

The role of pregnane X receptor (PXR) in cancer drug resistance and identification of novel PXR antagonists

Dissertation

der Mathematisch-Naturwissenschaftlichen Fakultät
der Eberhard Karls Universität Tübingen
zur Erlangung des Grades eines
Doktors der Naturwissenschaften
(Dr. rer. nat.)

vorgelegt von
Enni-Kaisa Mustonen
aus Nummi-Pusula/Finnland

Tübingen
2020

Gedruckt mit Genehmigung der Mathematisch-Naturwissenschaftlichen Fakultät der
Eberhard Karls Universität Tübingen.

Tag der mündlichen Qualifikation:

24.03.2021

Stellvertretender Dekan:

Prof. Dr. József Fortágh

1. Berichterstatter:

Prof. Dr. Matthias Schwab

2. Berichterstatter:

Prof. Dr. Peter Ruth

Contents

Abbreviations.....	III
Abstract.....	IV
Zusammenfassung.....	VI
1. Introduction.....	1
1.1. Structure and function.....	1
1.2. Cancer drug resistance.....	7
1.3. Role of PXR in carcinogenesis and cancer drug resistance.....	10
1.4. PXR antagonism in cancer drug resistance.....	13
1.5. Aims of the thesis.....	14
2. Material.....	15
3. Methods.....	24
3.1. Cell culture.....	24
3.2. Preparation of plasmids.....	26
3.3. Generation of drug-resistant cancer cells.....	26
3.4. Cell viability determination.....	27
3.5. Growth analysis.....	28
3.6. Resensitization of drug-resistant cells.....	28
3.7. RNA isolation and determination of RNA concentration.....	29
3.8. Test for RNA quality.....	29
3.9. Quantitative real-time PCR analysis.....	29
3.10. siRNA transfection of LS174T cells.....	31
3.11. Transient transfections and reporter gene assays.....	31
3.12. Batch transfections and reporter gene assays.....	32
3.13. Mammalian two hybrid assays.....	34
3.14. CaPO ₄ -transfections.....	34
3.15. Limited proteolytic digestion.....	35
3.15.1. Sample preparation.....	35
3.15.2. Proteolytic digestion.....	35
3.15.3. Protein gel electrophoresis and analysis.....	35
3.16. Protein analysis.....	35
3.16.1 Nuclear extraction.....	35
3.16.2. Total protein extraction.....	36
3.16.3. Determination of protein concentration.....	36
3.16.4. Western blot.....	36
3.17. Kinome profiling.....	37
4. Results.....	37
4.1. Generation and characterization of drug-resistant cancer cells.....	37
4.2. Determination of PXR levels in cisplatin- and irinotecan-resistant cells.....	43
4.3. Role of alternative splicing of PXR in cisplatin- and irinotecan resistance.....	44
4.4. Gene expression changes in cisplatin- and irinotecan-resistant cells.....	46
4.5. Cross-resistance of paclitaxel in irinotecan-resistant cells.....	50
4.6. Role of PXR in regulation of genes potentially involved in cisplatin or irinotecan resistance.....	50
4.7. Effect of PXR antagonism in irinotecan-resistant cells.....	55
4.8. Identification of novel PXR antagonists.....	57
4.9. Concentration-response analysis of potential PXR antagonists.....	63

4.10. Mode of antagonism of potential PXR antagonists.....	65
4.11. Binding of novel PXR ligands to PXR LBD.....	66
4.12. Relevance of specific amino acids for ligand binding of potential PXR ligands.....	68
4.13. Effects of novel PXR ligands on coregulatory protein interactions with PXR.....	71
4.14. Effects of novel PXR ligands on expression of endogenous PXR target genes.....	72
4.15. Nuclear receptor selectivity of novel PXR ligands.....	74
4.16. Structure-activity relationship (SAR) analysis.....	75
4.17. Inhibitory effects of compounds 100 and 109 on kinases.....	76
5. Discussion.....	78
5.1. Mechanism of resistance in cisplatin- and irinotecan-resistant cells.....	78
5.2. Role of PXR-dependent regulation on gene expression of cisplatin- and irinotecan-resistant cells.....	84
5.3. Resensitization of drug-resistant cancer cells by PXR antagonism.....	85
5.4. Identification of novel PXR antagonists and their mechanism of action.....	86
6. Conclusions.....	92
7. Declaration of collaboration.....	94
8. References.....	95
9. Appendices.....	109
10. Acknowledgements.....	113

Abbreviations

ABC	ATP-binding cassette
AF-2	activation function 2
CAR	constitutive androstane receptor
DBD	DNA binding domain
DMSO	dimethyl sulfoxide
DR	direct repeat
EC ₅₀	concentration that gives half maximal response
E _{max}	maximum response
EMT	epithelial-mesenchymal-transition
ER	everted repeat
GLUT-2	glucose 2 transporter
G6PC	glucose-6-phosphatase
HNF-4	hepatocyte nuclear factor 4
IC ₅₀	concentration of inhibitor that reduces response by half
IFD	induced fit docking
IR	inverted repeat
LBD	ligand binding domain
LBP	ligand binding pocket
Ls-P	parental LS174T cells
Ls-R-C	cisplatin-resistant LS174T cells
Ls-R-I	irinotecan-resistant LS174T cells
MDR1	multidrug resistance protein 1
PCK1	phosphoenolpyruvate carboxykinase
PHH	primary human hepatocyte
PROTAC	PROteolysis TArgeting Chimera
PXR	pregnane X receptor
RIF	rifampicin
ROS	reactive oxygen species
RT-qPCR	real-time quantitative polymerase chain reaction
RXR α	retinoid X receptor alpha
siRNA	small interfering RNA
SMRT	silencing mediator of retinoic acid and thyroid hormone receptor
sPXR	small PXR
SRC1	steroid receptor coactivator 1
SULT	sulfotransferase
TüKIC	Tübingen Kinase Inhibitor Collection
UGT	uridine 5'-diphospho-glucuronosyltransferase
VDR	vitamin D3 receptor
WT	wild-type
1 α ,25(OH) ₂ D ₃	1 α ,25-dihydroxy vitamin D3

Abstract

Pregnane X receptor (PXR) is a ligand-activated transcription factor, which belongs to the nuclear receptor family. PXR is mainly involved in regulating genes that metabolize and transport xenobiotics. Other PXR-regulated genes include those maintaining lipid and glucose homeostasis. In cancer cells, PXR activation appears to enhance cancer drug resistance and promote tumor growth. Therefore, PXR antagonism has been suggested as a potential approach in cancer therapy. However, several challenges related to utilizing PXR antagonism in cancer therapy remain, including insufficient knowledge about the consequences of PXR antagonism in drug-resistant cancer cells and the limited number of available PXR antagonists. Thus, the first aim of this work was to verify the putative role of PXR in cancer drug resistance and to investigate whether PXR antagonism has the capacity to resensitize drug-resistant cancer cells. To this end, cisplatin- and irinotecan-resistant colorectal cancer cells were generated. Colorectal cancer cell line LS174T was chosen due to its high PXR expression. Cisplatin and irinotecan were selected because these drugs have been demonstrated to possess PXR activating potential and acquired resistance can be developed against these drugs. Cisplatin is commonly used in the treatment of various solid tumors, whereas irinotecan is used in the treatment of colorectal cancer. Several cancer drug resistance-associated genes were differently expressed in these resistant cells compared to parental cells. To investigate the role of PXR in regulation of these genes, resistant cells were treated with PXR agonist rifampicin and antagonist SPA70. In cisplatin-resistant cells, none of the relevant genes associated with cisplatin resistance were affected by PXR modulation; therefore, PXR appears not to play a role in cisplatin resistance. On the contrary, in irinotecan-resistant cells specific resistance-associated genes were affected by PXR activation and inhibition. However, these cells were not resensitized to irinotecan with co-treatment of PXR antagonist SPA70. Irinotecan-resistant cells displayed increased expression of ABCB1 and CYP3A4, which have been shown to participate in paclitaxel metabolism and resistance. Accordingly, these cells exhibited cross-resistance towards paclitaxel. Moreover, irinotecan-resistant cells were resensitized to paclitaxel with co-treatment of PXR antagonist SPA70. These results suggest that PXR antagonism is a potential approach to attenuate drug resistance in cancer cells, if the resistance is for the most part dependent on PXR-regulated genes. Due to the limited number of available PXR antagonists, the second aim of this work was to identify novel PXR antagonists from the Tübingen Kinase Inhibitor Collection compound library, which contains 8,500 proprietary compounds comprising for the most part kinase inhibitors, which is one of the most relevant groups of molecularly targeted cancer drugs. These compounds were investigated in relation

to their PXR antagonism, because these compounds could be of special interest for the prevention of cancer drug resistance, if they could elicit a dual function of inhibiting both kinases and PXR. The combination of *in silico* and biological assays resulted in identification of four novel potential PXR antagonists and one potential full agonist, which displayed high structural similarity consisting of a benzosuberone moiety, two additional aromatic rings and an amide. These novel antagonists appeared to be passive, competitive antagonists with partial agonism activity. They also demonstrated direct binding to PXR and impaired the rifampicin-induced coactivator interactions with PXR. Moreover, these antagonists elicited gene-specific effects on endogenous PXR target gene expression. Finally, these antagonists displayed selectivity towards PXR among the NR1I group of nuclear receptors. Interestingly, the subtle changes in the functional groups of these compounds altered considerably the PXR activation and inhibition potential.

To summarize, PXR antagonism could be a potential approach to reduce cancer drug resistance in cases where resistance is mainly dependent on PXR-regulated genes. Overall, these results provide deeper understanding of drug-dependent resistance mechanisms in colorectal cancer with respect to gene expression changes and PXR-dependent regulation of these genes. In addition, to the best of our knowledge, this work shows for the first time successful resensitization of drug-resistant colorectal cancer cells by use of a PXR antagonist. Development of novel PXR antagonists is challenging not only due to the large and flexible ligand binding pocket of PXR, but also because subtle structural changes affect the activation and inhibition ability as was demonstrated by the identified PXR ligands in this work. Finally, our results provide further information regarding the structure-activity relationship and gene-specific effects of potential antagonists, which could aid in the demanding development of specific PXR antagonists in the future.

Zusammenfassung

Der Pregnan X-Rezeptor (PXR) ist ein ligandenaktivierter Transkriptionsfaktor, der zur Familie der Kernrezeptoren gehört. PXR ist hauptsächlich an der Regulation von Genen beteiligt, die Xenobiotika metabolisieren und transportieren. Aber auch Gene, welche an der Aufrechterhaltung der Lipid- und Glucosehomöostase beteiligt sind, werden von PXR reguliert. In Krebszellen scheint die PXR-Aktivierung die Resistenz gegen Krebsmedikamente zu erhöhen und das Tumorwachstum zu fördern. Daher wurde ein PXR-Antagonismus als möglicher Ansatz in der Krebstherapie vorgeschlagen. Es bestehen jedoch noch einige Herausforderungen im Zusammenhang mit der Verwendung von PXR-Antagonisten in der Krebstherapie, die insbesondere in unzureichenden Kenntnissen über die Folgen des PXR-Antagonismus in arzneimittelresistenten Zellen und in der begrenzten Anzahl verfügbarer PXR-Antagonisten begründet sind. Das erste Ziel dieser Arbeit war es daher, die mutmaßliche Rolle von PXR bei der Resistenz gegen Krebsmedikamente zu überprüfen und zu untersuchen, ob der PXR-Antagonismus die Fähigkeit besitzt, arzneimittelresistente Krebszellen erneut zu sensibilisieren. Zu diesem Zweck wurden Cisplatin- und Irinotecan-resistente Darmkrebszellen erzeugt. Die Darmkrebszelllinie LS174T wurde hierfür aufgrund ihrer hohen PXR-Expression ausgewählt. Cisplatin und Irinotecan wurden ausgewählt, da gezeigt wurde, dass diese Medikamente ein PXR-aktivierendes Potenzial haben und eine erworbene Resistenz gegen diese Medikamente entwickelt werden kann. Cisplatin wird üblicherweise zur Behandlung verschiedener solider Tumore verwendet, während Irinotecan zur Behandlung von Darmkrebs eingesetzt wird. Mehrere mit Krebsmedikamentenresistenz assoziierte Gene wurden in diesen resistenten Zellen im Vergleich zu den Elternzellen unterschiedlich exprimiert. Um die Rolle von PXR bei der Regulation dieser Gene zu untersuchen, wurden resistente Zellen mit dem PXR-Agonisten Rifampicin und dem Antagonisten SPA70 behandelt. In Cisplatin-resistenten Zellen wurde keines der relevanten Gene, die mit Cisplatin-Resistenz assoziiert sind, durch PXR-Modulation beeinflusst; Daher scheint PXR keine Rolle bei der Cisplatinresistenz zu spielen. Im Gegensatz dazu wurden in Irinotecan-resistenten Zellen spezifische resistenzassoziierte Gene durch PXR-Aktivierung und -Hemmung beeinflusst. Diese Zellen wurden jedoch, bei gleichzeitiger Behandlung mit dem PXR-Antagonisten SPA70, nicht gegen Irinotecan resensibilisiert. Irinotecan-resistente Zellen zeigten eine erhöhte Expression von ABCB1 und CYP3A4, von denen gezeigt wurde, dass sie am Paclitaxel-Metabolismus und an der Resistenz beteiligt sind. Dementsprechend zeigten diese Zellen auch eine Kreuzresistenz gegen Paclitaxel. Darüber hinaus wurden Irinotecan-resistente Zellen bei gleichzeitiger Behandlung mit SPA70 gegen Paclitaxel resensibilisiert. Diese Ergebnisse legen nahe, dass der

PXR-Antagonismus ein potenzieller Ansatz zur Abschwächung der Arzneimittelresistenz in Krebszellen ist, wenn die Resistenz größtenteils von PXR-regulierten Genen abhängt. Aufgrund der begrenzten Anzahl verfügbarer PXR-Antagonisten bestand das zweite Ziel dieser Arbeit darin, neue PXR-Antagonisten aus der Substanzbibliothek der Tübinger Kinase Inhibitor Collection zu identifizieren, die 8500 proprietäre Verbindungen enthält, welche größtenteils Kinase-Inhibitoren sind. Kinase-Inhibitoren stellen eine der bedeutsamsten Substanzgruppen molekular zielgerichteter Krebsmedikamente dar. Diese Verbindungen wurden hinsichtlich ihres PXR-Antagonismus untersucht, da sie für die Prävention von Krebsmedikamentenresistenz von besonderem Interesse sein könnten, wenn sie sowohl eine Hemmung von Kinasen wie auch von PXR hervorrufen könnten. Die Kombination von In-Silico- und biochemischen Assays führte zur Identifizierung von vier neuen potenziellen PXR-Antagonisten und einem potenziellen Vollagonisten, die eine hohe strukturelle Ähnlichkeit zeigten. Ihre gemeinsame Struktur aus einer Benzosuberoneinheit, zwei zusätzlichen aromatischen Ringen und einem Amid. Die neuen Antagonisten schienen passive, kompetitive Antagonisten mit partieller Agonismusaktivität zu sein. Sie zeigten auch eine direkte Bindung an PXR und beeinträchtigten die Rifampicin-induzierte Coaktivator-Interaktion mit PXR. Darüber hinaus wirkten diese Antagonisten genspezifisch auf die Expression endogener PXR-Zielgene. Schließlich zeigten sie eine Selektivität gegenüber PXR innerhalb der NR11-Gruppe von Kernrezeptoren. Interessanterweise veränderten die subtilen Änderungen in den funktionellen Gruppen dieser Verbindungen das PXR-Aktivierungs- und Inhibitionspotential erheblich.

Zusammenfassend zeigte sich, dass PXR-Antagonismus ein potenzieller Ansatz zur Verringerung der Resistenz gegen Krebsmedikamente ist, wenn die Resistenz hauptsächlich von PXR-regulierten Genen abhängt. Insgesamt liefern diese Ergebnisse ein tieferes Verständnis der arzneimittelabhängigen Resistenzmechanismen bei Darmkrebszellen in Bezug auf Genexpressionsänderungen und die PXR-abhängige Regulation dieser Gene. Darüber hinaus zeigt diese Arbeit erstmals eine erfolgreiche Resensibilisierung von arzneimittelresistenten Darmkrebszellen durch PXR-Antagonisten. Die Entwicklung neuer PXR-Antagonisten ist nicht nur aufgrund der großen und flexiblen Ligandenbindungstasche von PXR eine Herausforderung, sondern auch, weil subtile strukturelle Änderungen die Aktivierungs- und Inhibitionsfähigkeit beeinflussen, wie die in dieser Arbeit identifizierten PXR-Liganden gezeigt haben. Schließlich liefern unsere Ergebnisse weitere Informationen bezüglich der Strukturaktivitätsbeziehung und der genspezifischen Wirkungen potenzieller

Antagonisten, die in Zukunft die weitere Entwicklung spezifischer PXR-Antagonisten unterstützen könnten.

1. Introduction

1.1. Structure and function of pregnane X receptor

The family of nuclear receptors consists of 48 members, which act as transcription factors regulating genes that are involved in several important processes, such as cell proliferation, xenobiotic metabolism, lipid, glucose and bile acid homeostasis (reviewed in Cave et al. 2016; Garcia et al. 2018; Mazaira et al. 2018; Prakash et al. 2018). One of these ligand-activated transcription factors, is pregnane X receptor (PXR, NR1I2), which was first isolated in mouse liver (Kliewer et al., 1998) and soon after also human PXR was identified (Bertilsson et al., 1998; Blumberg et al., 1998; Lehmann et al., 1998). Similar to other nuclear receptors, PXR consists of the N-terminal domain, the DNA-binding domain (DBD), the hinge region connecting DBD to the ligand-binding domain (LBD) and the C-terminal domain (di Masi et al., 2009).

PXR forms a heterodimer with retinoid X receptor alpha (RXR α) and after activation by ligand this complex induces the target gene expression by binding to short DNA sequences called response elements in the DNA of the target gene (Goodwin et al., 1999; Lehmann et al., 1998). These response elements include three types of repeats of the canonical nuclear receptor hexamer half-site motif: direct repeats separated by three, four or five nucleotides (DR3, DR4, DR5), everted repeats separated by six, seven, eight or nine nucleotides (ER6, ER7, ER8, ER9) and inverted repeats separated by six nucleotides (IR6) (Blumberg et al., 1998; Frank et al., 2005; Lehmann et al., 1998). Transcriptional activity of PXR is also regulated by coactivators and corepressors that bind to the motifs in the activation function 2 (AF-2) region at the end of LBD (reviewed in Pavek, 2016). These coregulatory proteins include coactivators, such as steroid receptor coactivator 1 (SRC1, NCOA1) and corepressors, such as silencing mediator of retinoic acid and thyroid hormone receptor (SMRT, NCOR2). The binding of coactivators enhances the transcriptional activity of PXR, whereas corepressors repress it. Correspondingly, PXR agonists typically promote the interaction of PXR with coactivators (Kliewer et al., 1998; Lehmann et al., 1998) and interfere with the interaction of corepressors (Synold et al., 2001). In contrast, antagonists can impair the interaction of PXR with coactivators (Chen et al., 2010; Huang et al., 2007) or promote the interaction with corepressors (Lin et al., 2017).

Alternative splicing of the PXR gene results in various isoforms (reviewed in Brewer and Chen, 2016). Frequently studied variants are PXR1, PXR2, PXR3 and PXR4, which is also known as small PXR (sPXR) (Fig. 1). PXR1 is the reference variant, translating into a 434 amino acid containing protein (Bertilsson et al., 1998; Lehmann et al., 1998). PXR2 originates from a

different transcription initiation site than PXR1 resulting in an N-terminal 39 amino acid extension (Bertilsson et al., 1998). PXR3 is a splicing variant of PXR1 with a 111 bp deletion in exon 5 leading to a 37 amino acid deletion in the LBD (Dotzlaw et al., 1999). PXR1 and PXR2 elicit comparable gene activation properties, whereas PXR3 is deficient in ligand-induced gene activation (Gardner-Stephen et al., 2004; Lin et al., 2009). sPXR is derived from an alternative promoter in intron 3 and as a result contains only exons 4–9 of PXR1 (Breuker et al., 2014). Similar to PXR3, sPXR does not elicit any ligand-induced transcriptional activity, it is, however, able to suppress the transcriptional activity of functional PXR (Breuker et al., 2014). Furthermore, Breuker et al. (2014) detected that the expression of sPXR was decreased in certain aggressive hepatocellular carcinoma subgroups compared to the non-proliferative subgroups, which are usually related to better prognosis. Therefore, sPXR has been suggested to elicit tumor suppressing effects (Breuker et al., 2014).

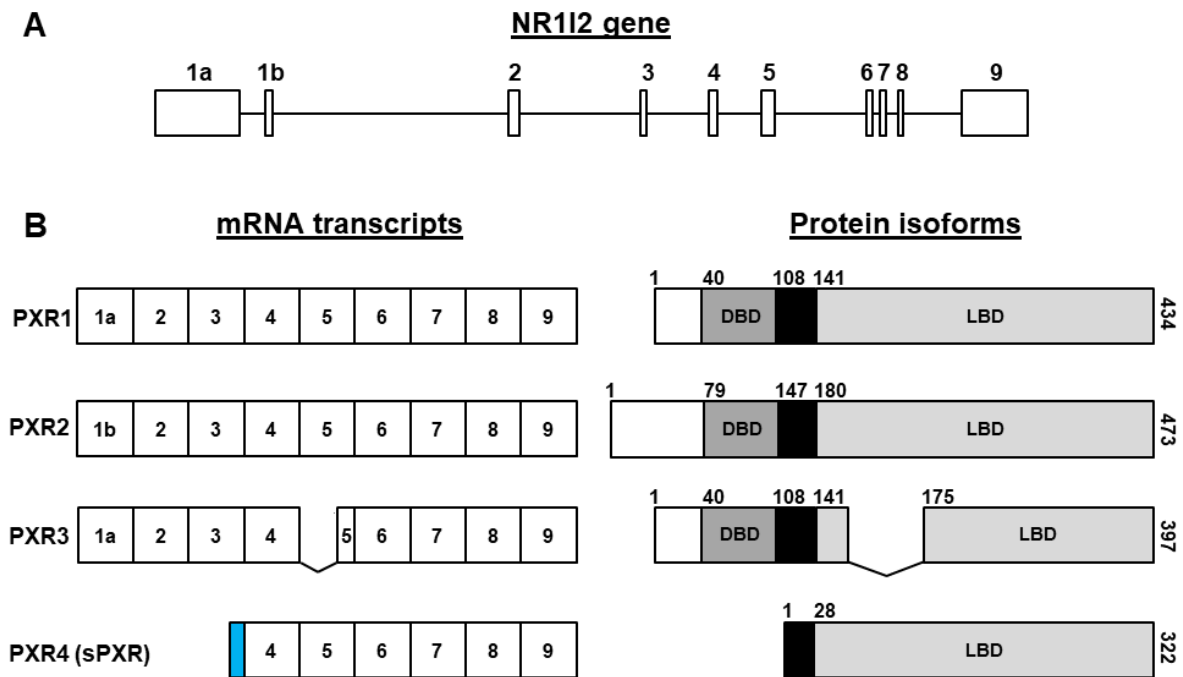


Figure 1. PXR gene, mRNA transcripts and protein isoforms. (A) PXR gene is located in chromosome 3 (3q12–q13.3). Exons are illustrated with rectangles and introns with horizontal lines. Numbers above exons depict the exon numbers. (B) Schematic representation of PXR mRNA transcripts and protein isoforms. White rectangles in the transcripts illustrate the exons and numbers inside rectangles depict the exon numbers. Exon deletion is demonstrated with a gap. Blue illustrates approximately 400 specific bases upstream of exon 4 in PXR4. In protein isoforms, white color illustrates N-terminal, dark grey DNA binding domain (DBD), black the hinge region and light grey the ligand binding domain (LBD). Numbers above schemes depict the first amino acid in the respective region. Vertical number at the end of schemes depicts the last amino acid in the respective isoform.

Human and mouse PXR share 96% sequence similarity in their DBDs, whereas LBDs similarity is only 76% between these two species (Lehmann et al., 1998). The differences in

the LBD explain the species-specific effects in the ligand-induced activation of PXR. For instance, rifampicin is a potent agonist for human PXR, but it activates mouse PXR only weakly (Lehmann et al., 1998). In contrast, pregnenolone-16 α -carbonitrile is a weak activator of human PXR, whereas it acts as a potent activator for mouse PXR.

PXR has a large and flexible ligand binding pocket (LBP), therefore, compounds with variable structures and molecular sizes act as PXR ligands (Fig. 2) (Jones et al., 2000; Lehmann et al., 1998; Watkins et al., 2003). The number of PXR agonists is vast. These agonists include xenobiotics such as drugs, drug metabolites, pesticides, environmental pollutants and natural products, but also endogenous molecules, such as bile acid derivatives. Table 1 shows selected PXR agonists with their respective EC₅₀ values.

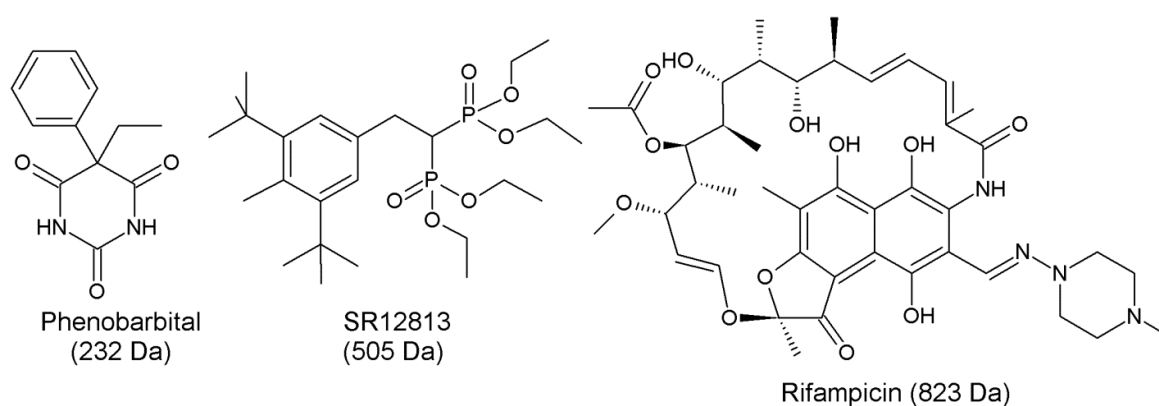


Figure 2. Examples of PXR agonists with their structures.

Table 1. PXR agonists with determined EC₅₀ values.

Compound	EC ₅₀ (μ M)	Reference
Artemisinin	5.4–34	Burk et al., 2005; Persson et al., 2006
Betamethasone	20	Persson et al., 2006
Bis(2-ethylhexyl) phthalate	2.5	Mnif et al., 2007
Carbamazepine	15.6	Persson et al., 2006
Carboxymefloquine	24	Piedade et al., 2015
C2BA-4	0.02	Lemaire et al., 2007
5 β -Cholestan-3 α ,7 α ,12 α -triol	5	Goodwin et al., 2003
Cholic acid	11.6	Krasowski et al., 2005
CITCO	3	Maglich et al., 2003
Clotrimazole	0.8–5	Bertilsson et al., 1998; Lehmann et al., 1998; Lemaire et al., 2004; Moore et al., 2000a
Corticosterone	30	Blumberg et al., 1998
Coumestrol	25	Blumberg et al., 1998
Deoxycholic acid	50.2	Krasowski et al., 2005
Deoxycholic acid-3,12-diacetate	9.1	Carazo et al., 2017
Dexamethasone	5.5–10	Lehmann et al., 1998; Persson et al., 2006
7,12-Diketolithocholic acid	35.5	Krasowski et al., 2005
6,16 α -Dimethyl pregnenolone	0.3	Kliwer et al., 1998
Echimidine	67.1	Luckert et al., 2018
Estradiol	30	Blumberg et al., 1998
Ferutinine	1.8	Mnif et al., 2007

Glycolithocholic acid	16.1	Krasowski et al., 2005
Glycolithocholic acid 3-sulfate	56.2	Krasowski et al., 2005
17-Hydroxy-pregnenolone	>10	Lehmann et al., 1998
Hyperforin	0.002–0.003	Moore et al., 2000b; Persson et al., 2006
ICI 182780	3.1	Mnif et al., 2007
Indomethacin	17.6	Persson et al., 2006
7-Ketodeoxycholic acid	58.2	Krasowski et al., 2005
3-Ketolithocholic acid	8,3	Krasowski et al., 2005
7-Ketolithocholic acid	21.5	Krasowski et al., 2005
12-Ketolithocholic acid	31.3	Krasowski et al., 2005
Lansoprazole	3.0	Persson et al., 2006
Lithocholic acid	10.2	Krasowski et al., 2005
Lithocholic acid acetate	1.2	Krasowski et al., 2005
Lithocholic acid acetate methyl ester	1.1	Krasowski et al., 2005
Lithocholic acid 3-sulfate	118	Krasowski et al., 2005
Lovastatin	1	Lehmann et al., 1998
Metolazone	0.7–1.5	Banerjee and Chen, 2014
Mifepristone (RU486)	5.5–10	Lehmann et al., 1998; Moore et al., 2000a
n-Butyl-p-aminobenzoate	8.0	Krasowski et al., 2005
Nifedipine	4.3	Bertilsson et al., 1998
23-Norcholeic acid	96.0	Krasowski et al., 2005
23-Nordeoxycholic acid	16.4	Krasowski et al., 2005
4-OHT	3.0	Mnif et al., 2007
Omeprazole	8.6	Persson et al., 2006
Paclitaxel	5.0	Synold et al., 2001
Pantoprazole	6.8	Persson et al., 2006
PCB153	1.5	Al-Salman and Plant, 2012
Phenobarbital	169–370	Lemaire et al., 2004; Persson et al., 2006
Phenytoin	8.0	Persson et al., 2006
Pregnenolone-16 α -carbonitrile	>10	Moore et al., 2000a
5 β -Pregnane-3,20-dione	3.1–20	Lehmann et al., 1998; Lemaire et al., 2004; Moore et al., 2000a
Primaquine	13.6	Persson et al., 2006
Rabeprazole	1.5	Persson et al., 2006
Rifampicin	0.1–10	Al-Salman and Plant, 2012; Banerjee and Chen, 2014; Berthier et al., 2012; Blumberg et al., 1998; Lehmann et al., 1998; Lemaire et al., 2004; Mu et al., 2006; Persson et al., 2006
RU58668	0.21	Mnif et al., 2007
Schisandrin	1.25	Mu et al., 2006
SJB7	0.88	Lin et al., 2017
SR12813	0.12–0.14	Lemaire et al., 2007; Mnif et al., 2007; Moore et al., 2000a
Taurochenodeoxycholic acid	104	Krasowski et al., 2005
Tauroolithocholic acid	19.8	Krasowski et al., 2005
Tauroolithocholic acid 3-sulfate	83.2	Krasowski et al., 2005
TCPOBOP	3.9	Moore et al., 2000a
4-tert-octylphenol	2.7	Mnif et al., 2007
T0901317	7.9	Xue et al., 2007
Troglitazone	3.5	Persson et al., 2006
Walrycin A	30	Berthier et al., 2012
Warfarin	49.5	Persson et al., 2006
Verapamil	3.2	Persson et al., 2006
α -Zearalenone	1.3–1.8	Mnif et al., 2007

PXR is most abundantly expressed in the liver and the intestine, and to lesser extent in other tissues, such as the kidney, the heart and the bone marrow (Blumberg et al., 1998; Lamba et al., 2004; Lehmann et al., 1998; Miki et al., 2005). The prominent expression of PXR in the liver and the intestine is obvious because PXR is largely involved in the regulation of xenobiotic detoxification. PXR activation induces expression of many metabolizing enzymes and transporters (Fig. 3) (reviewed in di Masi et al., 2009). These transcriptional targets include genes encoding several CYP P450 metabolizing enzymes, including CYP3A4, ATP-binding cassette (ABC) transporters and conjugating enzymes such as uridine 5'-diphosphoglucuronosyltransferases (UGTs) and sulfotransferases (SULTs). PXR has a vital role in drug metabolism as, for instance CYP3A4 participates in the metabolism of over 50% of marketed drugs (Harmsen et al., 2009). In addition to this vital role in xenobiotic metabolism, PXR is one of the nuclear receptors that maintains glucose, lipid and bile acid homeostasis (Fig. 3) (reviewed in Hakkola et al., 2016; Li and Chiang, 2013).

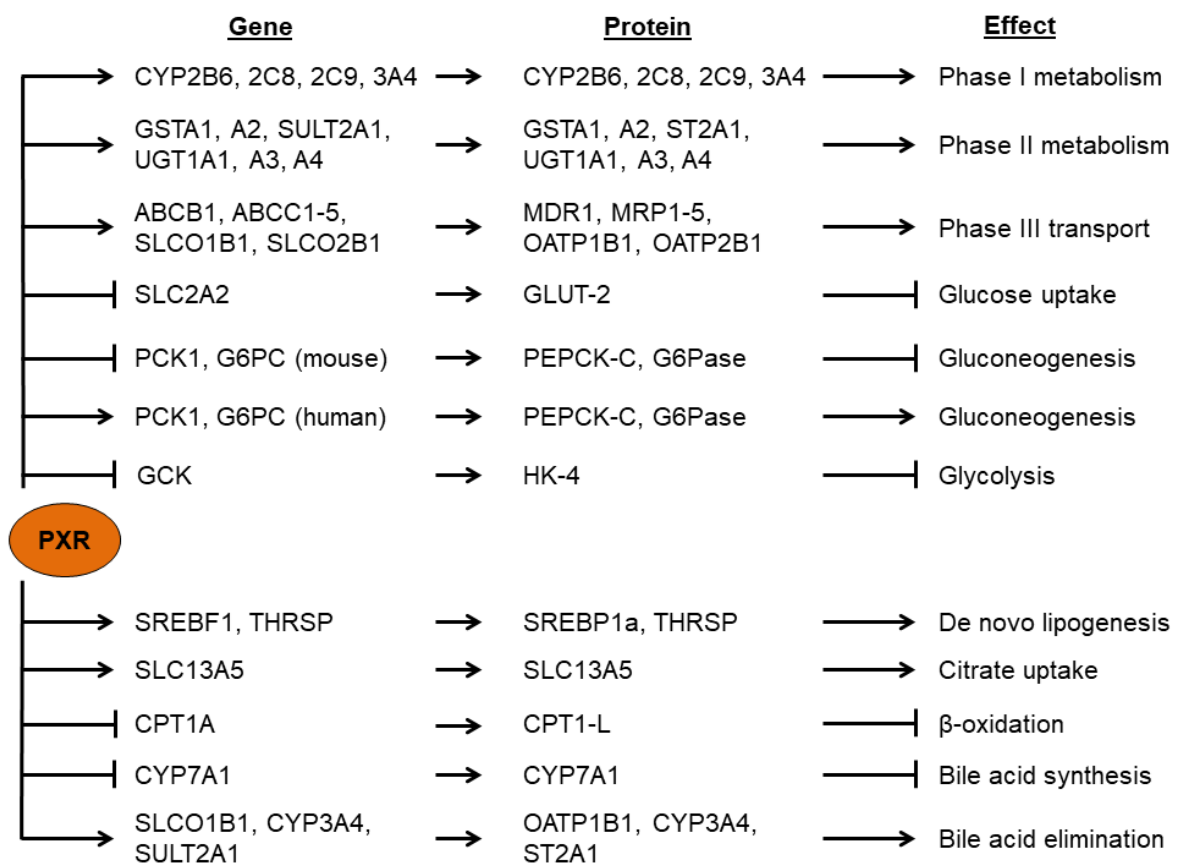


Figure 3. Function of PXR in xenobiotic metabolism, glucose, lipid and bile acid homeostasis. For example, activated PXR induces expression of CYP2B6, which increases phase I metabolism, whereas expression of SLC2A2 gene is suppressed by PXR activation, which decreases the expression of GLUT-2 transporter protein and results in decreased glucose uptake. Arrowhead arrow, induction; blunt head arrow, suppression.

The effect of PXR activation in glucose homeostasis is complex. Treatment with PXR agonists has shown to reduce the expression of gluconeogenic genes glucose-6-phosphatase (G6PC) and phosphoenolpyruvate carboxykinase (PCK1) in human liver cancer cells and in mouse hepatocytes (Bhalla et al., 2004; Kodama et al., 2007, 2004). Different mechanisms behind the attenuated gluconeogenesis have been suggested. On one hand ligand-activated PXR has been observed to compete with hepatocyte nuclear factor 4 (HNF-4) in binding to peroxisome proliferator activating receptor- γ coactivator-1 (PGC-1) (Bhalla et al., 2004). As a result this suppressed the activation of PCK1 by HNF-4 in human liver cancer cells (Bhalla et al., 2004). On the other hand, also in human liver cancer cells ligand-activated PXR repressed the activity of forkhead box protein O1 (FOXO1) (Kodama et al., 2004). FOXO1 activates G6PC and PCK1, and thereby promotes gluconeogenesis. Ligand-activated PXR has also demonstrated to bind to the cyclic AMP-response element-binding protein (CREB) suppressing the cAMP-dependent induction of G6PC in mouse hepatocytes (Kodama et al., 2007). Opposite results, however, were observed in human liver cancer cells overexpressing PXR, where rifampicin treatment resulted in upregulation of G6PC (Gotoh and Negishi, 2014). On the contrary, this effect was not detected in parental cells. PXR activation increased expression of G6PC and PCK1 also in primary human hepatocytes (Gotoh and Negishi, 2015). Correspondingly, when human volunteers were treated with PXR agonists, they displayed impaired glucose tolerance (Rysä et al., 2013; Stage et al., 2016). Postprandial hyperglycemia was also observed in PXR agonist-treated rats that displayed reduced expression of glucose 2 transporter (GLUT-2, SLC2A2) (Rysä et al., 2013). Similarly, GLUT-2 protein levels were reduced by PXR activation in human liver cancer cells (Ling et al., 2016). In addition to downregulated GLUT-2, PXR activation impaired glucose utilization in human liver cancer cells by reducing protein levels of hexokinase (HK-4). Overall, effects of PXR activation in relation to glucose homeostasis are complex and species-specific.

Compared to glucose homeostasis, effects of PXR activation in lipid homeostasis are more similar between species. In general, PXR activation induces expression of several lipogenic genes, therefore, causing lipid accumulation and eventually hepatic steatosis (Bitter et al., 2015; Li et al., 2015; Moreau et al., 2009; Nakamura et al., 2007). In primary human hepatocytes, PXR activation induced for example thyroid hormone-inducible hepatic protein (THRSP) and sterol regulatory element-binding protein 1 (SREBP1a), which subsequently increased expression of their lipogenic target genes, including fatty acid synthase (FAS), ATP-citrate synthase (ACLY) and acetyl-CoA carboxylase 1 (ACACA) (Bitter et al., 2015; Moreau

et al., 2009). PXR activation in mouse induced distinct lipogenic genes, such as lipin-1 (*Lpin1*) and stearoyl-CoA desaturase 1 (*Scd1*) (He et al., 2013; Nakamura et al., 2007; Zhou et al., 2006a). In addition to induction of lipogenic genes, PXR activation suppressed carnitine O-palmitoyltransferase 1 (*CPT1A*) and as a result reduced β -oxidation in both primary human hepatocytes and in mice (Moreau et al., 2009; Nakamura et al., 2007). In primary human hepatocytes and in humanized PXR transgenic mice, PXR activation increased both mRNA and protein levels of *SLC13A5* that transports citrate from circulation into the hepatocytes (Li et al., 2015). In addition, PXR activation in mice increased fatty acid transport by inducing *Cd36* and its positive regulator peroxisome proliferator-activated receptor gamma (*PPAR γ*) (Zhou et al., 2006a). In contrast, rifampicin treatment did not induce these genes in primary human hepatocytes (Moreau et al., 2009). Given the above, PXR activation induces lipid accumulation; despite that partially distinct genes are affected in a species-specific manner.

Some of the same PXR-regulated xenobiotic metabolizing enzymes and transporters are also involved in bile acid homeostasis. These include bile acid hydroxylating or conjugating enzymes, such as CYP 450s, SULTs and UGTs and *SLCO* family uptake transporters (reviewed in Li and Chiang, 2013; Staudinger et al., 2013). In addition, PXR activation has shown to reduce the bile acid synthesis from cholesterol via suppressing the rate-limiting enzyme *CYP7A1* (Bhalla et al., 2004; Li and Chiang, 2005; Staudinger et al., 2001). Ultimately, PXR activation decreases the synthesis of bile acids and enhances the metabolism and excretion. Moreover, in mice PXR was activated by the toxic secondary bile acid, lithocholic acid (Staudinger et al., 2001; Wistuba et al., 2007). Therefore, PXR activation can protect against harmful effects of the toxic bile acids by enhancing the elimination of them.

1.2. Cancer drug resistance

The cancer incidence and mortality are currently increasing globally. This is due to aging population, continued population growth and improved socioeconomic aspects, which has increased the prevalence of many cancer risk factors (Bray et al., 2018). Cancer is the second leading cause of mortality in the United States and in Europe (Eurostat, 2016; Siegel et al., 2019). In 2018, there were estimated to be 18.1 million new cancer cases and 9.6 million cancer deaths in the world (Bray et al., 2018). The most frequently diagnosed cancer is lung cancer, which is also causing most of the cancer-related deaths. By incidence the next most common cancers are breast cancer, prostate cancer and colorectal cancer, whereas by mortality lung cancer is followed by colorectal, stomach and liver cancer.

Chemotherapy is one of the leading treatment options in cancer. However, treatment failure caused by cancer drug resistance is frequent (Holohan et al., 2013). The resistance can be intrinsic, meaning that cells are initially resistant towards the drug or cancer cells acquire resistance towards drug during the treatment. Cancer drug resistance can be caused by several mechanisms (Fig. 4) (reviewed in Holohan et al., 2013; Marin et al., 2010; Pan et al., 2016).

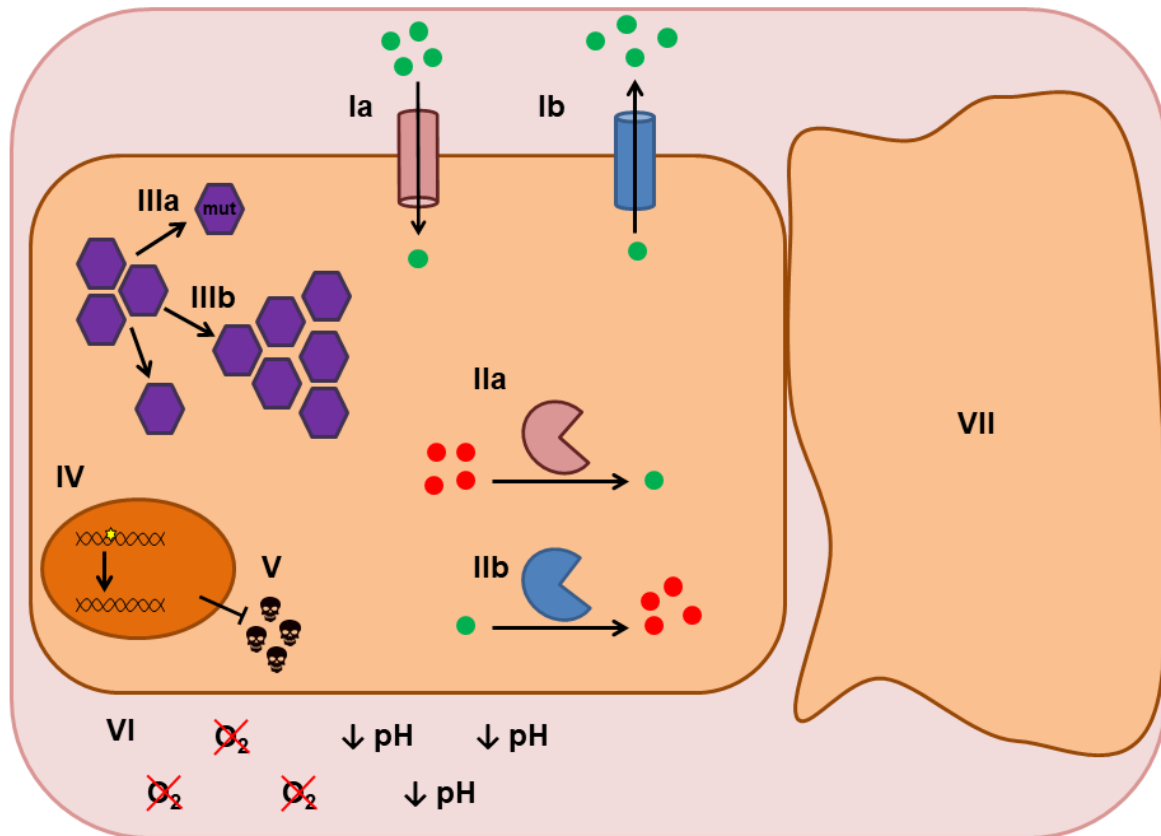


Figure 4. Mechanisms of cancer drug resistance. Cancer drug resistance can be caused by reduced uptake of drug (Ia), increased drug efflux (Ib), reduced prodrug activation (IIa), increased drug inactivation (IIb), alterations in molecular targets, including mutations (IIIa) and altered expression level of target (IIIb), enhanced repair of drug-induced DNA damage (IV), alterations in balance of apoptosis and survival pathways (V), altered cancer cell microenvironment (VI), or by phenotype transition (VII).

First, reduced uptake of drug into the cells (Ia) or enhanced drug efflux out of the cells (Ib) can lead to reduced intracellular drug concentration (Marin et al., 2010). For instance, several kinase inhibitors are substrates or modulators of multidrug resistance protein 1 (MDR1), therefore, MDR1 can transport these drugs out of cancer cells or these drugs can enhance the efflux of other MDR1 substrate drugs that are administered simultaneously (Dohse et al., 2010; Harmsen et al., 2013).

In addition to the transporters, metabolizing enzymes can alter the intracellular concentration of active drug (Pan et al., 2016). On one hand the metabolism of prodrug to active metabolite

can be reduced (IIa), on the other hand the metabolism of active drug into inactive metabolites can be enhanced (IIb). For instance, CYP3A4 metabolizes several kinase inhibitors and camptothecin derivatives, such as irinotecan (Marin et al., 2010).

Cancer drug resistance can result from alterations in molecular targets (Holohan et al., 2013). The target of a cancer drug can be mutated (IIIa) or the expression level of the target can be changed (IIIb). There are several examples where the drug target is mutated initially or during the treatment especially with molecularly targeted drugs leading at worst case to treatment failure (reviewed in Ward et al., 2020). Imatinib, which is a tyrosine kinase inhibitor and used for the treatment of chronic myeloid leukemia, targets the fusion protein of ABL1 and BCR genes. So far over 40 mutations have been identified for this gene fusion that are associated with resistance towards imatinib (reviewed in Linev et al., 2018). This has led to development of further kinase inhibitors targeting these mutated proteins. Marketing authorizations for the treatment of imatinib-resistant chronic myeloid leukemia are granted for example for dasatinib and nilotinib, which are effective against several imatinib-resistant mutations (EMA, 2019a, 2018; Ward et al., 2020).

Alterations in levels of drug targets have been observed to occur in both directions. Methotrexate-resistant sarcoma cells displayed increased gene copy number of the molecular target of methotrexate, dihydrofolate reductase (Alt et al., 1978). In contrast, irinotecan-resistant non-small cell lung cancer cells exhibited reduced activity and amount of topoisomerase 1 (TOP1) (Kanzawa et al., 1990).

Several chemotherapeutics are directly targeting the DNA and cause DNA damage (Holohan et al., 2013). For this type of drugs, enhanced DNA repair can lead to cancer drug resistance (IV). For instance, ERCC1 has been shown to repair cisplatin-induced DNA damage and downregulation of this gene increased the sensitivity of cancer cells towards cisplatin (Arora et al., 2010).

Additionally, alterations in balance of apoptosis and survival pathways (V) resulting from increased expression of antiapoptotic proteins and reduced expression of proapoptotic proteins can enhance the survival of cancer cells during drug treatment (Marin et al., 2010). For example, estrogen treatment increased expression of antiapoptotic Bcl-2 in breast cancer cells and subsequently reduced cytotoxicity of doxorubicin (Teixeira et al., 1995). Similarly, Bcl-2 transfection increased the resistance. Treatment with estrogen free medium decreased Bcl-2 levels, and as a result enhanced sensitivity towards doxorubicin.

In addition to above mentioned mechanism that are related to gene alterations, altered cancer cell microenvironment can also enhance cancer drug resistance (VI) (Marin et al., 2018). Typical microenvironmental change is hypoxia. Hypoxia has been shown to induce expression of ABCB1 and ABCC1 transporters via induction of hypoxia-inducible factor 1 α (HIF-1 α), which regulates cellular responses to hypoxia (Lv et al., 2015; Min et al., 2012; Yang et al., 2016). Furthermore, hypoxia has been demonstrated to suppress the expression of proapoptotic proteins, including BAX and BAD (Yang et al., 2016).

Finally, cancer drug resistance can be affected by phenotype transition (VII) (Marin et al., 2018). For instance, epithelial-to-mesenchymal transition (EMT) is a phenotypic change of cells, in which cells lose their cell-cell adhesion and gain properties of mesenchymal cells, such as enhanced migration and invasion (Zhang et al., 2012). Increased expression of EMT markers, migration and invasion have been observed in drug-resistant cancer cell lines (Wu et al., 2013a; Zhang et al., 2012). EMT can also be linked to other drug resistance mechanism, as demonstrated by increased expression of ABC transporters after induction of EMT (Saxena et al., 2011). Moreover, EMT-inducing transcription factors were observed to bind directly to the promoters of ABC transporters.

1.3. Role of PXR in carcinogenesis and cancer drug resistance

PXR is expressed in many cancer cell lines and cancer tissues, including colon cancer (Dong et al., 2017; Pfrunder et al., 2003; Raynal et al., 2010). Dong et al. (2017) discovered an association between PXR expression and poor overall survival in colorectal cancer patients. Overall, PXR activation appears to have tissue- and context-specific effects in cancer cells (Fig. 5) (reviewed in Pondugula et al., 2016).

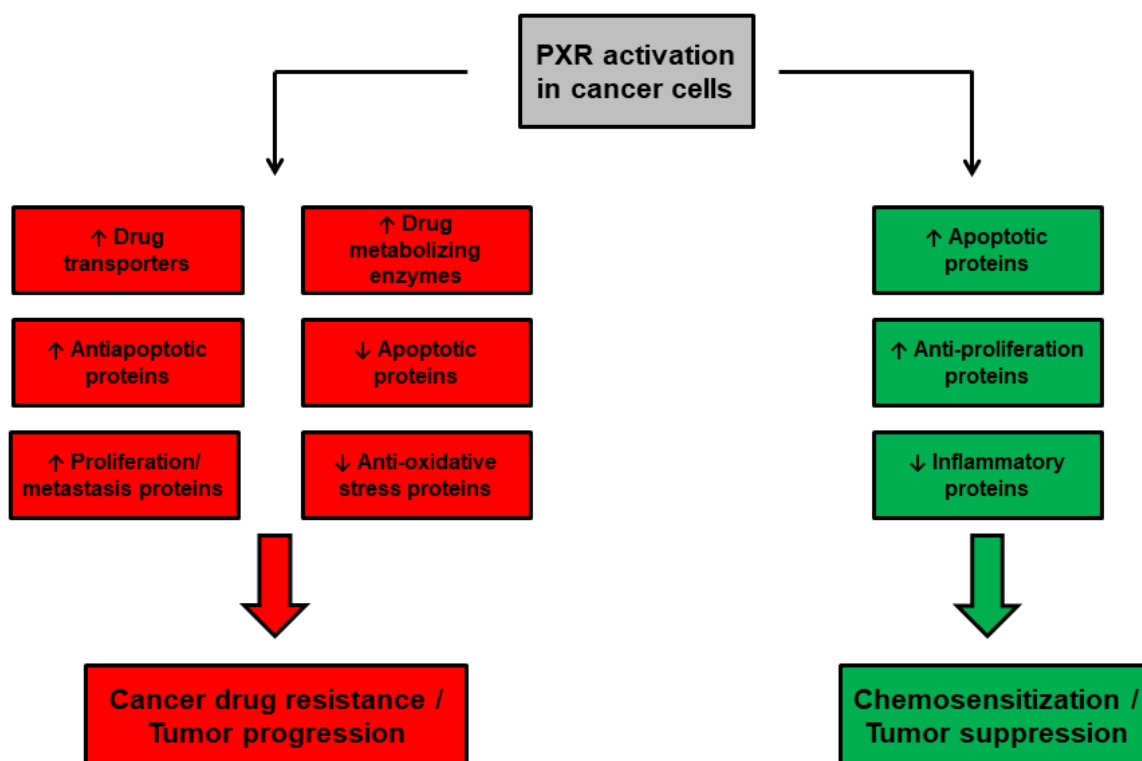


Figure 5. Effects of PXR activation in cancer. On one hand PXR activation has been shown to promote cancer drug resistance and tumor progression. On the other hand, PXR activation has also been demonstrated to promote opposite effects. Adapted from Pondugula et al. 2016.

Several chemotherapeutics are substrates of MDR1 drug transporter; therefore, PXR activation can enhance the efflux of these drugs out of cancer cells, and as a result reduce the cytotoxicity (Pan et al., 2016; Pondugula et al., 2016). For instance, rifampicin treatment of colorectal cancer cells decreased the intracellular amount of MDR1 substrate doxorubicin (Harmsen et al., 2010). PXR activation can also enhance the metabolism of active drug to inactive metabolite. Chen et al. (2016) showed that PXR activation increased the metabolism of paclitaxel, which lead to enhanced resistance. Likewise, PXR activation by rifampicin treatment or by overexpression increased glucuronidation of SN38 to inactive metabolite SN38G, thereby decreasing the cytotoxicity of this active metabolite of irinotecan (Gupta et al., 2008; Raynal et al., 2010).

In addition to the induction of metabolism and efflux of cancer drugs, PXR activation elicits additional effects that can enhance tumor progression. For instance, in colon cancer cells PXR activation by rifampicin or using constitutive active PXR upregulated antiapoptotic genes BAG3, BIRC2 and MCL-1, whereas proapoptotic genes BAK1 and TP53 were downregulated (Zhou et al., 2008). Similarly in colon cancer cells, PXR activation by rifampicin enhanced cell proliferation and migration via upregulation of FGF19 (Wang et al., 2011). Pretreatment with

PXR agonist of prostate and breast cancer cells reduced the cytotoxicity of tested cancer drugs, including paclitaxel, while PXR knock down increased the sensitivity of cells for this drug (Chen et al., 2009, 2007). In the same way, PXR overexpression enhanced drug resistance and PXR ablation increased sensitivity of paclitaxel and cisplatin in endometrial cancer cells (Masuyama et al., 2007). Opposite effects, however, have also been observed. For example, in breast cancer cells PXR activation induced expression of proapoptotic genes BAX and BBC3 and reduced the cell growth (Verma et al., 2009). PXR overexpression also suppressed the cervical cancer cell growth and xenograft tumor growth in mice via causing G2/M cell cycle arrest (Niu et al., 2014). Similarly, PXR overexpression induced G0/G1 cell cycle arrest, which inhibited the growth of not only colon and liver cancer cells but also xenograft tumors in mice (Ouyang et al., 2010).

Oxidative stress caused by increased formation of reactive oxygen species (ROS) has been associated with several important parts of cancer formation such as carcinogenesis, angiogenesis, metastasis and cancer drug resistance (reviewed in Galadari et al., 2017). ROS has also been linked to tumor suppressive effects, including enhanced apoptosis, autophagy and increased sensitivity towards cancer drugs (Galadari et al., 2017). ROS can be formed as a byproduct in the CYP-mediated metabolism process (reviewed in Hrycay and Bandiera, 2015). As described above, PXR is a well-known regulator of CYP enzymes; therefore, PXR-induced xenobiotic metabolism could lead to formation of ROS and as a result promote tumor progression. In addition, PXR activation can sensitize to oxidative stress as was demonstrated with humanized PXR transgenic mice, which were more sensitive to the treatment with oxidative stress causing agent paraquat than wild-type (WT) mice (Gong et al., 2006). Similarly, WT mice treated with PXR agonist were more sensitive to paraquat than their vehicle-treated controls. The paraquat sensitive mice had reduced activities of ROS detoxifying enzymes: superoxide dismutase and catalase. Likewise, PXR overexpressing colon and liver cancer cells were sensitized to oxidative stress (Gong et al., 2006). The sensitized cells produced elevated amounts of ROS. Moreover, hPXR/CYP3A4 transgenic mice showed increased level of oxidative stress marker after co-treatment with rifampicin and ritonavir, which was not observed in null mice (Shehu et al., 2019). Conversely, Tanshinone IIA suppressed the oxidative stress damage and inflammatory response in human umbilical vein endothelial cells in a PXR-dependent manner (Zhu et al., 2017a). These controversies could be explained by the differences in experimental methods to induce oxidative stress and cell models. Even though PXR activation has been observed to sensitize to oxidative stress, PXR

activation has also demonstrated to reduce inflammation by inhibition of NF-KB (Deuring et al., 2019; Zhou et al., 2006b).

Not only several cancer drugs act as substrates for the PXR-induced metabolizing enzymes and transporters, but many cancer drugs also activate PXR (Table 2). These compounds, therefore, could enhance the development of cancer drug resistance via above described mechanisms.

Table 2. Examples of PXR-activating cancer drugs.

Cancer drug	Reference
Cisplatin	Masuyama et al., 2005
Cyclophosphamide	Harmsen et al., 2009
Docetaxel	Harmsen et al., 2010, 2009
Erlotinib	Harmsen et al., 2013, 2009
Flutamide	Harmsen et al., 2010, 2009
Gefinitib	Harmsen et al., 2013
Ifosfamide	Harmsen et al., 2010, 2009
Irinotecan/SN38	Basseville et al., 2011; Chen et al., 2010
Nilotinib	Harmsen et al., 2013
Paclitaxel	Harmsen et al., 2010; Masuyama et al., 2005
Sorafenib	Harmsen et al., 2013
Tamoxifen	Harmsen et al., 2010, 2009
Vandetanib	Harmsen et al., 2013

1.4. PXR antagonism in cancer drug resistance

Due to the putative role of PXR in tumor progression and cancer drug resistance, PXR antagonism has been suggested as a potential approach to attenuate these effects. This was recently shown with cisplatin-resistant liver cancer cells that displayed increased caspase-3 activity suggesting enhanced apoptosis after co-treatment of cisplatin with PXR antagonist leflunomide (Yasuda et al., 2019). Compared to the vast number of PXR agonists, the amount of PXR antagonists is few (Table 3). Not only a limited number of PXR antagonists are available, but also, many of these compounds are not specific or potent. Moreover, for most of these compounds the mechanism of antagonism is not comprehensively investigated (Chai et al., 2020). Antagonism can occur either by direct competitive binding with an agonist to the LBP or by binding to allosteric sites outside of LBP (Staudinger, 2019). For instance, SPA70 is a potent and specific PXR antagonist, which has been shown to bind to the LBP (Lin et al., 2017). SPA70 suppressed in primary human hepatocytes the expression of many PXR agonist-induced target genes. In addition, SPA70 increased the sensitivity to paclitaxel in PXR overexpressing colon cancer cells. Belinostat is a histone deacetylase inhibitor, which has already marketing authorization for the treatment of peripheral T-cell lymphoma (FDA, 2014). Not only belinostat repressed the PXR agonist-induced gene expression in primary human

hepatocytes, but also it reduced the PXR agonist-induced resistance towards SN38 (Abbott et al., 2019). Even though there is no direct experimental data confirming that belinostat directly interacts with the PXR LBP, molecular docking data implies that belinostat could directly bind to the LBP (Abbott et al., 2019). Other binding sites outside LBP, however, were also suggested. These included the AF-2 region and $\alpha 8$ pocket. Therefore, the exact mechanism of action of belinostat is unclear.

Table 3. PXR antagonists with their respective IC₅₀ values.

Compound	IC₅₀ (μM)	Reference
A-792611 (HIV-protease inhibitor)	2	Healan-Greenberg et al., 2008
Allyl isothiocyanate	-	Lim et al., 2015
Belinostat	-	Abbott et al., 2019
Camptothecin	0.58	Chen et al., 2010
Coumestrol	11.6	Wang et al., 2008
ET-743	0.003	Synold et al., 2001
Fucoxanthin	-	Liu et al., 2012
Isosilybin	74	Mooiman et al., 2013
Itraconazole	8.9	Ekins et al., 2008
Metformin	-	Krausova et al., 2011
(+)-2R,4S-Ketoconazole	5.6	Ekins et al., 2008
(-)-2S,4R-Ketoconazole	5.6	Ekins et al., 2008
Ketoconazole	9.7–13.4	Wang et al., 2007
Leflunomide	6.8	Ekins et al., 2008
Pazopanib	4.1	Burk et al., 2018
Pimecrolimus	1.2	Burk et al., 2018
Resveratrol	-	Deng et al., 2014
Sesamin	-	Lim et al., 2012
Silybin	135	Mooiman et al., 2013
SPA70	0.5	Lin et al., 2017
SPB03256	6.2	Ekins et al., 2008
SPB06061	5.2	Ekins et al., 2008
SPB06257	16.4	Ekins et al., 2008
R-/S-Sulforaphane	5.6	Ekins et al., 2008
Sulforaphane (racemate)	12	Zhou et al., 2007

1.5. Aims of the thesis

Cancer drug resistance is a major challenge in the treatment of cancer. This resistance is associated with several mechanisms, such as increased metabolism and efflux of cancer drugs and altered balance of apoptotic and survival proteins. PXR is involved in multitude of cellular processes related to cancer drug resistance. Not only PXR is well-known regulator of metabolizing enzymes and transporters, but also PXR activation has been shown to upregulate antiapoptotic and proliferation-related genes. Moreover, several cancer drugs have been demonstrated to activate PXR. Therefore, PXR antagonism has been proposed to be a potential approach to overcome cancer drug resistance. Challenges, however, remain to disclose the

validity of this approach. These include the limited number of PXR antagonists and insufficient knowledge about the consequences of PXR antagonism in relation to resensitization of drug-resistant cancer cells.

To address this, the aims of this work were the following:

- I. Generation and characterization of drug-resistant cancer cells.
- II. Investigate the role of PXR in cancer drug resistance.
- III. To disclose if PXR antagonism can resensitize cancer drug-resistant cells.
- IV. Identification and characterization of novel PXR antagonists.

To this end, cisplatin- and irinotecan-resistant LS174T cells were generated and characterized in respect to their growth properties and gene expression. Furthermore, the role of PXR in regulation of resistance-associated genes was investigated by activating and antagonizing PXR. Finally, PXR antagonism was utilized at aiming to resensitize drug-resistant cancer cells. To meet the need for more PXR antagonists, compounds from Tübingen Kinase Inhibitor Collection (TüKIC) compound library were investigated in respect to their potential for PXR antagonism. Then, the potential PXR antagonists were characterized in more detail.

2. Material

Table 4. Chemicals and reagents.

Chemicals and reagents	Company
1 α ,25-dihydroxy vitamin D ₃	Sigma-Aldrich, Taufkirchen, Germany
Adenosine 5'-triphosphate (ATP)	Alfa Aesar, Kandel Germany
Bicinchoninic acid	Sigma-Aldrich, Taufkirchen, Germany
Bromophenol blue	Fluka, Buchs, Switzerland
β -mercaptoethanol	Sigma-Aldrich, Taufkirchen, Germany
Calcium chloride	Sigma-Aldrich, Taufkirchen, Germany
Cisplatin	Selleckchem, Houston, TX, USA
CITCO	ENZO Life Sciences, Lörrach, Germany
Coelenterazine	Biotium, Hayward, CA, USA
Coenzyme A	Cayman Chemical, Ann Arbor, MI, USA
4% Copper(II) sulfate	Sigma-Aldrich, Taufkirchen, Germany
Dextran 70	Amersham Biosciences, Little Chalfont, UK
Dimethylsulfoxide (DMSO)	Sigma-Aldrich, Taufkirchen, Germany
1,4-Dithiotreitol (DTT)	Roth, Karlsruhe, Germany
DMEM	Thermo Fischer Scientific, Waltham, MA, USA
EDTA	Sigma-Aldrich, Taufkirchen, Germany
Ethidiumbromide	Roth, Karlsruhe, Germany
Fetal bovine serum (FBS)	Biowest, Nuaille, France
Ficoll	Roth, Karlsruhe, Germany

Formaldehyde	Sigma-Aldrich, Taufkirchen, Germany
Formamide	Sigma-Aldrich, Taufkirchen, Germany
Glycerol	Sigma-Aldrich, Taufkirchen, Germany
Glycine	Merck, Darmstadt, Germany
Halt protease inhibitor cocktail	Thermo Fischer Scientific, Waltham, MA, USA
HEPES	Roth, Karlsruhe, Germany
Irinotecan HCl trihydrate	Selleckchem, Houston, TX, USA
jetPEI	Polyplus, Illkirch, France
jetPRIME	Polyplus, Illkirch, France
KCl	Merck, Darmstadt, Germany
KH ₂ PO ₄	Roth, Karlsruhe, Germany
L-glutamine	Biozym, Niedersachsen, Germany
Lipofectamine RNAiMAX	Thermo Fischer Scientific, Waltham, MA, USA
Luciferin	PanReac AppliChem, Darmstadt, Germany
MEM	Thermo Fischer Scientific, Waltham, MA, USA
MgCl ₂	Sigma-Aldrich, Taufkirchen, Germany
MOPS	Merck, Darmstadt, Germany
Na ₂ HPO ₄ x 2 H ₂ O	Fluka, Buchs, Switzerland
100x Non-Essential Amino Acids	Biozym, Niedersachsen, Germany
Norit A (active coal)	Serva, Heidelberg, Germany
NP-40	Roche Diagnostics, Mannheim, Germany
Opti-MEM	Thermo Fischer Scientific, Waltham, MA, USA
5x Passive lysis buffer	Promega, Madison, WI, USA
Penicillin/streptomycin	Biozym, Niedersachsen, Germany
Phenylmethylsulfonyl fluoride (PMSF)	Sigma-Aldrich, Taufkirchen, Germany
10x Phosphate buffered saline	Biozym, Niedersachsen, Germany
2x qPCR Master Mix	Eurogentec, Liège, Belgium
Rifampicin	Tocris Bioscience, Bristol, UK
RPMI 1640	Thermo Fischer Scientific, Waltham, MA, USA
Skim milk powder	Merck, Darmstadt, Germany
Sodium acetate	Roth, Karlsruhe, Germany
Sodium chloride	Merck, Darmstadt, Germany
Sodium deoxycholate	Sigma-Aldrich, Taufkirchen, Germany
Sodium orthovanadate	Sigma-Aldrich, Taufkirchen, Germany
Sodium pyruvate	Biozym, Niedersachsen, Germany
SPA70	Axon Medchem, Groningen, Netherlands
SR12813	Tocris Bioscience, Bristol, UK
SuperSignal West Dura Extended Duration Substrate	Thermo Fischer Scientific, Waltham, MA, USA
2x TaqMan™ PreAmp Master Mix	Thermo Fischer Scientific, Waltham, MA, USA
TRIS base	Roth, Karlsruhe, Germany
TRIS Cl	Roth, Karlsruhe, Germany
Trypsin-EDTA	Thermo Fischer Scientific, Waltham, MA, USA
TWEEN 20	Sigma-Aldrich, Taufkirchen, Germany

Table 5. Culture mediums for cell lines.

Cell line	Final concentration	Components
HepG2		MEM
	10%	FBS
	2 mM	L-glutamine
	100 U/ml	Penicillin
	100 µg/ml	Streptomycin
LS174T / Huh7		DMEM
	10%	FBS
	2 mM	L-glutamine
	100 U/ml	Penicillin
	100 µg/ml	Streptomycin
	1%	100x Non-Essential Amino Acids
LoVo	1 mM	Sodium pyruvate
		RPMI 1640
	10%	FBS
	100 U/ml	Penicillin
	100 µg/ml	Streptomycin
	1%	β-mercaptoethanol
	10 µM	HEPES pH 7.2
	1 mM	Na-pyruvate
	2 mM	Glutamine
	0.6%	100x Non-Essential Amino Acids
LS174T freezing medium	0.02 mg/ml	Asparagine
	5%	Culture medium DMSO

Table 6. Plasmids.

Plasmids	Reference
pcDNA3	Thermo Fischer Scientific, Waltham, MA, USA
pcDhuCAR1	Burk et al., 2002
pcDhuCAR3	Burk et al., 2002
pcDhuPXR	Geick et al., 2001
pcDhuPXR(Q285A)	See section 3.2.
pcDhuPXR(Y306A)	See section 3.2.
pcDhuPXR(S247A)	See section 3.2.
pcDhuPXR(H407A)	See section 3.2.
pcDhuPXR(W299A)	See section 3.2.
pcDhuPXR(H327A)	See section 3.2.
pcDhu-sPXR	Jeske et al., 2017
pcDhuPXR(S208W/S247W/C284W)	Burk et al., 2018
pcDhuRXRα(orf)	Mathäs et al., 2012
pcDhuVDR	Burk et al., 2005
pGL3(DR3) ₃ Tk	Hustert et al., 2001
pGL4-CYP3A4(-7830Δ7208-364)	Burk et al., 2018
pGL4-G5	Arnold et al., 2004
pMetLuc2Control	Takara-Clontech, Mountain View, CA, USA
pM-SRC1(583-783)	Arnold et al., 2004
pM-SMRT(1109-1330)	Burk et al., 2005

pVP16-PXR(108-434)
pGL4.75[hRLuc/CMV]

Burk et al., 2005
Promega, Madison, WI, USA

Table 7. Antibodies.

Antibodies	Final concentration in WB	Company
Mouse monoclonal anti-PXR, H4417	2 µg/ml in 1% MM-TBS-T	Perseus Proteomix Inc., Tokyo, Japan
Mouse monoclonal anti-TBP, mAbcam 51841	2 µg/ml in 1% MM-TBS-T	Abcam, Cambridge, UK
Rabbit polyclonal anti-mouse / HRP-conjugate, Dako P0260	0.13 µg/ml in 5% MM-TBS-T	Dako, Glostrup, Denmark

Table 8. Kits.

Kit	Company
CellTiter-Glo Luminescent Cell Viability assay	Promega, Madison, WI, USA
FLEX Six™ Gene Expression Kit FLEX Six™ Gene Expression IFC Control Line Fluid for 96.96 IFCs 2x Assay Loading Reagent 20x GE Sample Loading Reagent	Fluidigm, South San Francisco, CA, USA
48.48 Gene Expression Kit 48.48 Gene Expression IFC Control Line Fluid for 48.48 IFCs 2x Assay Loading Reagent 20x GE Sample Loading Reagent	Fluidigm, South San Francisco, CA, USA
NucleoSpin RNA Kit	Macherey-Nagel, Düren, Germany
PureYield Plasmid Midiprep System	Promega, Madison, WI, USA
Q5 Site-Directed Mutagenesis Kit	New England Biolabs, Ipswich, MA, USA
TaqMan Reverse Transcription kit MgCl ₂ Multiscribe Reverse Transcriptase 50 U/µl Random hexamers 50 µM RNase inhibitor 20 U/µl 10x TaqMan RT Buffer	Thermo Fischer Scientific, Waltham, MA, USA

Table 9. Primers and probes for qPCR.

Assay	Location (concentration)	Sequence (5' to 3')
18S	Forward (400 nM)	ACC GCA GCT AGG AAT ATT GGA
	Reverse (400 nM)	GCC TCA GTT CCG AAA ACC A
	Probe (200 nM)	FAM-ACC GCG GTT CTA TTT-MGB
CYP2B6	Forward (400 nM)	GCT GAA CTT GTT CTA CCA GAC TTT TTC
	Reverse (400 nM)	GAA AGT ATT TCA AGA AGC CAG AGA AGA
	Probe (400 nM)	FAM.TGT ATT CGG CCA GCT GT-MGB/NFG
PXR1	Forward (400 nM)	TCC TTT GCA CCG GAT TGT TC
	Reverse (400 nM)	TCC AGC TTT CTT TGG GTC TCA
	Probe (200 nM)	FAM-CAC CAA GCA GTC CAA GA-MGB
PXR2	Forward (400 nM)	AGTGCTGCGGCTGAGTTGG
	Reverse (400 nM)	TCTTTGGGTCTCACCTCCAGG
	Probe (200 nM)	FAM-TTCAAACCATCCAAGAGGCCAGAA-TAMRA
sPXR	Forward (900 nM)	TCT GCT GCC TTG AGA GGG TTA
	Reverse (900 nM)	CCC TGT CCG TTC ACT TTT CTT C
	Probe (250 nM)	FAM-CCC TGC AGT GAT CA-MGB

Table 10. Commercial predesigned gene expression assays (Thermo Fischer Scientific).

Gene	Assay ID	Exon/exon	Ref Seq	Context sequence	Location	Amplicon size	
ABCA2	Hs00242232	m1	10/11	NM_001606	GTCATCCTCAAGGCCAACGAGACTT	1574	58
ABCB1	Hs00184500	m1	6/7	NM_000927	AGACATGACCAGGTATGCCTATTAT	832	67
ABCB11	Hs00994811	m1	16/17	NM_003742	CATAAAGGATGCAACTGAAGATGAC	2142	77
ABCC1	Hs01561483	m1	11/12	NM_004996	CAAGACGTATCAGGTGGCCACATG	1648	65
ABCC2	Hs00166123	m1	25/26	NM_000392	CTCCAACAGGTGGCTTGCAATTCGC	3757	75
ABCC3	Hs00978452	m1	11/12	NM_003786	GCCTTCCAGGTAAAGCAAATGAAAT	1515	64
ABCC4	Hs00988717	m1	6/7	NM_005845	CATCACTGAGGAGTAAAACCTGCAAC	920	63
ABCC5	Hs00981089	m1	4/5	NM_005688	ACTGCAGAAGACTAGAGAGACTGTG	632	68
ABCG2	Hs01053790	m1	3/4	NM_004827	GGAGGCAAATCTTCGTTATTAGATG	755	83
ALDH1A1	Hs00946916	m1	8/9	NM_000689	GCCGACTTGGACAATGCTGTTGAAT	1173	61
AKR1B10	Hs01546975	gH	9/10	NM_020299	AACGTGTTGCAATCCTCTCATTTGG	1230	75
ATP7A	Hs00163707	m1	12/13	NM_000052	GTCCCTCATCACAGGGGAGGCAATG	2826	88
ATP7B	Hs00163739	m1	4/5	NM_000053	CATTGAGCTGACAATCACAGGGATG	1864	83
BAG3	Hs00188713	m1	1/2	NM_004281	AGGGCCCCAAGGAGACTCCATCCTC	488	83
BAK1	Hs00832876	g1	6	NM_001188	CTAAGCATGTGTCCAGGAGCAGGA	1465	176
BAX	Hs00180269	m1	3/4	NM_001291429	CTGGTGCTCAAGGCCCTGTGCACCA	387	62
BBC3	Hs00248075	m1	3/4	NM_014417	GAGCGGCGGAGACAAGAGGAGCAGC	750	101
BCL2	Hs04986394	s1	2	NM_0006332	GGAGGAGCTCTTCAGGGACGGGGTG	907	73
BCL2L1	Hs00236329	m1	2/3	NM_001317920	GAACGGCGGCTGGGATACTTTTGTG	812	65
BIRC2	Hs01112284	m1	5/6	NM_001256166	GCTGACCCACCAATTATTCATTTTG	1172	84
CDKN1A	Hs00355782	m1	2/3	NM_001220778	GCAGACCAGCATGACAGATTTCTA	676	66
CES1	Hs00275607	m1	8/9	NM_001025195	GAGACCCCAGAGAGAGTCAACCCCT	1052	95
CES2	Hs01077945	m1	2/3	NM_003869	CCCATCCGGCCATGTGTCTACAGGG	NA	90
CYP1A1	Hs00153120	m1	1/2	NM_000499	AGCTCAGTACCTCAGCCACCTCCAA	168	91
CYP1A2	Hs00167927	m1	2/3	NM_000761	GGACTTTGACAAGAACAGTGTCCGG	895	67
CYP3A4	Hs00604506	m1	2/3	NM_017460	ATTTTGTCTACCATAAGGGCTTTT	267	119
CXCR4	Hs00976734	m1	1/2	NM_003467	AGGGGATCAGTATATACACTTCAGA	112	79
EGFR	Hs01076090	m1	5/6	NM_005228	ACTGCCAGAACTGACCAAAATCAT	875	57
ERCC1	Hs01012158	m1	4/5	NM_001983	CCTGTTCTCAGCCTCCGCTACCAC	572	55
FGF19	Hs00192780	m1	2/3	NM_005117	TGCAGGGGCTGCTTCAGTACTCGGA	801	54
GADD45A	Hs00169255	m1	2/3	NM_001199741	CGTGCTGGTGACGAATCCACATTCA	600	123
GADD45B	Hs00169587	m1	2/3	NM_015675	AGTTGATGAATGTGGACCCAGACAG	380	74
GSTA1	Hs07292901	gH	6/6	NM_001319059	AATTAATAATAACAACCTCCTATTTCG	888	141
GSTP1	Hs00943350	g1	3/4	NM_000852	No info provided	391	67

MCL1	Hs01050896	m1	2/3	NM_021960	TAAACAAAGAGGCTGGGATGGGTTT	1141	89
MSH2	Hs00953527	m1	6/7	NM_000251	AACAGAATAGAGGAGAGATTGAATT	1197	71
NFKB1	Hs00765730	m1	22/23	NM_001319226	ACAACATATGAGGCTCTGGGGGTAC	2868	66
NR0B2	Hs00222677	m1	1/2	NM_021969	TCAACCCCGATGTGCCAGGCCTCCA	672	87
NR1H4	Hs01026596	m1	6/7	NM_005123	CAAAGTCATGCAGGGAGAAAAGTGA	1195	112
NR1I2	Hs01114267	m1	8/9	NM_003889	GCCCCAGCCTGCTCATAGGTTCTTG	2994	103
OLFM4	Hs00197437	m1	4/5	NM_006418	TCCCACTCCAGGGAGCTGTGGTCAT	828	85
PRAMEF10	Hs04185201	m1	1/2	NM_001291381	AGTCCAGATCTGAGTTTTTCCTCGG	49	66
PRAMEF17	Hs01685002	g1	2/3	NM_001099851	ACCTGCTCAGGTGCCTCAAGAACCC	895	163
SLC10A1	Hs00161820	m1	1/2	NM_003049	GGACATGAACCTCAGCATTGTGATG	488	68
SLC10A2	Hs01001557	m1	5/6	NM_000452	TCTTAGGATTTTTATGTGGCATAACA	1520	81
SLC22A1	Hs00427552	m1	6/7	NM_003057	GTACCTGTGGTTCACGGACTCTGTG	1170	79
SLC31A1	Hs00741015	m1	1/2	NM_001859	ACTTGACCTGGAAAAGAATCTTCTGC	149	151
SLC31A2	Hs00156984	m1	2/3	NM_001860	TCCTGCTGGCATGGCCCTTTCGGTG	195	70
SLCO1B1	Hs00272374	m1	14/15	NM_006446	AATTCCACATCATTTTCAAGGGTCT	1965	77
SLCO2B1	Hs00200670	m1	7/8	NM_007256	TGCCAGGAAGGGCAAGGACTCTCCC	1370	113
TBP	Hs00427620	m1	2/3	NM_001172085	GCAGCTGCAAAAATATTGTATCCACA	578	91
TOP1	Hs00243257	m1	13/14	NM_003286	TTCACGAATCAAGGGTGAGAAGGAC	1554	101
TP53	Hs01034249	m1	10/11	NM_000546	GCTCACTCCAGCCACCTGAAGTCCA	1304	108
UGT1A1	Hs02511055	s1	1	NM_000463	TTCAGAGAGAGGTGACTGTCCAGGA	740	134
UGT1A9	Hs02516855	sH	1	NM_021027	CGTGGTCTTCGCCAGGGGAATACTT	544	113

Table 11. Buffers and solutions.

Buffer / solution	Final Concentration
Blotting buffer	
TRIS base	25 mM
Glycine	192 mM
Denatured ethanol	20%
Buffer A	
HEPES-KOH pH 7.9	10 mM
KCl	10 mM
MgCl ₂	1.5 mM
DTT	1 mM
HALT protease inhibitor cocktail	1x
PMSF	0.5 mM
Buffer A + NP-40	
HEPES-KOH pH 7.9	10 mM
KCl	10 mM
MgCl ₂	1.5 mM
DTT	1 mM
HALT protease inhibitor cocktail	1x
PMSF	0.5 mM
NP-40	0.4%
Buffer B	
HEPES-KOH pH 7.9	20 mM
NaCl	420 mM
MgCl ₂	1.5 mM
DTT	1 mM
EDTA pH 8.0	0.2 mM
HALT protease inhibitor cocktail	1x
PMSF	0.5 mM
Coomassie-staining solution	
Coomassie Brilliant Blue	0.125%
Ethanol	45%
Acetic acid	10%
Fixing/destaining solution	
Ethanol	9%
Acetic acid	6%
2x HBS	
NaCl	280 mM
Na ₂ HPO ₄ x 2 H ₂ O	1.5 mM
HEPES	50 mM
1x MOPS buffer	
MOPS	20 mM
Sodium acetate	5 mM
EDTA	1 mM
1x PBS	
NaCl	137 mM
KCl	2.7 mM
Na ₂ HPO ₄ x 2 H ₂ O	4.3 mM
KH ₂ PO ₄	1.4 mM
Protein lysis buffer	
HEPES-KOH pH 7.9	50 mM
NaCl	150 mM
EDTA	1 mM

Sodium fluoride	20 mM
Sodium orthovanadate	2 mM
B-glycerolphosphate	10 mM
Triton-X-100	1%
Glycerol	10%
Sodium butyrate	10 mM
Sodium dodecyl sulfate	0.1%
Sodium deoxycholate	0.5%
Halt Protease Inhibitor cocktail	1x
PMSF	1 mM
5x Protein sample buffer (5x Lämmli)	
SDS	10 mM
1 M TRIS-HCl pH 6.8	312.5 mM
β-Mercaptoethanol	25%
Glycerol	20%
Bromophenol blue	0.1%
RNA color marker	
Ficoll	10%
Bromophenol blue	0.1%
RNA sample buffer	
Formamide	50%
Formaldehyde	2.2 M
1x MOPS pH 7.0	
Reaction-Injection-Mix (RIM+)	
Luciferin	0.05 mM
ATP	2 mM
MgCl ₂	10 mM
Coenzyme A	0.027 mM
DTT	30 mM
Glycylglycine ph 7.8	25 mM
Renilla Luciferase Assay Buffer	
Coelenterazine	1 μM
Tris-Cl pH 7.5	25 mM
NaCl	100 mM
CaCl ₂	1 mM
1x Running buffer for protein electrophoresis	
TRIS Base	25 mM
Glycine	192 mM
SDS	0.1%
Smith reagent	
Bicinchoninic acid	98%
4% Copper(II) sulfate	2%
1x TAE	
TRIS Base	40 mM
Acetic Acid	0.4 mM
EDTA	1 mM
TBS-T	
NaCl	137 Mm
KCl	2.68 Mm
TRIS Base	0.03%
TRIS-Cl	0.27%
TWEEN-20	0.1%

Table 12. Instruments.

Instrument	Company
Autolumat Plus LB953	Berthold, Bad Wildbad, Germany
Bioruptor UCD200	Diagenode, Liège, Belgium
CR35 Bio radioluminography	Raytest, Straubenhardt, Germany
EnSpire Multimode Plate Reader	PerkinElmer, Waltham, MA, USA
Fluidigm BioMark HD System	Fluidigm, South San Francisco, CA, USA
Heidolph Titramax 101	Heidolph Instruments, Schwabach, Germany
Nanodrop UV-VIS Spectrophotometer	Thermo Fischer Scientific, Waltham, MA, USA
7900 Real Time PCR System	Applied Biosciences, Foster City, CA, USA
STELLA 3200	Raytest, Straubenhardt, Germany

3. Methods

3.1. Cell culture

All cells were cultured at 37°C and 5% CO₂. Mediums were changed every two to three days, unless otherwise stated. Cells were passaged when they reached $\geq 70\%$ confluency. For passaging, cells were washed with 1x phosphate buffered saline (PBS) and 0.25% trypsin-EDTA was added before incubation for 5-8 min at 37°C and 5% CO₂. Trypsinization was stopped with medium and cell suspension was centrifuged at 235 g for 5 min. After centrifugation, supernatant was aspirated, and cell pellet was resuspended with medium. Depending on cell line, split ratio was adjusted accordingly, and cells were seeded on a new dish. When necessary, cells were counted with Neubauer cell counting chamber.

Human hepatocellular carcinoma HepG2 cells (HB-8065, lot number 58341723, ATCC, Manassas, VA, USA) and stably transfected HepG2 cells with PXR overexpression (HP cells) were cultivated in Minimal Essential Media (MEM)-based culture medium (Table 5). Duke's type B colorectal adenocarcinoma LS174T cells (ATCC, Manassas, VA, USA) and human hepatocellular carcinoma Huh7 cells (Gift from U. Brinkmann, Epidauros) were cultivated in Dulbecco's Modified Eagles Medium (DMEM)-based culture medium (Table 5). Duke's type C colorectal adenocarcinoma LoVo (Gift from N. Janssen, IKP) cells were cultivated in Roswell Park Memorial Institute (RPMI 1640)-based culture medium (Table 5). FBS was replaced by dextran-charcoal-stripped FBS in drug treatments.

Parental HepG2 cells were propagated at passage 74 and used in the experiments between passages 90 and 118. HP cells were used up to passage 30 after validation of clones. LS174T cells were obtained at passage 104, which was then re-set as 1 and used in the experiments between passages 8 and 30. In addition, as a control to minimize the effects of culture duration, LS174T cells were cultured as long as resistant cells up to passage 64. Huh7 cells were obtained

and assigned as passage 1 and used in the experiment at passage 16. LoVo cells were obtained and assigned as passage 1 and used in the experiment at passage 7.

For absolute copy number determination of PXR variants in different cell lines, $0.3\text{--}0.75 \times 10^6$ HepG2, Huh7, LoVo and LS174T cells per well in a volume of 2 ml in 6-well plate were seeded and cultured in culture medium for 2 to 4 days before cell harvesting and RNA isolation as described above in section 3.7. Absolute copy number quantification was conducted as described in section 3.9.

For investigation of effects of rifampicin, cisplatin, irinotecan and SN38 on gene expression of established PXR target genes, 1×10^6 LS174T cells were seeded in a volume of 2 ml in a 6-well plate. Then on next day cells were treated with 0.2% DMSO, 10 μM rifampicin, 10 μM cisplatin, 1.5 μM irinotecan or 25 nM SN38 for 72 h before cell harvesting and RNA isolation as described in section 3.7. Medium was changed every 24 h. Relative quantification analyses were conducted as described in section 3.9.

For investigation of PXR dependency on expression of rifampicin-induced established PXR target genes, 1×10^6 LS174T cells were seeded in a volume of 2 ml in a 6-well plate. Then on next day cells were treated with 0.2% DMSO, 10 μM rifampicin, 10 μM SPA70, or 10 μM rifampicin and 10 μM SPA70 for 72 h before cell harvesting and RNA isolation as described in section 3.7. Medium was changed every 24 h. Relative quantification analyses were conducted as described in section 3.9.

For investigation of gene expression in cisplatin-resistant LS174T cells (Ls-R-C), irinotecan-resistant LS174T cells (Ls-R-I) and equally long cultured parental LS174T cells (Ls-P), 0.4×10^6 cells were seeded in a volume of 1 ml in a 12-well plate in two wells per cell line. Ls-R-C cells were cultured in 30 μM cisplatin-containing culture medium, Ls-R-I cells in 40 μM irinotecan-containing culture medium and Ls-P cells in drug-free culture medium until nearly confluency. Then one well was harvested as described in section 3.7 and the other well was passaged into two new wells. Relative quantification analyses were conducted as described in section 3.9.

For investigation of effect of PXR activation and inhibition on expression of cancer drug resistance-associated genes in Ls-P, Ls-R-C and Ls-R-I cells, 0.6×10^6 cells were seeded in a volume of 1 ml in a 12-well plate. Then on next day cells were treated with 0.2% DMSO, 10 μM rifampicin, 10 μM SPA70, or 10 μM rifampicin and 10 μM SPA70 for 48 h before cell

harvesting and RNA isolation as described in section 3.7. Medium was changed every 24 h. Relative quantification analyses were conducted as described in section 3.9.

For investigation of the effect of selected TüKIC compounds on gene expression, 0.3×10^6 or 0.6×10^6 (for compound 109) LS174T cells were seeded in a volume of 1 ml in a 12-well plate. Then on next day, cells were treated with 0.1–0.2% DMSO, 10 μ M RIF, 10 μ M of compounds 12/73/100 for 72 h and compound 109 for 48 h or co-treated with 10 μ M RIF and 10 μ M compounds 12/73/100 for 72 h before cell harvest and RNA isolation as described in section 3.7. Relative quantification analyses were conducted as described in section 3.9.

3.2. Preparation of plasmids

Site-directed mutagenesis of the full-length PXR expression plasmid with suitable oligonucleotides designed with NEBaseChanger using Q5 Site-Directed Mutagenesis kit (New England Biolabs, Ipswich, MA, USA) was utilized to generate PXR mutants Q285A, Y306A, S247A, H407A, W299A and H327A. The mutations were confirmed by sequencing. Plasmids were purified using PureYield Plasmid Midiprep System (Promega, Madison, WI, USA).

3.3. Generation of drug-resistant cancer cells

Cisplatin-resistant (Ls-R-C) and irinotecan-resistant (Ls-R-I) LS174T cells were generated by continuous exposure of LS174T cells to cisplatin (Table 13) or irinotecan (Table 14) by gradually increasing the concentration in a stepwise manner during approximately five to seven months. The cells were passaged 3–5 times at each concentration. At every concentration increase, cells were frozen as back up. Cells were trypsinized as described in section 3.1., after centrifugation and aspiration of supernatant; cell pellet was resuspended in freezing medium (Table 5). Cells were aliquoted in 1 ml sterile Nalgene cryovials (Thermo Fischer Scientific, Waltham, MA, USA) and placed in -80°C for at least 48 h before long-term storage in liquid nitrogen. When necessary, cells were thawed quickly in 37°C water bath, transferred in culture medium, centrifuged (at 235 g, 5 min) and resuspended in culture medium before seeding on a dish. Cells were cultured for 2–3 passages before used in the experiments for up to one month after thawing.

Before subsequent experiments, cells were cultured in a drug-free culture medium for at least five days. Ls-P cells were cultured parallel in drug-free culture medium the same duration as resistant cells were generated. After generation of resistance, Ls-R-C cells and Ls-R-I were cultivated in maintenance concentration of 30 μ M cisplatin and 40 μ M irinotecan, respectively,

until characterization including confirmation of resistance after selection, long-term stability, freeze-thaw stability and growth analysis, was completed.

Table 13. Cisplatin concentrations used for generating resistant cells.

Concentration of cisplatin	Drug exposure (passages)	Drug exposure (days)
10 μ M	5	52
15 μ M	3	116
20 μ M	3	27
30 μ M	3 + maintaining	21 + maintaining

Table 14. Irinotecan concentrations used for generating resistant cells.

Concentration of irinotecan	Drug exposure (passages)	Drug exposure (days)
1 μ M	4	67
1.5 μ M	3	8
2.5 μ M	3	11
5 μ M	4	19
10 μ M	3	13
20 μ M	3	16
40 μ M	3 + maintaining	15 + maintaining

3.4. Cell viability determination

For cell viability determination Ls-P, Ls-R-C and Ls-R-I cells were seeded at density of 8,000 cells per well in 100 μ l in a Greiner (#655098) white, clear flat bottom CellStar 96-well plate (Greiner Bio-One GmbH, Frickenhausen, Germany). On following day, cells were treated with increasing cisplatin (0.3–1,000 μ M), irinotecan (0.3–1,000 μ M) or paclitaxel (1–3,000 nM) concentrations. Treatment medium was changed every 24 h. After 72 h of exposure, cell viabilities were determined by quantifying ATP content with CellTiter-Glo Luminescent Cell Viability Assay according to the manufacturer’s instructions (Promega, Madison, WI, USA). Briefly, plate was equilibrated at room temperature for 30 min. Then 100 μ l of CellTiter-Glo Reagent was added to each well. Mixture was incubated on an orbital shaker (450 rpm, Heidolph Titramax 101) for 2 min while protected from light. Before luminescence measurement, cell lysates were incubated at room temperature for 10 min while protected from light. Luminescence was measured using EnSpire multimode plate reader with a 0.1 second measurement time (PerkinElmer, Waltham, MA, USA). After subtracting background, cell viability was calculated in percent by dividing the value of treated cells by the value of DMSO-treated control cells. Experiment was conducted three times independently with technical triplicates. Log concentrations were plotted to cell viability percentages and mean

IC₅₀ was determined using nonlinear regression with GraphPad Prism version 8.3.0 for Windows (GraphPad Software, San Diego, California, USA).

For determination of long-term stability of resistance, Ls-R cells were cultured in drug-free medium for one month. Then cells were seeded in a Greiner (#655098) white, clear flat bottom CellStar 96-well plate (Greiner Bio-One GmbH), treated with increasing concentrations of cisplatin or irinotecan and cell viability was determined as described above. Ls-P cells that had been maintained for the same time from beginning were used as controls to minimize effects caused by culture duration.

For determination of resistance stability of Ls-R cells after freezing and thawing, Ls-R and Ls-P cells were frozen as described above. After keeping cells in liquid nitrogen for 72 h, cells were thawed and cultured for 3–4 passages. Ls-P and Ls-R-I cells were cultured in drug-free culture medium, whereas Ls-R-C cells were cultured in culture medium containing 30 µM cisplatin due to the possible reduction of resistance, if cultured in drug-free medium for longer time. Ls-R-C cells were cultured in drug-free culture medium for five days before cell viability determination as described above.

To assess the cellular toxicity of TüKIC compounds, HepG2 cells were seeded at density of 40,000 cells per well in 100 µl in a Greiner (#655098) white, clear flat bottom CellStar 96-well plate (Greiner Bio-One GmbH). On following day, cells were treated with 3, 10 or 30 µM of test compounds. After 24 h, cell viabilities were determined as described above.

3.5. Growth analysis

For growth analysis, 0.4×10^6 Ls-P, Ls-R-C and Ls-R-I cells per well were seeded in a volume of 2 ml in 6-well plate (Sarstedt, Nümbrecht, Germany). Cells were manually counted every 24 h for 4 days. Drug-free culture medium was changed every second day. Doubling time was calculated at the exponential growth phase with following formula: Doubling time = $h \times \ln(2)/\ln(c_2/c_1)$, where c_1 is the amount of cells in the beginning and c_2 amount of cells in the end of the exponential growth phase (Jensen et al. 2015). Experiment was conducted three times.

3.6. Resensitization of drug-resistant cells

Ls-R-I cells were cultured in a dish with 6 cm diameter and treated with 0.1% DMSO or 10 µM SPA70 for 48 h. Medium was changed every day. At 48 h, cells were trypsinized and cells were seeded at density of 10,000 cells per well in 100 µl in a Greiner (#655098) white, clear flat bottom CellStar 96-well plate (Greiner Bio-One GmbH) supplemented with 0.1% DMSO

or 10 μ M SPA70. After 24 h, cells were treated with increasing concentrations of irinotecan (0.3 μ M–1,000 μ M) or paclitaxel (1–3,000 nM) with or without 10 μ M SPA70. After 72 h, cell viabilities were determined using CellTiter-Glo Luminescent Cell Viability Assay (Promega) as described in section 3.4. Experiment was conducted three times independently with technical triplicates.

3.7. RNA isolation and determination of RNA concentration

Total RNA was isolated with the NucleoSpin RNA kit (Machery-Nagel, Düren, Germany). Briefly, cells were lysed by adding 350 μ l of buffer RA1 supplemented with 3.5 μ l β -mercaptoethanol and scraped. Cell lysates were stored at -80°C until RNA isolation. The viscosity of thawed cell lysates was reduced by filtering. Before binding the RNA to the column, the binding conditions were adjusted with ethanol. After RNA binding, silica membrane was desalted, and DNA was digested on-column with rDNase. Then after three washing steps and drying of the column, RNA was eluted with 40 μ l of RNase free water.

UV-VIS spectrophotometer Nanodrop (Thermo Fischer Scientific) was used for the determination of RNA concentration. RNA concentration was determined based on the absorbed light. The more the sample absorbs light the higher is the optical density (OD), which reflects the RNA concentration. The amount of RNA was calculated using following equation: RNA (μ g/ μ l) = OD₂₆₀ * 40 (factor for RNA). The purity was determined using the ratio A₂₆₀ nm / 280 nm. Value of approximately 2 reflects pure RNA.

3.8. Test for RNA quality

RNA quality was assessed using characteristic separation of RNA into ribosomal 18S and approximately twice as strong band of ribosomal 28S on agarose gel. RNA samples were adjusted to the amount of 1 μ g and to a volume of 16 μ l with RNA sample buffer. Then 0.6 μ l of 0.025% ethidium bromide solution was added to the RNA solution. After incubation for 10 min at 65°C, samples were placed on ice, 4 μ l RNA color marker was added, and samples were loaded onto 1% agarose gel with 1x MOPS buffer. Electrophoresis was conducted with 125 V for approximately 30 minutes.

3.9. Quantitative real-time PCR analysis

Primers and probe were designed to sPXR mRNA with ABI Primer Express software (version 3.0.1, Applied Biosciences, Foster City, CA, USA). Specificity of the primers and probe were analyzed using the basic logarithmic alignment tool (BLAST) by National Center for Biotechnological Information (NCBI). In addition, primers and probe were checked for their

ability to form hairpins, secondary structures or cross dimers with OligoEvaluator by Sigma-Aldrich and Multiple Primer Analyzer by Thermo Fischer Scientific. Different primer and probe concentrations were tested to obtain as sensitive and specific assay as possible. In the assay establishment, qPCR products were always analyzed also in agarose gel with 1x TAE. The assay specificity was determined using cDNA plasmid of PXR1 variant, which the assay did not detect. In addition, using excess PXR1 cDNA plasmid over sPXR, assay demonstrated specificity towards sPXR.

TaqMan reverse transcription reagents (Thermo Fischer Scientific) were utilized to synthesize first strand cDNA according to manufacturer's instructions from either 0.25 µg or 0.32 µg of total RNA with 1x RT buffer, 5.5 mM MgCl₂, 0.5 mM each dNTP, 2.5 µM random hexamer primers, 0.4 units/µl RNase inhibitor and 1.25 units/µl multiscribe reverse transcriptase in a total volume of 25 µl or 16 µl.

cDNA samples corresponding to 0.25 µg RNA were 1:2 diluted with nuclease-free water and quantified with 7900 HT Real-time PCR system (Applied Biosciences) with following thermal cycling parameters 10 min at 95°C, 40 cycles 15 sec at 95°C/1 min at 60°C. PCR reactions were set up with cDNA corresponding to 2 pg (18S rRNA) or 10 ng (all other assays) of total RNA and 1x qPCR Master Mix (Eurogentec, Liège, Belgium) and specifically designed primers/probes (Table 9). For absolute copy number determination, serial dilutions of plasmids containing respective PXR variants were used for generating standard curves ranging from 12 to 12x10⁶ copies with following performance: PXR1 (slope: -3.62, R²: 0.994, efficiency: 88.7%), PXR2 (slope: -3.46, R²: 0.999, efficiency: 94.6%), sPXR (slope: -3.45, R²: 0.997, efficiency: 94.9%), 18S (slope: -3.28, R²: 0.997, efficiency: 101.7%). Assays were done in triplicates. 18S and PXR1-specific assay has been described before (Hoffart et al., 2012). PXR2-specific assay has been designed and validated previously in a Bachelor's thesis by Nina Dedic (IKP, 2007). Gene expression levels were normalized to respective 18S rRNA levels and calculated as copies per 10⁶ copies of 18S rRNA. Relative quantification analyses of the PXR variants in the resistant cells was conducted using the 2^{-ΔΔCt} method (Livak and Schmittgen, 2001) with 7900 HT Real-time PCR system (Applied Biosciences). Gene expression levels were normalized to the respective TBP levels.

Relative quantification analyses were conducted with TaqMan RT-PCR utilizing the BioMark HD system and 48.48 or FLEX Six Gene Expression Integrated Fluidic Circuits (IFC) according to manufacturer's instruction (Fluidigm, South San Francisco, CA, USA). For the IFCs a preamplification with 14 or 17 cycles of cDNA corresponding to 25 ng RNA was

performed using TaqMan PreAmp Master Mix (Applied Biosciences) and specific primers/probes of respective target genes (excluding 18S). Assays were either predesigned TaqMan assays purchased from Thermo Fischer Scientific (Table 10), or described previously: CYP2B6 (Burk et al., 2005), 18S (Hoffart et al., 2012) (Table 9). Pre-amplified cDNA was 1:5 diluted with 5 mM Tris/HCl (pH 8.5). Reaction mixtures consisting of the preamplified cDNA samples, 1x GE sample loading reagent and 1x PCR Mastermix (Eurogentec) or respective gene expression assays of the target genes and 1x assay loading reagent were prepared according to manufacturer's instructions and loaded to either FLEX Six or 48.48 Gene Expression IFCs to perform TaqMan RT-PCR with the BioMark HD system (Fluidigm). Either assays or samples were done as triplicates. Data was analyzed with Fluidigm Real-time PCR Analysis software (version 4.1.3) with a quality threshold set at 0.65, baseline correction method set at linear (derivative) and C_t threshold set at auto (detectors) and further processed with the $2^{-\Delta\Delta C_t}$ method (Livak and Schmittgen, 2001). Gene expression levels were normalized either to respective 18S rRNA or mean levels of 18S rRNA and TBP.

3.10. siRNA transfection of LS174T cells

Reverse transfection of LS174T cells was conducted according to the instructions of the manufacturer (Thermo Fischer Scientific). Per well, 6 μ l of 10 μ M pool of double-stranded non-targeted negative control siRNAs or double-stranded siRNAs targeting NR1I2 (Thermo Fischer Scientific) were diluted in Opti-MEM in a total volume of 500 μ l. 6 μ l Lipofectamine RNAiMAX was added. Mixture was incubated for 20 min at room temperature. 0.35×10^6 LS174T cells were resuspended and added into the wells making a total volume of 3 ml. The final concentration of siRNAs was 20 nM. After 48 h incubation, cells were treated with 0.1% DMSO or 10 μ M rifampicin for 24 h before cells were harvested and RNA isolated as described in section 3.7.

3.11. Transient transfections and reporter gene assays

HepG2 cells were seeded at 1.5×10^5 cells per well into 24-well plates one day prior to transfection. Transient transfections were conducted using jetPRIME transfection reagent (Polyplus, Illkirch, France). Per well, a mixture containing 0.3 μ g pGL4-CYP3A4(-7830 Δ 7208-364) luciferase reporter gene plasmid, 0.005 μ g Renilla luciferase expression plasmid pGL4.75[hRluc/CMV] and pcDhuPXR expression plasmid with equal ratio (0.02/0.02 μ g) or four-fold excess (0.01/0.04 μ g) of empty expression vector pcDNA3 or pcDhusPXR expression plasmid were prepared. The total amount of DNA was adjusted to 0.5 μ g with pUC18 in all transfections. The DNA mixture was diluted with

jetPRIME buffer to achieve a volume of 50 μ l. 1 μ l of jetPRIME transfection reagent was added, mixed and incubated at room temperature for 10 minutes. Then the reaction mixture was added onto cells. After incubation for 22–24 h, cells were treated with 0.1% DMSO or 10 μ M rifampicin for 24 h before cell lysis with 150 μ l of passive lysis buffer (Promega). Luminescence of firefly luciferase was measured from 20 μ l of sample with automatically injected 300 μ l of firefly luciferase assay solution (Geick et al. 2001) using the AutoLumat Plus LB953 (Berthold Technologies, Bad Wildbad, Germany). Similarly, Renilla luciferase was measured from 10 μ l sample with injection of 100 μ l of Renilla assay solution (Piedade et al. 2015). Results were normalized by dividing firefly luciferase activity by Renilla luciferase activity measured in the same well. Each transfection was done five times independently in technical triplicates.

3.12. Batch transfections and reporter gene assays

Transient batch transfection with HP cells was conducted using JetPEI transfection reagent (Polyplus). Per well, 0.6 μ l of JetPEI transfection reagent was diluted in 150 mM NaCl to a final volume of 25 μ l. For investigation of PXR activation, per well, 0.3 μ g pGL4-CYP3A4(-7830 Δ 7208-364) luciferase reporter gene plasmid and 0.01 μ g Renilla luciferase plasmid pGL4.75[hRluc/CMV] were diluted in 150 mM NaCl to a final volume of 25 μ l. JetPEI dilution was added to DNA dilution and incubated at room temperature for 15 min. Simultaneously, HP cells were trypsinized, counted and cell number adjusted to 40,000 cells in 200 μ l, per well. JetPEI/DNA mixture was added to cell suspension and 250 μ l of this mixture was pipetted into a Cell+ 96-well plate (Sarstedt). After at least 24 h incubation, cells were treated with 0.1–0.2% DMSO, 10 μ M rifampicin, 1 μ M SR18213, 10 μ M test compounds or co-treated with 10 μ M of rifampicin or 1 μ M SR18213 and 10 μ M of test compounds. Concentration-response experiments were conducted by treating the cells with 0.1–0.2% DMSO, 10 μ M rifampicin and i) increasing concentrations of test compounds, ii) co-treated with 10 μ M rifampicin and increasing concentrations of compounds or iii) co-treated with increasing concentrations of rifampicin and three fixed concentrations of test compounds. After 24 h treatment, medium was removed, 100 μ l of 1x PBS per well was added and aspirated. Cells were then lysed with 50 μ l of passive lysis buffer (Promega) and incubated for 20 min at room temperature in orbital shaker (750 rpm, Heidolph Titramax 101). Cell lysate was transferred to a conical 96-well plate and centrifuged for 5 min at 440 g, and then 10 μ l of cell lysate was transferred to a white OptiPlate-96 measuring plate (PerkinElmer). Per well, 150 μ l of RIM+ or 100 μ l of Renilla-Luciferase Assay Buffer was added. Mixture was

incubated in an orbital shaker (350 rpm, Heidolph Titramax 101) for 10 min while protected from light. Luminescence was measured using 0.1 s measurement time with EnSpire multimode plate reader (PerkinElmer). Results were normalized by dividing Firefly luciferase activity by Renilla luciferase activity measured in the same well. Experiments were conducted three times independently with technical triplicates.

For testing activity of PXR mutants, transient batch transfection was conducted similarly as above, but with HepG2 cells and following expression plasmids: per well, 0.27 µg pGL4-CYP3A4(-7830Δ7208-364) luciferase reporter gene plasmid, 0.01 µg Metridia luciferase plasmid pMetLuc2-control and 0.03 µg either pcDhuPXR, pcDhuPXR(Q25A), pcDhuPXR(Y306A), pcDhuPXR(S247A), pcDhuPXR(S407A), pcDhuPXR(W299A), pcDhuPXR(H327A) or pcDhuPXR(S208W/S247W/C284W) were diluted in 150 mM NaCl to a final volume of 25 µl. After at least 24 h incubation, cells were treated with 0.1% DMSO, 10 µM rifampicin and 10 µM test compounds. After 24 h medium was transferred to a conical 96-well plate, centrifuged for 5 min at 440 g and then 10 µl of medium was transferred to a white OptiPlate-96 measuring plate. Next, 100 µl Renilla-Luciferase Assay Buffer was added and Metridia luciferase activity was measured immediately using 0.1 s measurement time with EnSpire multimode plate reader. Cell lysis and firefly luciferase measurements were conducted as above. Results were normalized by dividing Firefly luciferase activity by Metridia luciferase activity measured in the same well. Experiments were conducted five times independently with technical triplicates.

For testing nuclear receptor selectivity, transient batch transfection was conducted similarly as above, but with HepG2 cells and following plasmids. Per well, 0.26 or 0.23 µg pGL4-CYP3A4(-7830Δ7208-364) luciferase reporter gene plasmid, 0.01 µg Metridia luciferase plasmid pMetLuc2control and 0.03 µg either pcDhuCAR1, pcDhuCAR3 or pcDhuVDR expression plasmids were diluted in 150 mM NaCl to a final volume of 25 µl. In addition, 0.03 µg pcDhuRXRα(orf) expression plasmid was added to CAR3 transfection. After at least 24 h incubation, cells were treated with 0.2% DMSO, 10 µM CITCO, 0.1 µM 1α,25-dihydroxy vitamin D3 (1α,25(OH)₂D₃) or 10 µM test compounds or co-treated with 10 µM of CITCO or 0.1 µM 1α,25(OH)₂D₃ and 10 µM of test compounds. After 24 h incubation Metridia and firefly luciferases were measured as described above. Results were normalized by dividing Firefly luciferase activity by Metridia luciferase activity measured in the same well. Experiments were conducted five times independently with technical triplicates.

3.13. Mammalian two hybrid assays

Transient batch transfection with HepG2 cells was conducted using JetPEI transfection reagent (Polyplus). Per well, 0.6 μ l of JetPEI transfection reagent was diluted in 150 mM NaCl to a final volume of 25 μ l. Similarly per well, for coactivator interaction assay 0.24 μ g pGL4-G5 luciferase reporter gene plasmid, 0.01 μ g Renilla luciferase plasmid pGL4.75[hRluc/CMV], 0.03 μ g pVP16-PXR(108-434) and 0.03 μ g pM-SRC1(583-783) were diluted in 150 mM NaCl to a final volume of 25 μ l. Likewise for corepressor interaction assay per well, 0.24 μ g pGL4-G5 luciferase reporter gene plasmid, 0.01 μ g Renilla luciferase plasmid pGL4.75[hRluc/CMV], 0.03 μ g pVP16-PXR(108-434), 0.03 μ g pM-SMRT(1109-1330) and 0.015 μ g pcDhuRXR α (orf) were diluted in 150 mM NaCl to a final volume of 25 μ l. JetPEI dilution was added to DNA dilution and incubated at room temperature for 15 min. Preparation of cells and transfection were conducted as described above in section 3.12. After at least 24 h incubation, cells were treated with 0.2% DMSO, 10 μ M rifampicin or co-treated with 10 μ M of rifampicin and 10 μ M of test compounds. After 24 h treatment, reporter gene assays were performed as described above in section 3.12. Results were normalized by dividing Firefly luciferase activity by Renilla luciferase activity measured in the same well. Experiments were conducted five times independently with technical triplicates.

3.14. CaPO₄-transfections

5.0×10^6 HepG2 cells were seeded a day before transfection in a dish with 10 cm diameter. Next day, 1 h before transfection, medium was aspirated and 9 ml fresh culture medium was added. Aqueous DNA solution of 450 μ l, containing 2 μ g pMetLuc2control and 10 μ g expression plasmid encoding wild-type PXR or PXR mutants [pcDhuPXR, pcDhuPXR(Q25A), pcDhuPXR(Y306A), pcDhuPXR(S247A), pcDhuPXR(S407A), pcDhuPXR(W299A), pcDhuPXR(H327A) or pcDhuPXR(S208W/S247W/C284W)], was prepared. Total amount of DNA was adjusted to 25 μ g with pUC18. 50 μ l of 2.5 M CaCl₂ was added to each DNA solution. This DNA/CaCl₂ solution was added dropwise to an equal volume of 2x HBS while simultaneously mixing with vortex. Then, this mixture was added dropwise onto cells. Cells were incubated for 5 h, then medium was aspirated, 3 ml 15% glycerol-PBS solution was added. Cells were incubated for 3 min at room temperature before washing the cells twice with 1x PBS. Then, 10 ml culture medium was added and cells were incubated for two days before Metridia luciferase measurement, as described in section 3.12., and total protein extraction, as described in section 3.16.2, were executed.

3.15. Limited proteolytic digestion

3.15.1. Sample preparation

Per ligand, 12.5 μ l H₂O, 2 μ l 10 mM Tris-Cl pH7.6, 0.5 μ l 40x ligand stock or vehicle (final vehicle 2.5%) and 5 μ l ³⁵S-TNT protein of sPXR were mixed, incubated for 30 min at 25°C and then put on ice for 30 seconds.

3.15.2. Proteolytic digestion

1 μ l of 5 mg/ml trypsin (final concentration of 250 μ g/ml) was added to incubated samples. Samples were incubated for 10 min at 25°C for proteolytic digestion and then put on ice. After 30 seconds, 6 μ l 5x protein sample buffer supplemented with β -mercaptoethanol was added and mixed. To achieve final volume of 30 μ l, 3 μ l of H₂O was added. After mixing, samples were incubated at 95°C for 5 min. Samples were immediately processed with gel electrophoresis or stored at -80°C.

3.15.3. Protein gel electrophoresis and analysis

15 μ l of samples were loaded to a 12% polyacrylamide protein gel with 10% input control and molecular weight marker. Gel was run with 200 V for approximately 45 min, then stained with Coomassie for 15–30 min and fixed/destained for 45 min up to overnight (solution was changed after 1 h). After destaining, gel was watered for 5 min and incubated for 30 min in 0.5 M sodium salicylate. Then gel was dried for at least 30 min. Samples were exposed to imaging plates and analyzed with CR35 Bio radioluminography laser scanner and quantified with AIDA software (version 4.50.010, Raytest, Straubenhardt, Germany).

3.16. Protein analysis

3.16.1. Nuclear extraction

Samples were kept on ice and all buffers were ice-cold during nuclear extraction. Cells were washed with PBS. Then cells were scraped with PBS and transferred to a reaction tube. Cell suspension was centrifuged for 5 min at 750 g at 4°C. Supernatant was discarded and cell pellet was resuspended in Buffer A, centrifuged as above and supernatant was discarded. Then, cell pellet was resuspended in Buffer A+0.4% NP-40, incubated on ice for 20 min, until cells were lysed. Cell lysis was controlled with microscope. After lysis, cell lysate was centrifuged as above and supernatant discarded. Buffer B was added in a volume of approximately 5 times of the volume of nuclear pellet and mixed with a magnetic stirrer for 30 min at 4°C and centrifuged for 15 min at 16,000 x g at 4°C. Supernatant was then aliquoted and stored at -80°C.

3.16.2. Total protein extraction

Samples were kept on ice and all buffers were ice-cold during total protein extraction. Cells were washed with PBS. Then cells were scraped with PBS and transferred to a reaction tube. Cell suspension was centrifuged for 5 min at 750 g at 4°C. Supernatant was discarded and cell pellet was resuspended in protein lysis buffer (Sundqvist et al., 2005), incubated on ice for 15 min while resuspended by pipetting every three minutes. Then, lysate was homogenized with ultrasonication (2x30s) using Bioruptor UCD200 (Diagenode, Liège, Belgium). Extracts were aliquoted and stored at -80°C.

3.16.3. Determination of protein concentration

Protein concentration was determined with bicinchoninic acid protein assay, which is based on the reduction of Cu^{2+} to Cu^+ by the peptide bonds of protein and subsequent binding of the reduced Cu^+ to bicinchoninic acid, which causes formation of violet color. The intensity of this color is proportional to the amount of protein. Briefly, 200 μl of Smith reagent was combined with 10 μl of protein sample and incubated for 1 h at 37°C. After incubation, absorbance was measured with EnSpire Multimode Plate Reader (PerkinElmer). Protein concentration of samples was determined based on the standard curve of bovine serum albumin.

3.16.4. Western blot

Protein samples were analyzed using sodium dodecyl sulfate-polyacrylamide gel electrophoresis (SDS-PAGE) and Western blot. 30 μg of protein was combined with 6 μl of 5x Lämmli and H_2O in a total volume of 30 μl and incubated at 95°C for 5 min before loading onto 10% polyacrylamide gel. For transfected PXR mutants, protein amount was adjusted to the transfection efficiency, as determined by measurement of Metridia luciferase activity. The gel electrophoresis was applied with 1x running buffer for 50–60 min using 200 V. Then the samples were blotted onto nitrocellulose membrane using 150 V for 45 min in blotting buffer. Protein transfer was confirmed with Ponceau staining. After destaining the membrane with TBS-T, membrane was blocked with 5% skim milk solution in TBS-T for 1 h at room temperature. Then membrane was incubated with primary anti-PXR antibody (Table 7) for overnight at 4°C. On next day, membrane was washed with TBS-T for 3 x 10 min and incubated with secondary antibody (Table 7) for 1 h at room temperature. After washing the membrane again with TBS-T for 3 x 10 min, the membrane was incubated at room temperature for 5 min in detection solution (SuperSignal West Dura Extended Duration Substrate, Thermo Fischer Scientific) before chemiluminescence detection with STELLA 3200 bio-imaging system (Raytest, Straubenhardt, Germany). The presence of equal amounts of protein in nuclear

extract samples was checked with anti-TBP antibody (Table 7) in a similar procedure. The intensity of the specific protein bands was quantified using the AIDA software (version 4.50.010, Raytest, Straubenhardt, Germany).

3.17. Kinome profiling

Compounds 100 and 109 were profiled at concentrations 1 μ M and 10 μ M against 335 wild-type protein kinases with single measurements. Kinome profiling was performed by ProKinase GmbH (Freiburg, Germany).

4. Results

4.1. Generation and characterization of drug-resistant cancer cells

For the generation of potentially drug-resistant cancer cells due to activation of PXR, a cell line with high PXR expression is essential. To this end, mRNA levels of PXR variants were quantified in four different human cancer cell lines, including two liver cancer cell lines (HepG2, Huh7) and two colon cancer cell lines (LoVo, LS174T). PXR is typically highly expressed in human liver; therefore, primary human hepatocytes (PHHs) were used as positive control. From the tested cell lines, LS174T cells had the highest mRNA expression of PXR1 (35.5% of PHHs) and sPXR (48.9% of PHHs) (Fig. 6A). The PXR1/sPXR ratio in PHHs and in LS174T cells was 4 and 3, respectively. These comparable ratios suggest a similar PXR activation system in these cells. Levels of PXR2 were undetectable in Huh7, LoVo and LS174T cells. However, primary human hepatocytes and HepG2 cells expressed PXR2, but at very low level (data not shown). The expression of PXR in LS174T cells was confirmed performing Western blot with nuclear extracts from LS174T cells. PXR protein was detected at approximately 50 kDa (Fig. 6B).

Functionality of PXR in LS174T cells was verified by treating the cells with the prototypical PXR agonist rifampicin and measuring the expression of established PXR target genes. Rifampicin-treatment induced ABCB1 and CYP3A4 3.5- and 7.4-fold, respectively (Fig. 6C). To confirm the dependency of rifampicin-induced gene expression on PXR in LS174T cells, a respective knock down experiment was conducted. After PXR knock down, induction of ABCB1 and CYP3A4 was reduced by 54% and 78%, respectively (Fig. 6D). Hence, rifampicin-induced gene expression appears to be dependent on PXR activation in LS174T cells. This was also confirmed with the co-treatment of rifampicin with a specific PXR antagonist, which suppressed rifampicin-induced ABCB1 and CYP3A4 expression (Fig. 6E). Overall, these results support the selection of human colorectal adenocarcinoma LS174T cells as a suitable cell line for development of potentially PXR dependent drug-resistant cancer cells.

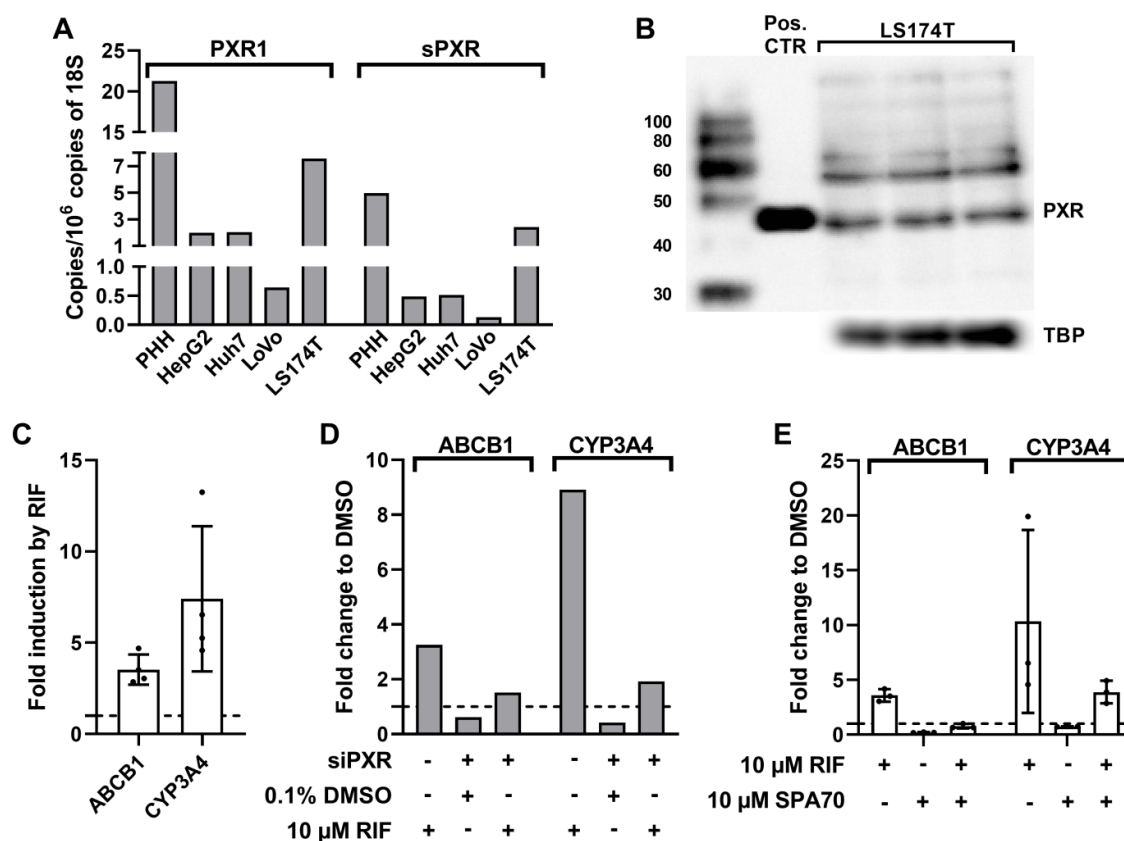


Figure 6. PXR is expressed and functional in LS174T cells. (A) LS174T cells express highest levels of PXR variants among tested cell lines. mRNA levels of PXR variants were quantified with RT-qPCR from HepG2, Huh7, LoVo and LS174T cell lines. Primary human hepatocytes of single donor were used as a positive control. (B) Expression of PXR protein in nuclear extracts of LS174T cells. PXR protein was detectable at approximately 50 kDa. Positive control (Pos.CTR) was in vitro translated PXR protein. (C) Rifampicin induces expression of PXR target genes in LS174T cells. LS174T cells were treated with 0.1% DMSO or 10 μM rifampicin for 72 h. mRNA was quantified using RT-qPCR and normalized to the expression of 18S. (D, E) Rifampicin induces expression of ABCB1 and CYP3A4 in a PXR-dependent manner. (D) LS174T cells were transfected with siRNA pool targeting PXR (+) or negative control siRNA pool (-) and treated for 24 h with 0.1% DMSO or 10 μM rifampicin. mRNA was quantified as in C. (E) LS174T cells were treated with 10 μM RIF, 10 μM SPA70 or co-treated with both for 72 h. mRNA was quantified as in C. Data in A and D is mean of technical triplicates from one experiment, and in C and E mean ±SD from three independent experiments and individual experiments illustrated with dots.

Cisplatin and irinotecan were used for the generation of drug-resistant cancer cells. Cisplatin was selected, because of its well-known ability to cause acquired resistance and its use as a chemotherapeutic in the treatment of several types of solid tumors (Amable, 2016). In addition, cisplatin has demonstrated PXR activation potential (Masuyama et al., 2016, 2005). Irinotecan was chosen because it is commonly used in the treatment of colorectal cancer (Basseville et al., 2011). Similar to cisplatin, irinotecan itself and its active metabolite SN38 have been shown to potentially activate PXR (Basseville et al., 2011; Chen et al., 2010). Accordingly, cisplatin,

irinotecan and its active metabolite SN38 demonstrated here PXR activation potential by inducing the expression of established PXR target genes ABCB1 and CYP3A4 (Fig. 7).

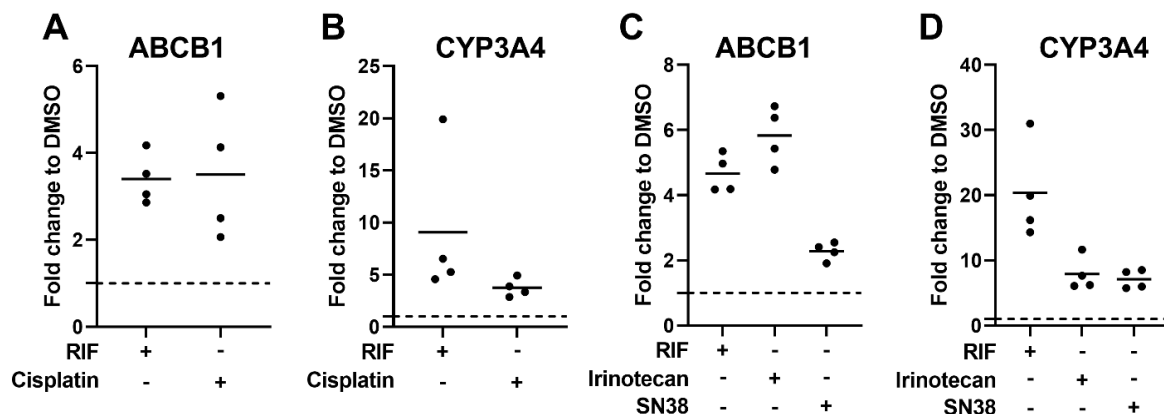


Figure 7. Cisplatin, irinotecan, and its active metabolite SN38 induce expression of established PXR target genes. Effect of cisplatin, irinotecan and SN38 on expression of (A, C) ABCB1 and (B, D) CYP3A4. LS174T cells were treated with 0.2% DMSO, 10 μ M rifampicin, 10 μ M cisplatin, 1.5 μ M irinotecan and 25 nM SN38 for 72 h. mRNA was quantified using RT-qPCR and normalized to the corresponding expression of 18S. Data is shown as mean fold change to DMSO-treated cells (set as 1, illustrated with dashed line) of four samples per group and individual samples illustrated with dots.

Before starting the generation of drug-resistant cancer cells, the sensitivity of parental LS174T cells towards cisplatin and irinotecan was assessed. LS174T cells were more sensitive towards irinotecan (Fig. 8B) than to cisplatin (Figure 8A, Table 15). The IC_{50} values for cisplatin and irinotecan were 13.6 μ M and 4.5 μ M, respectively. Both drugs killed nearly all of the cells at 100 μ M.

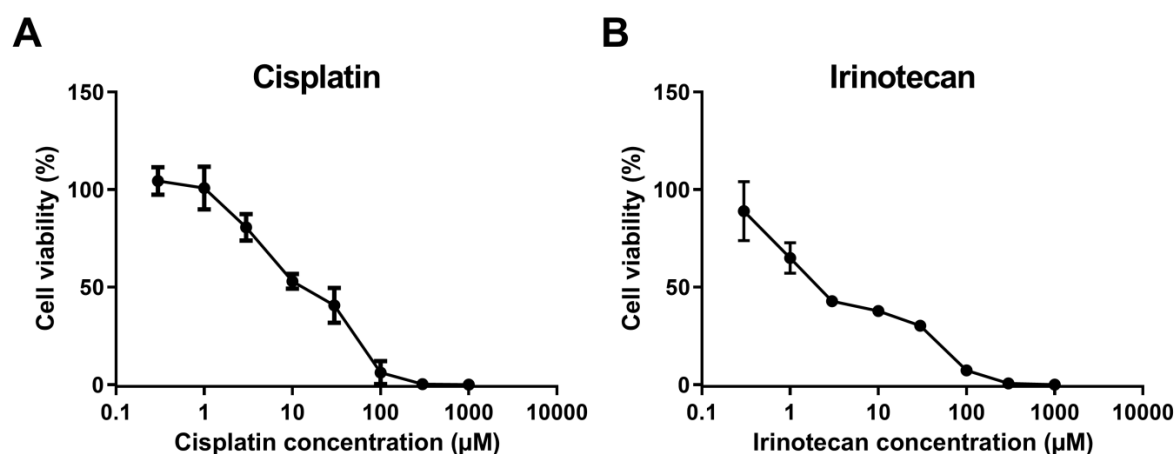


Figure 8. Sensitivity of parental LS174T cells towards cisplatin and irinotecan. LS174T cells were treated for 72 h with 0.3–1,000 μ M (A) cisplatin or (B) irinotecan. Cell viabilities were determined with CellTiter-Glo cell viability assay. Cell viability in the presence of vehicle DMSO only was set as 100%. Data is expressed as mean cell viability \pm SD from three independent experiments with technical triplicates.

To generate cisplatin and irinotecan-resistant cells, LS174T cells were continuously cultured in either cisplatin- or irinotecan-containing medium and the concentration was gradually increased as described in section 3.3. After treatment of cells for several months, cells were tested for their sensitivity towards these drugs. Compared to parental LS174T cells (Ls-P), cisplatin-resistant cells (Ls-R-C) were 6-fold more resistant to cisplatin, whereas irinotecan-resistant cells (Ls-R-I) were 78-fold more resistant to irinotecan (Fig. 9, Table 15). The concentration of cisplatin and irinotecan that killed nearly all of the Ls-P cells was 100 μ M. At that concentration approximately 65% of Ls-R-C cells and 80% of Ls-R-I cells were still viable. It can be concluded that both newly generated cell lines had acquired resistance towards cisplatin or irinotecan.

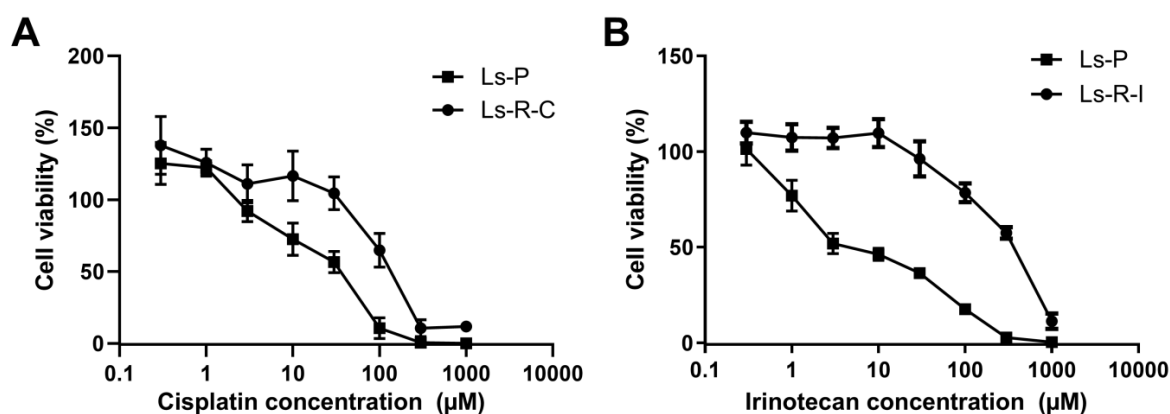


Figure 9. (A) Ls-R-C and (B) Ls-R-I cells acquire resistance towards cisplatin or irinotecan after continuous long-term treatment. After culturing LS174T cells with gradually increasing concentrations of cisplatin for 7 months or irinotecan for 5 months cell viabilities were determined with CellTiter-Glo cell viability assay. Cell viability of in the presence of vehicle DMSO only was set as 100%. Data is expressed as mean cell viability \pm SD from three independent experiments with technical triplicates.

In addition, cross-resistance of Ls-R-C cells towards irinotecan and of Ls-R-I towards cisplatin was evaluated. Ls-R-C cells were as sensitive towards irinotecan as parental cells, whereas Ls-R-I cells displayed marginally improved (2-fold) resistance to cisplatin (Fig. 10, Table 15). Therefore, no remarkable cross-resistance had been developed with either of the cells.

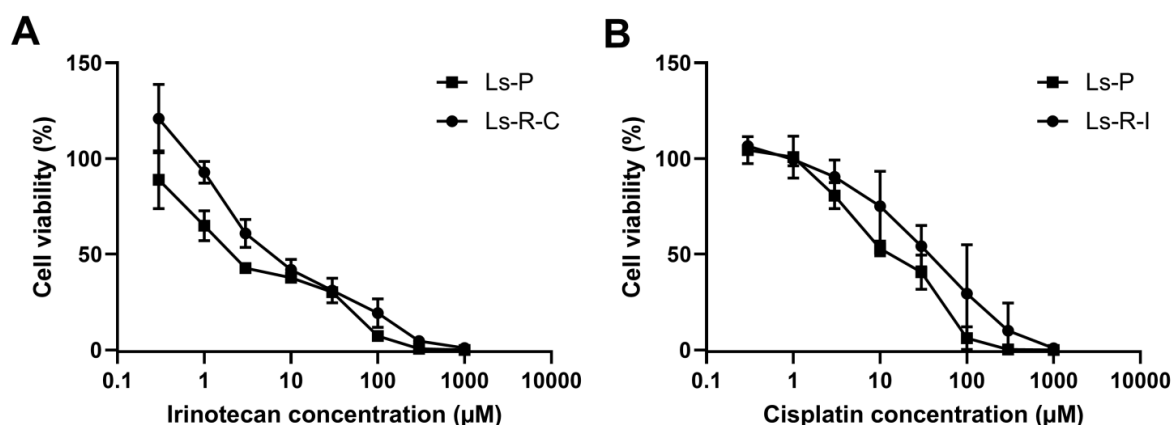


Figure 10. Cross-resistance of Ls-R-C and Ls-R-I cells. (A) Ls-R-C cells showed no cross-resistance towards irinotecan. (B) Ls-R-I cells displayed slight cross-resistance towards cisplatin. Ls-R-C cells were treated for 72 h with 0.3–1,000- μM irinotecan and Ls-R-I cells with 0.3–1,000 μM cisplatin. Cell viabilities were determined with CellTiter-Glo cell viability assay. Cell viability of in the presence of vehicle DMSO only was set as 100%. Data is expressed as mean cell viability \pm SD from three independent experiments with technical triplicates.

To evaluate the long-term stability of the acquired resistance, resistant cells were cultured in drug-free medium for one month and then cell viabilities were determined as described in section 3.4. Ls-R-C cells showed 4-fold resistance and L-R-I cells 141-fold resistance compared to Ls-P cells (Table 15); therefore both resistant cells maintained their resistance in the long-term (Fig. 11). Although the IC_{50} value of Ls-R-C cells was slightly, but not significantly reduced compared earlier.

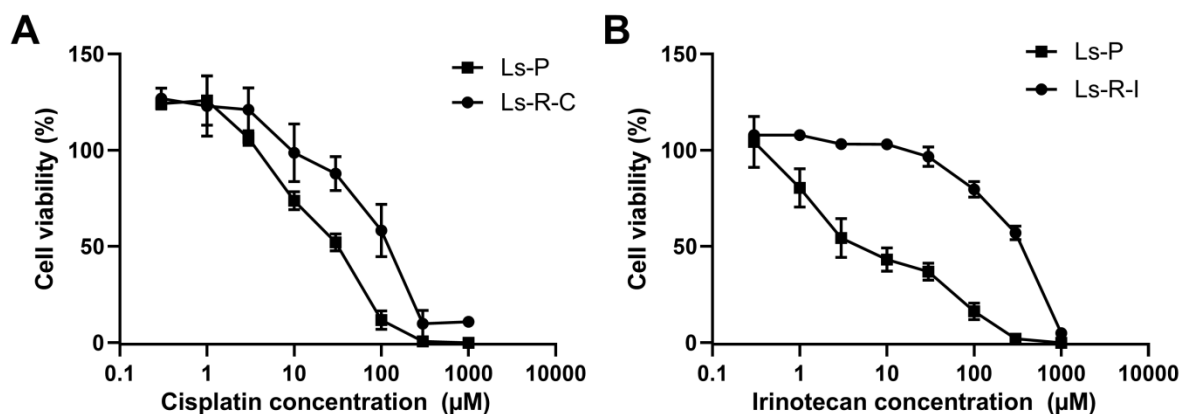


Figure 11. Long-term stability of resistance in Ls-R-C and Ls-R-I cells. (A) Ls-R-C and (B) Ls-R-I cells maintain their resistance after long-term culture without drug. Cells were cultured for one month in drug-free medium and cell viabilities were determined with CellTiter-Glo cell viability assay. Cell viability in the presence of vehicle DMSO only was set as 100%. Data is expressed as mean cell viability \pm SD from three independent experiments with technical triplicates.

Stability of resistance was assessed also after freezing and thawing of the cells, because a reliable drug resistance model should maintain the resistant phenotype after freeze/thaw cycle (McDermott et al., 2014). Compared to Ls-P, Ls-R-C demonstrated still 5-fold resistance and

Ls-R-I cells 180-fold resistance. In addition, the IC₅₀ values were not reduced compared to earlier, therefore both resistant cells maintained their acquired resistance after freezing and thawing (Fig. 12, Table 15).

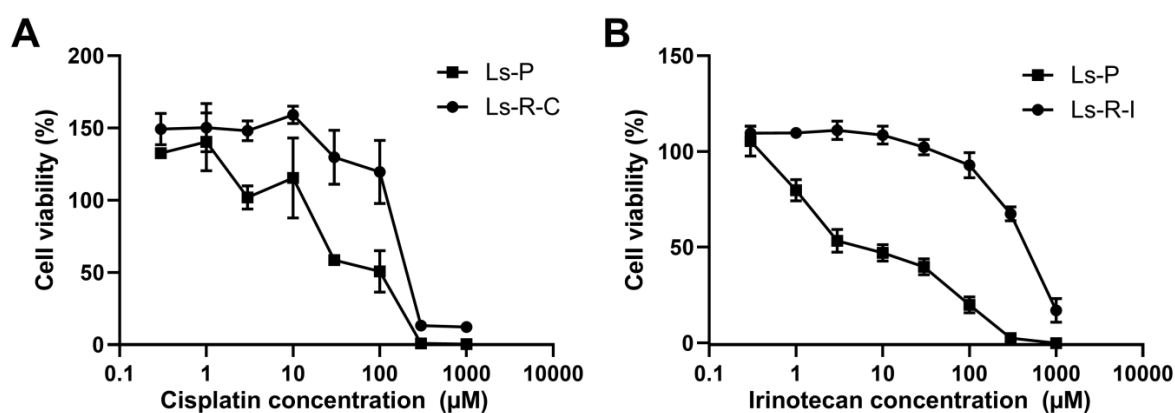


Figure 12. Effect of freezing and thawing on the stability of resistance in Ls-R-C and Ls-R-I cells. (A) Ls-R-C and (B) Ls-R-I cells maintained their resistance after freezing and thawing. Cells were frozen, thawed and cultured for 3–4 passages before determination of cell viabilities for Ls-R-C and Ls-R-I cells. Cell viability in the presence of vehicle DMSO only was set as 100%. Data is expressed as mean cell viability \pm SD from three independent experiments with technical triplicates.

Table 15. Drug sensitivity IC₅₀ values and relative resistances for Ls-R-C and Ls-R-I cells.

Cell line	Cisplatin: IC ₅₀ µM (95% CI)	Fold resistance	Irinotecan: IC ₅₀ µM (95% CI)	Fold resistance
Initial				
Ls-P	13.6 (8.7–21.1)	1	4.5 (1.4–14.9)	1
After selection				
Ls-P	17.9 (11.0–28.9)	1	5.9 (1.9–18.1)	1
Ls-R-C	101.1* (56.4–180.5)	6	-	-
Ls-R-I	-	-	457.9** (285.4–789.6)	78
Long-term stability				
Ls-P	17.2 (13.1–22.6)	1	4.7 (1.7–13.7)	1
Ls-R-C	70.7** (41.1–119.8)	4	-	-
Ls-R-I	-	-	661.9* (493.4–923.8)	141
Freeze-thaw stability				
Ls-P	39.5 (18.7–85.0)	1	5.5 (1.6–20.5)	1
Ls-R-C	204.2* [†] (108.6–397.8)	5	-	-
Ls-R-I	-	-	991.6* ^{††} (649.0–1727)	180
Cross-resistance				
Ls-R-C	-	-	2.7 (1.4–5.2)	<1
Ls-R-I	32.6 (16.6–64.2)	2	-	-

IC₅₀ values were calculated from experiments shown in Fig. 8–12 with nonlinear regression using GraphPadPrism (version 8.3.0). Statistical significances are illustrated with asterisks and daggers, * p <0.05, ** p <0.01 compared to the IC₅₀ value of Ls-P, analyzed with paired t-test. [†] p <0.05, ^{††} p <0.01 compared to the IC₅₀ after selection of respective cells analyzed with unpaired t-test.

Petitprez et al. (2013) have previously shown that acquired resistance towards cancer drugs can be associated with increased doubling time. Therefore, growth analysis was performed to

calculate the doubling times. Compared to Ls-P, Ls-R-C demonstrated 2.7-fold increase (Fig. 13A), while Ls-R-I displayed only 1.2-fold increase in doubling time (Fig. 13B).

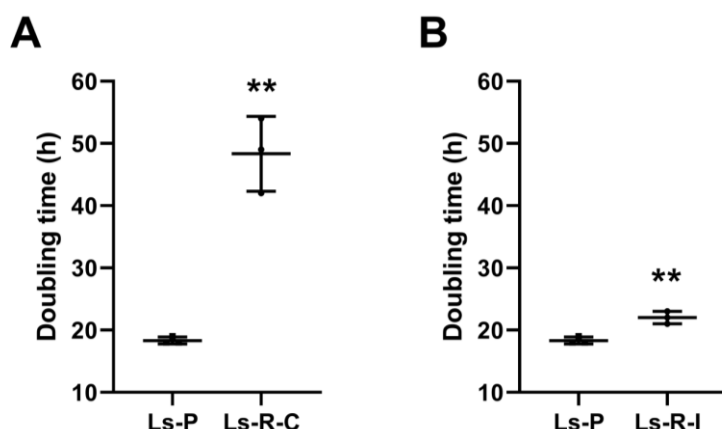


Figure 13. (A) Ls-R-C and (B) Ls-R-I cells demonstrate increased doubling times compared to Ls-P cells. Cells were grown in drug-free culture medium for 4 days and manually counted every 24 h. Doubling time was calculated at exponential growth phase. Data is expressed as mean doubling time \pm SD from three independent experiments and individual experiments illustrated with dots. Statistically significant differences are illustrated with asterisks. ** p <0.01 compared to Ls-P cells analyzed by unpaired t-test.

4.2. Determination of PXR levels in cisplatin and irinotecan-resistant cells

To assess if expression of PXR was altered in resistant cells, mRNA and protein levels of PXR were determined. Ls-R-C demonstrated reduced mRNA expression compared to the mean expression of Ls-P (Fig. 14A), albeit this could be also due to the high variability in Ls-P samples. The protein expression of PXR was also reduced by nearly 50% in Ls-R-C (Fig. 14C-D). In contrast, Ls-R-I cells showed comparable mRNA (Fig. 14B) expression, while the protein expression was increased by 45% compared to the Ls-P (Fig. 14C-D).

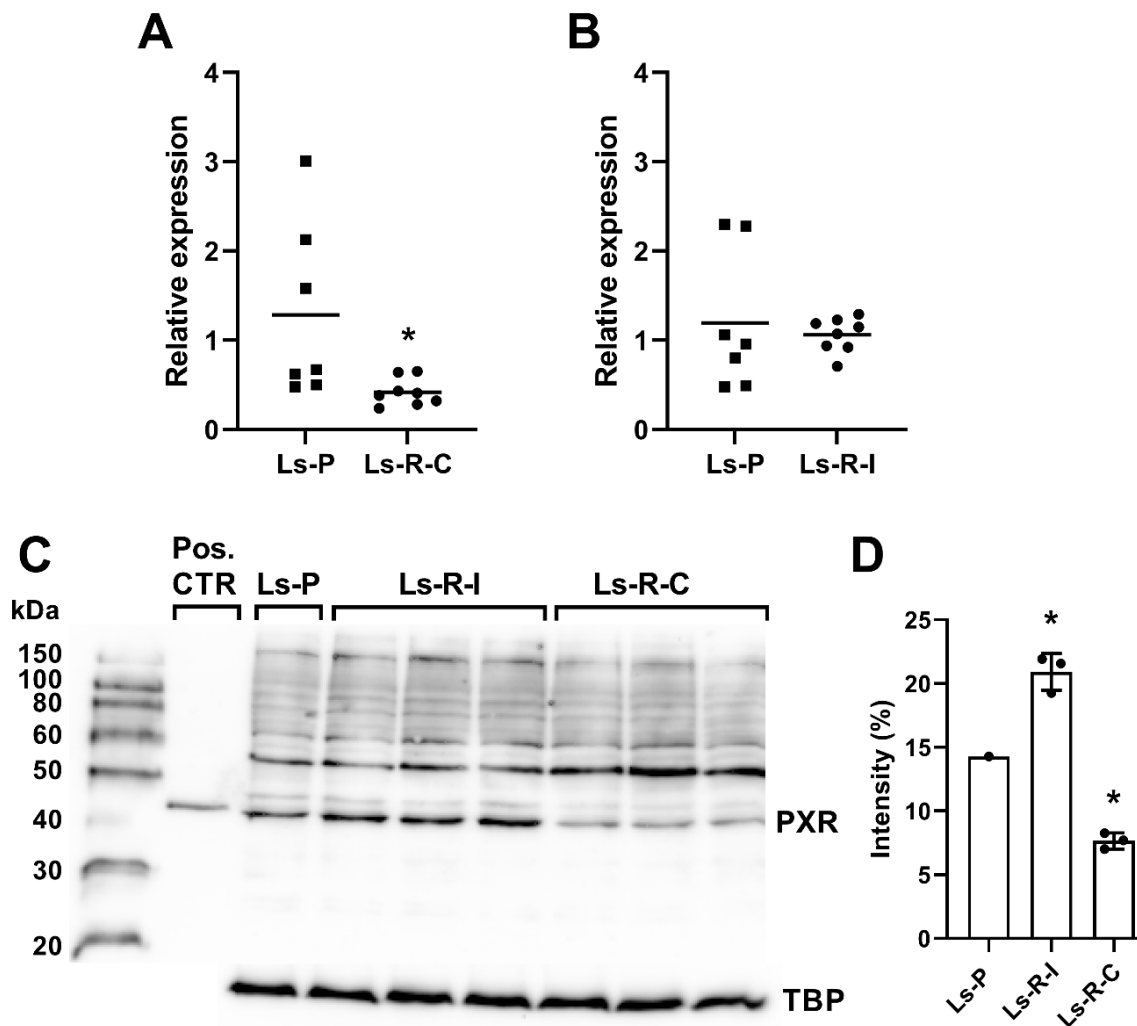


Figure 14. Expression levels of PXR in Ls-R-C and Ls-R-I cells. (A) Ls-R-C cells display reduced mRNA expression of total PXR. (B) Ls-R-I cells demonstrate comparable mRNA expression as Ls-P cells. Ls-R-C cells were continuously cultured with 30 μ M cisplatin, Ls-R-I in 40 μ M irinotecan and Ls-P cells in drug-free medium before cell harvest and subsequent RNA isolation. mRNA was quantified by RT-qPCR and normalized to the corresponding mean expression of 18S and TBP. Data is shown as mean relative expression compared to the normalized mean expression of Ls-P containing 8 samples per group and individual samples illustrated with dots. Statistically significant differences are illustrated with asterisks. * p <0.05, compared to Ls-P cells analyzed by unpaired t-test. (C) Expression of PXR protein in nuclear extracts of Ls-R-C, Ls-R-I and Ls-P cells. PXR protein was detectable at approximately 50 kDa. Positive control (Pos.CTR) was in vitro translated PXR protein. (D) Quantification of protein expression. Data is expressed as mean intensity (%) \pm SD from three samples per group. Except only one sample in Ls-P group due to technical reasons. Statistical significance are illustrated with asterisks. * p <0.05, compared Ls-P analyzed by one-way ANOVA with Dunnett's multiple comparisons test.

4.3. Role of alternative splicing of PXR in cisplatin and irinotecan resistance

sPXR has been suggested to have tumor suppressive effects by inhibiting the functional PXR (Breuker et al., 2014). The dominant negative effect of sPXR was confirmed here in transfection experiments. Equal amount of sPXR reduced the rifampicin-induced activity of

PXR1 by 55% (Fig. 15A). Similarly, four-fold excess of sPXR suppressed the rifampicin-induced activity by 78% and also the basal PXR activity (Fig. 15B).

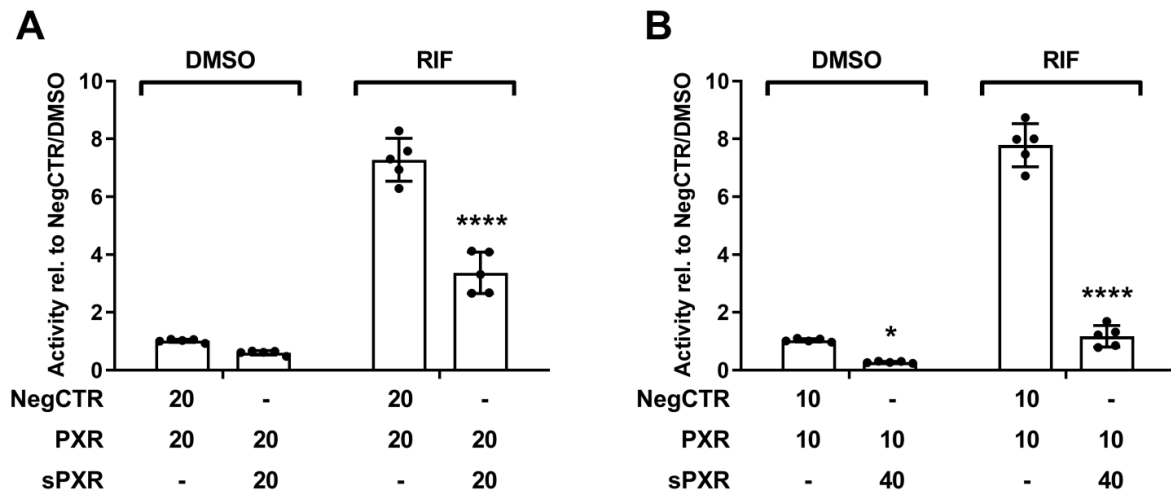


Figure 15. sPXR displays dominant negative activity. HepG2 cells were transiently transfected with CYP3A4 reporter gene, pcDhuPXR and either with pcDNA3 as negative control (NegCTR) or pcDhusPXR in (A) equal or (B) 4-fold excess ratio in nanograms and treated with 0.1% DMSO or 10 μ M rifampicin. Luciferase activities were measured after 24 h treatment. Data is expressed as mean \pm SD normalized luciferase activity relative to the activity of cells co-transfected with pcDNA3 and pcDhuPXR and treated with DMSO only from five independent experiments with technical triplicates and individual experiments illustrated with dots. Statistically significant differences are illustrated with asterisks. * p <0.05, **** p <0.0001 compared to similarly treated pcDhuPXR + NegCTR analyzed by two-way ANOVA with Sidak's post-test.

To investigate if altered splicing of PXR could be a possible mechanism behind cisplatin or irinotecan resistance, PXR1 and sPXR levels were measured from Ls-P, Ls-R-C and Ls-R-I cells. Compared to the Ls-P cells neither PXR1 nor sPXR levels were markedly altered in Ls-R-C (Fig. 16A) or in Ls-R-I (Fig. 16B) cells.

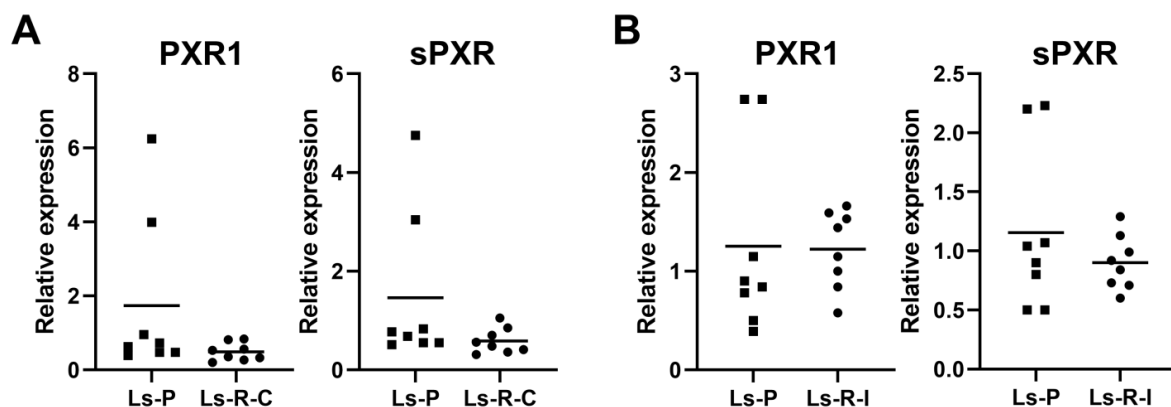


Figure 16. No remarkable changes in expression of PXR variants in resistant cells compared to parental LS174T cells. Ls-R-C and Ls-R-I cells were cultured continuously with 30 μ M cisplatin and 40 μ M irinotecan, respectively. Ls-P cells were cultured in drug-free medium before cell harvest and subsequent RNA isolation. mRNA was quantified by RT-qPCR and normalized to the corresponding expression of TBP. Two outliers of Ls-P in PXR1 and sPXR correspond to same samples. Data is shown

as mean relative expression compared to the normalized mean expression of Ls-P containing 8 samples per group and individual samples illustrated with dots. Statistical significance was compared to Ls-P cells, analyzed by unpaired t-test.

4.4. Gene expression changes in cisplatin- and irinotecan-resistant cells

To identify the possible gene related mechanisms behind acquired cancer drug resistance in cisplatin- and irinotecan-resistant cells, gene expression analysis was performed. Measured genes (46 genes for both resistant cells) were selected based on three reasons (Appendix Table 1): first, genes that have been shown to be involved in cisplatin or irinotecan metabolism or resistance; furthermore, genes that proved to be or are possibly regulated by PXR; finally, genes that are in general involved in cancer drug resistance. Compared to parental cells several genes associated with cancer drug resistance were differentially expressed in Ls-R-C cells (Fig. 17, Appendix Table 2). As expected, several efflux transporters were upregulated in Ls-R-C cells (2- to 33-fold), including ABCB11, ABCC1–3, ABCG2 and ATP7A. On the contrary, ABCB1 and ABCA2 were reduced by 135-fold and 1.4-fold, respectively. Ls-R-C cells displayed also increased expression of BCL2L1 (4.0-fold), CDKN1A (5.1-fold) and GADD45A (4.4-fold). In addition, ERCC1 and SLC31A2 showed 1.6- and 1.5-fold higher expression, respectively. In contrast, expression of SLC31A1 was reduced by 2-fold. Other downregulated genes included BCL2 with 1.9-fold reduction, CYP1A2 (1.9-fold reduction), GSTP1 (1.6-fold reduction), OLFM4 (59-fold reduction), SLC10A2 (14-fold reduction) and SLCO2B1 (2.7-fold reduction).

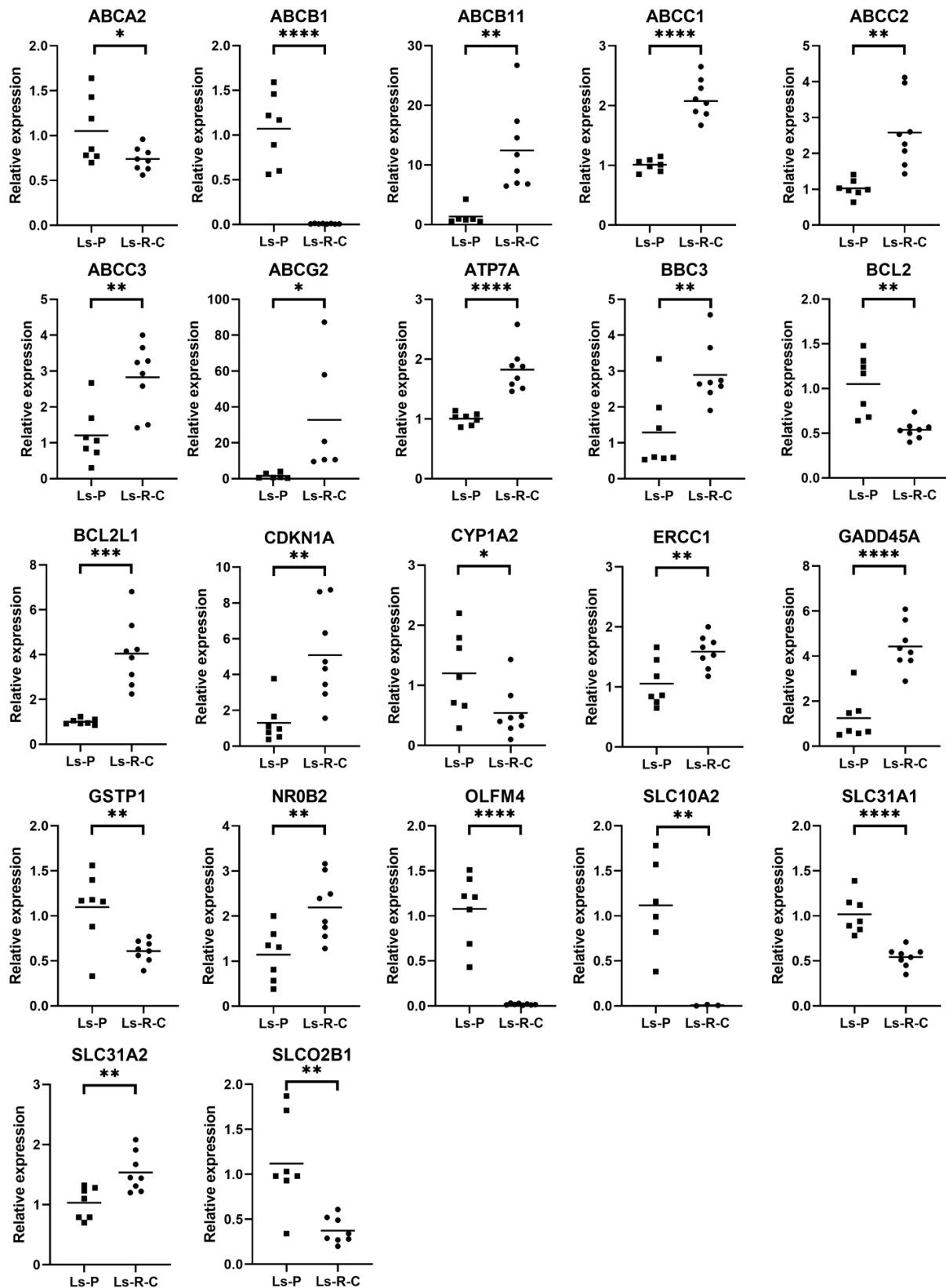


Figure 17. Gene expression alterations in Ls-R-C cells. Ls-R-C cells were continuously cultured with 30 μ M cisplatin and Ls-P cells in drug-free medium before cell harvest and subsequent RNA isolation. mRNA was quantified by RT-qPCR and normalized to the corresponding mean expression of 18S and TBP. Data is shown as mean relative expression compared to the normalized mean expression of Ls-P containing 6–8 samples per group and individual samples illustrated with dots. Only significant relative

expression changes >1.5 or <0.75 to Ls-P cells were included. Ls-R-C/SLC10A2 contains only three samples because the expression of SLC10A2 in other three samples was below detection limit and/or failed in quality. Statistically significant differences are illustrated with asterisks. * $p<0.05$, ** $p<0.01$, *** $p<0.0001$ compared to Ls-P cells analyzed by unpaired t-test.

Similar to Ls-R-C cells, Ls-R-I showed increased expression of BCL2L1 (2.3-fold), CDKN1A (3.3-fold), GADD45A (2.1-fold) and NR0B2 (4.3-fold) and reduced expression of OLFM4 (7.7-fold reduction) and SLC10A2 (12-fold reduction) (Fig. 18, Appendix Table 3). In contrast to Ls-R-C cells, ABCB1 and SLCO2B1 were upregulated 1.8- and 2.5-fold, respectively. In addition, the following genes were upregulated: CES2 (1.6-fold), CYP3A4 (4.6-fold), CXCR4 (16.3-fold), EGFR (1.6-fold) and FGF19 (3.3-fold). Instead, following genes were reduced: ALDH1A1 (11-fold reduction), TOP1 (1.7-fold reduction), UGT1A1 (1.7-fold reduction) and UGT1A9 (3.6-fold reduction).

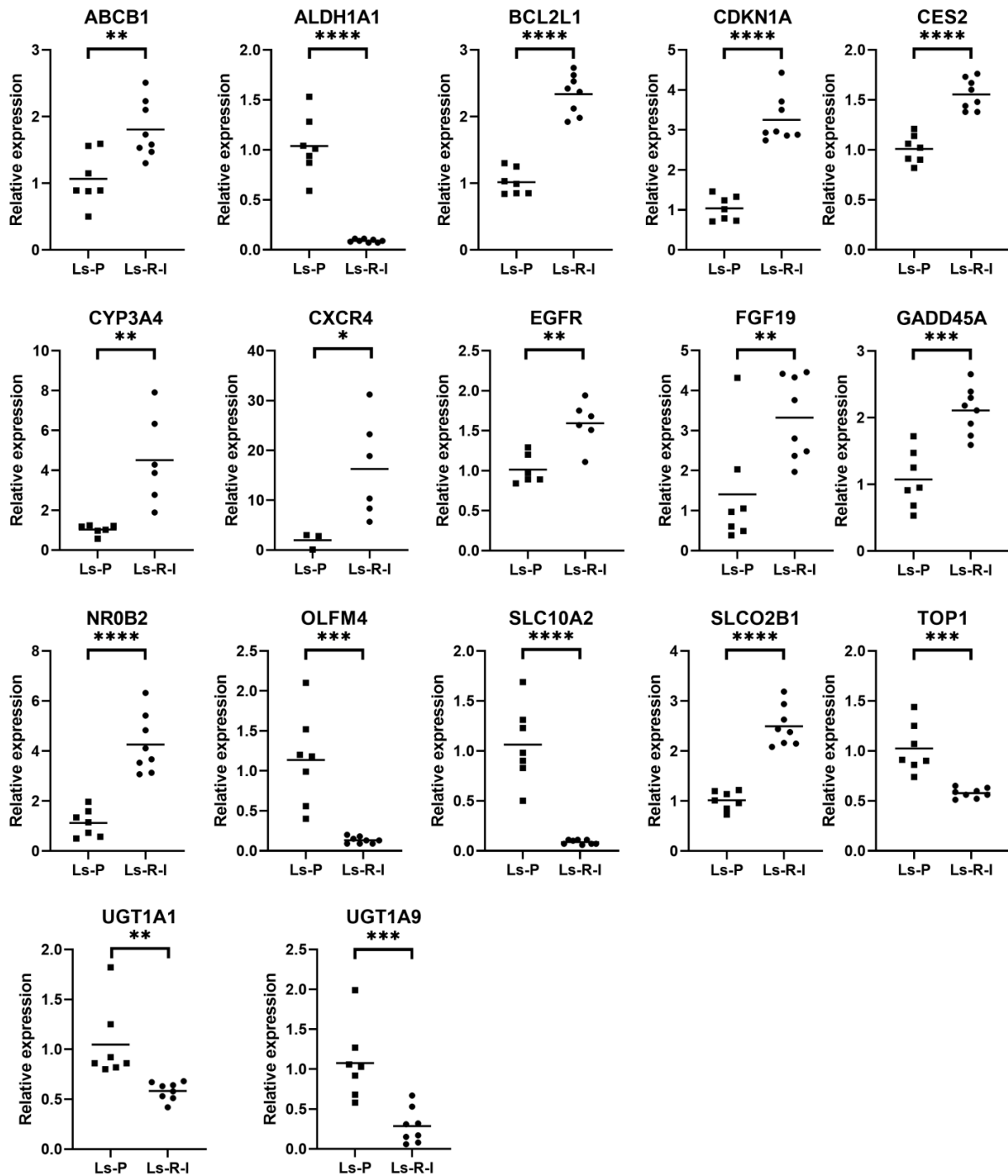


Figure 18. Gene expression alterations in Ls-R-I cells. Ls-R-I cells were continuously cultured with 40 μ M irinotecan and Ls-P cells in drug-free medium before cell harvest and subsequent RNA isolation. mRNA was quantified by RT-qPCR and normalized to the corresponding mean expression of 18S and TBP. Data is shown as mean relative expression compared to the normalized mean expression of Ls-P containing 6–8 samples per group and the individual samples illustrated with dots. Only significant relative expression changes >1.5 or <0.75 to Ls-P cells were included. Ls-P/CXCR4 contains only three samples because the expression of CXCR4 in other three samples was below detection limit and/or failed in quality. Statistically significant differences are illustrated with asterisks. * $p < 0.05$, ** $p < 0.01$, *** $p < 0.001$, **** $p < 0.0001$ compared to Ls-P cells analyzed by unpaired t-test.

4.5. Cross-resistance of paclitaxel in irinotecan-resistant cells

Ls-R-I cells showed increased expression of ABCB1 (MDR1) and CYP3A4. MDR1 acts as an efflux transporter for paclitaxel (Hendriks et al., 2013; Sparreboom et al., 1997). ABCB1 upregulation has been observed in paclitaxel-resistant cancer cells (Januchowski et al., 2013; Němcová-Fürstová et al., 2016; Takeda et al., 2007; Vaidyanathan et al., 2016). Moreover, inhibition of ABCB1 increased paclitaxel sensitivity in ABCB1 overexpressing cells, but not in parental cells (Shi et al., 2009; Vaidyanathan et al., 2016; Zhang et al., 2016). In addition, paclitaxel is not only metabolized by CYP2C8, but to a large extent also by CYP3A4 (Cresteil et al., 1994; Hendriks et al., 2013; Taniguchi et al., 2005). Given the above, the potential cross-resistance of paclitaxel in Ls-R-I cells was investigated. Ls-R-I cells indeed displayed approximately 3-fold higher resistance to paclitaxel compared to parental cells (Fig. 19). IC₅₀ values with 95% confidence intervals for paclitaxel in Ls-P and Ls-R-I cells were 3.0 nM (2.0–4.6) and 10.1 nM (6.8–14.9), respectively.

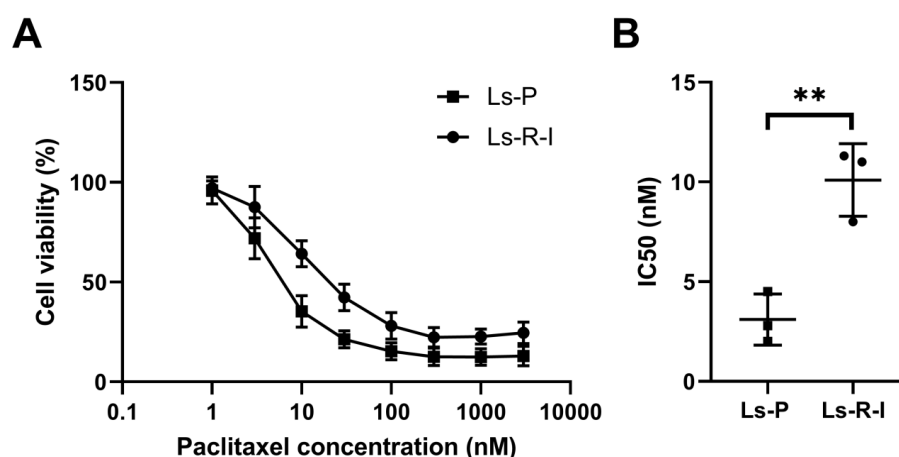


Figure 19. Ls-R-I cells demonstrate cross-resistance towards paclitaxel. (A) Ls-R-I cells display increased cell viability after paclitaxel treatment compared to parental Ls-P cells. Ls-P and Ls-R-I cells were treated for 72 h with 1–3,000 nM paclitaxel. Cell viabilities were determined with CellTiter-Glo cell viability assay. Cell viability in the presence of vehicle DMSO only was set as 100%. Data is expressed as mean cell viability \pm SD from three independent experiments with technical triplicates. (B) Ls-R-I cells showed increased resistance towards paclitaxel. IC₅₀ values were calculated from experiments shown in A with nonlinear regression using GrapPadPrism (version 8.3.0). IC₅₀ is expressed as mean \pm SD from three independent experiments and individual experiments illustrated with dots. Statistical significances illustrated with asterisks, ** p <0.01 compared to the IC₅₀ value of Ls-P, analyzed with paired t-test.

4.6. Role of PXR in regulation of genes potentially involved in cisplatin or irinotecan resistance

To investigate the possible role of PXR in the regulation of differentially expressed genes in resistant cells, Ls-P, Ls-R-C and Ls-R-I cells were treated with prototypical PXR agonist rifampicin, specific PXR antagonist SPA70 or co-treated with both. In Ls-P cells, rifampicin

treatment induced expression of ABCB1 (6.5-fold), BCL2L1 (3.0-fold), CYP3A4 (10.1-fold) and FGF19 (6.6-fold) (Fig. 20). Rifampicin-dependent induction of these genes was also suppressed by SPA70 co-treatment. Therefore, these genes appear to be regulated by PXR in LS174T cells.

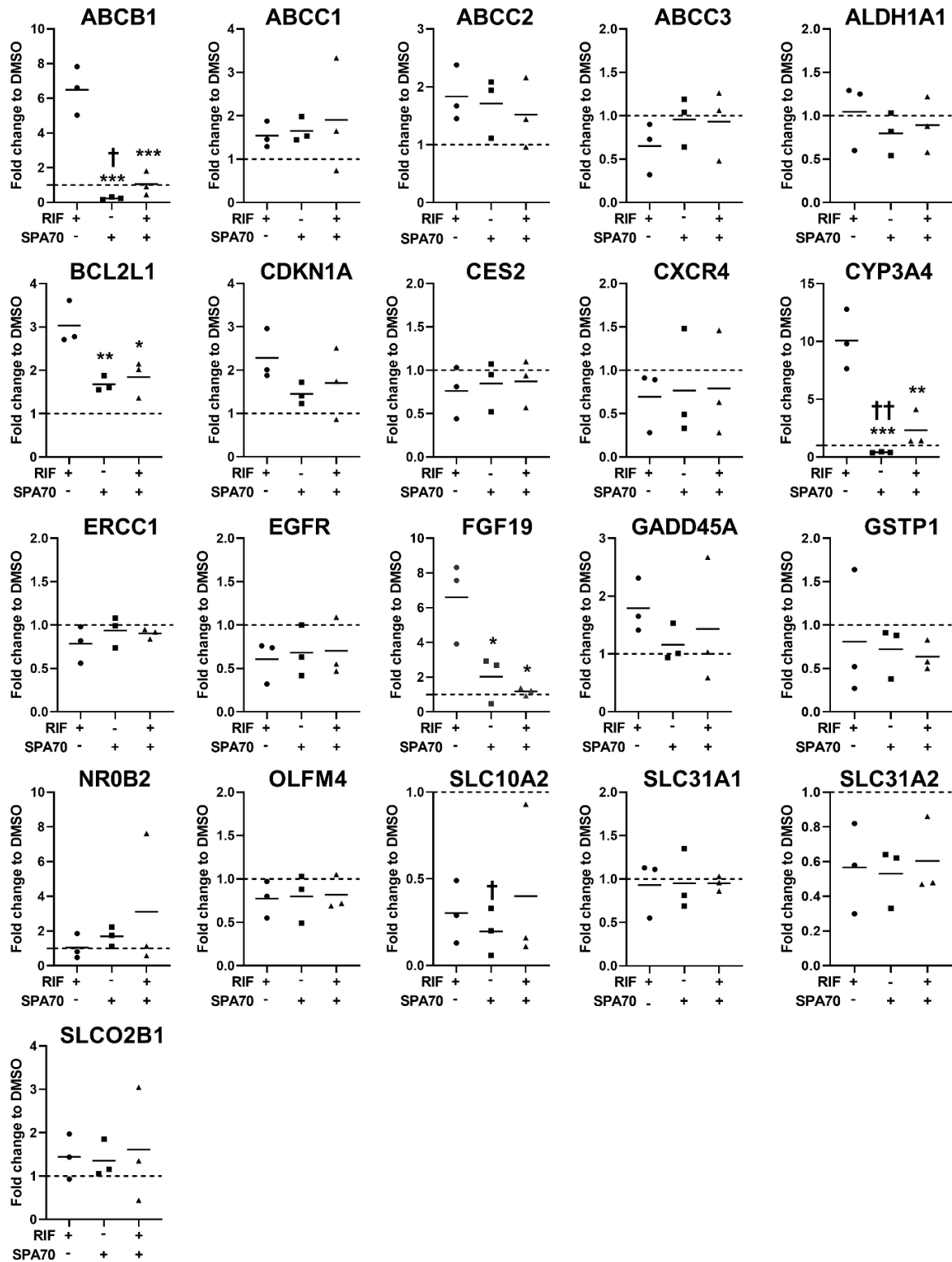


Figure 20. Effect of PXR antagonism on gene expression in Ls-P cells. Specific PXR antagonist SPA70 attenuates rifampicin-induced expression of part of the genes that were differentially expressed in Ls-R-C or Ls-R-I cells. LS174T cells were treated with 0.2% DMSO, 10 μ M rifampicin, 10 μ M SPA70 or co-treated with 10 μ M rifampicin and 10 μ M SPA70 for 48 h. mRNA was quantified using RT-qPCR and normalized to the corresponding mean expression of 18S and TBP. Data is shown as mean fold change to DMSO-treated cells of three experiments per group and individual experiments illustrated with dots. Statistically significant differences are illustrated with asterisks and daggers.

* $p < 0.05$, ** $p < 0.01$, *** $p < 0.001$ compared to 10 μM rifampicin treatment analyzed by one-way ANOVA with Dunnett's multiple comparisons test. † $p < 0.05$, †† $p < 0.01$, compared to 1 (DMSO) analyzed by one sample t-test corrected by the method of Bonferroni.

In Ls-R-C cells, only ABCB1 and ABCB11 were suppressed by SPA70 treatment alone or as a co-treatment with rifampicin (Fig. 21). The expression of all the other genes was not affected by PXR activation or inhibition. Therefore, PXR appears not to regulate the genes that are potentially relevant for cisplatin resistance.

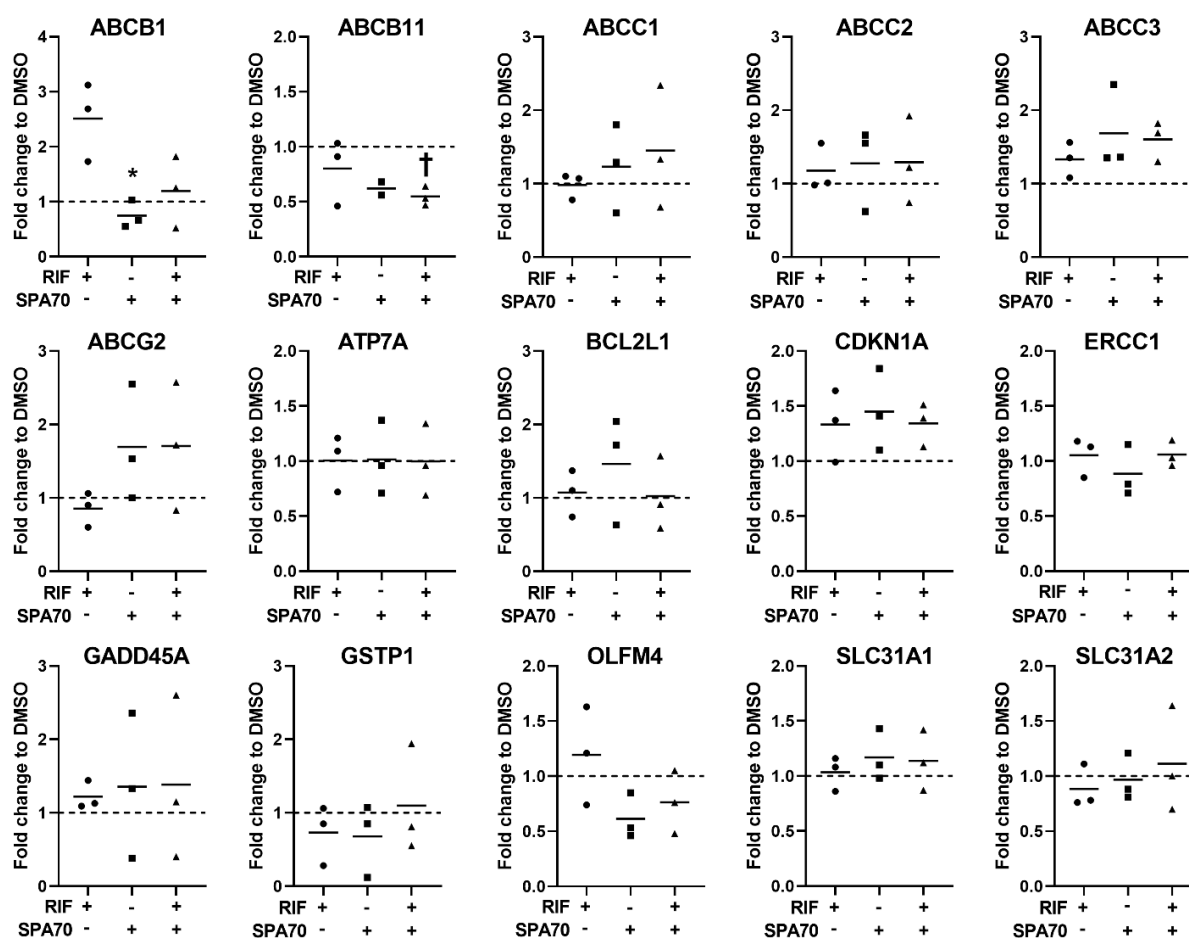


Figure 21. PXR activation or antagonism has no effect on expression of selected genes in Ls-R-C cells. Ls-R-C cells were treated with 0.2% DMSO, 10 μM rifampicin, 10 μM SPA70 or co-treated with 10 μM rifampicin and 10 μM SPA70 for 48 h. mRNA was quantified using RT-qPCR and normalized to the corresponding mean expression of 18S and TBP. Data is shown as mean fold change to DMSO-treated cells of three samples per group and individual experiments illustrated with dots. Statistically significant differences are illustrated with asterisks and daggers. * $p < 0.05$, compared to 10 μM rifampicin treatment analyzed by one-way ANOVA with Dunnett's multiple comparisons test. † $p < 0.05$, compared to 1 (DMSO) analyzed by one sample t-test corrected by the method of Bonferroni.

The effects of rifampicin and SPA70 in Ls-R-I cells resembled the effects of parental Ls-P cells. Similar to Ls-P cells, SPA70 suppressed the basal and rifampicin-induced ABCB1 and CYP3A4 expression in Ls-R-I cells (Fig. 22). In addition, single treatment of SPA70 and as

co-treatment with rifampicin showed a slight declining trend in expression of CDKN1A, FGF19 and GADD45A. PXR antagonism reduced also the elevated expression of ABCB1, CYP3A4 and FGF19 in Ls-R-I near to the basal levels of Ls-P (Fig. 23). This effect was not observed with CDKN1A or GADD45A (data not shown).

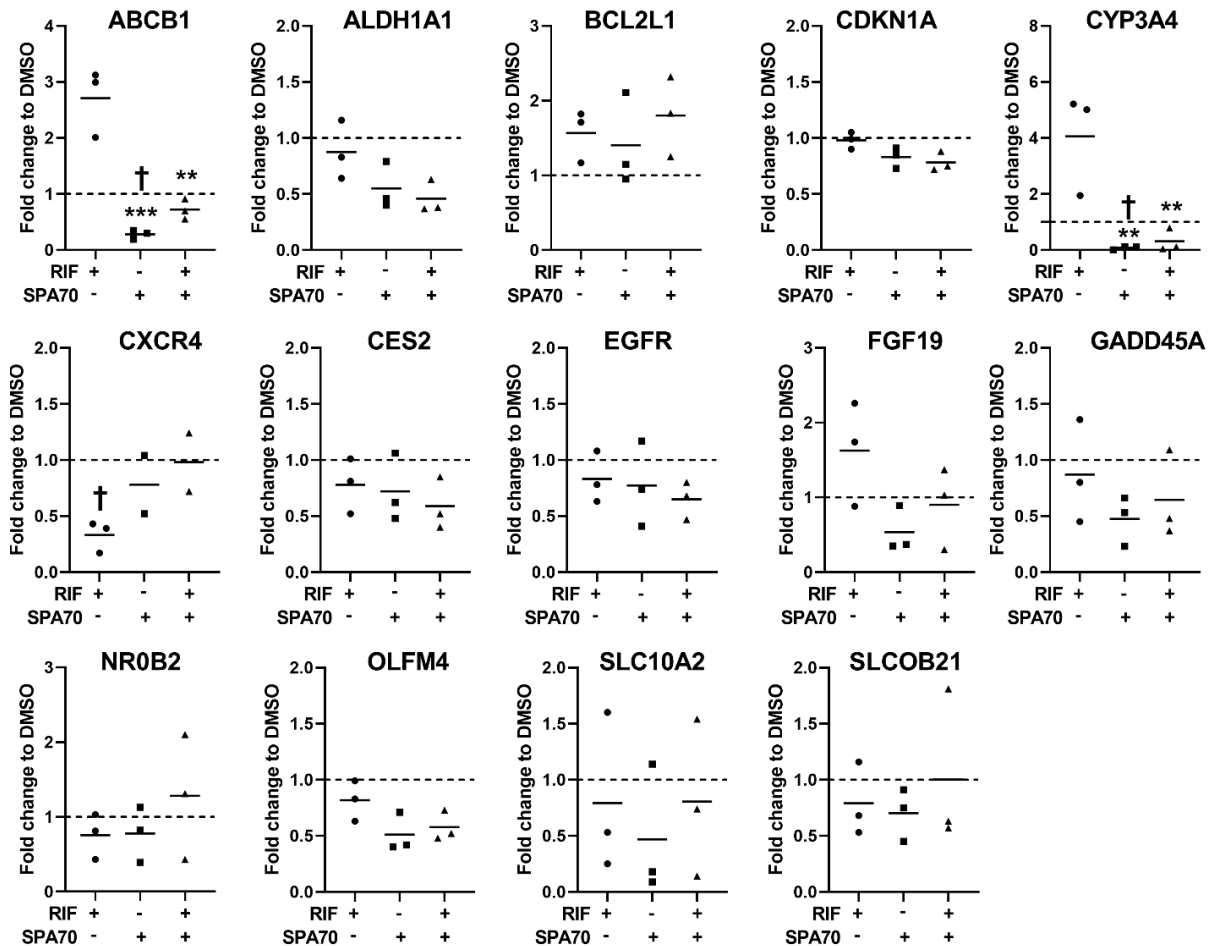


Figure 22. Effect of PXR antagonism on expression of selected genes in Ls-R-I cells. Specific PXR antagonist SPA70 attenuates rifampicin-induced expression of part of the genes that were induced in Ls-R-I cells. Ls-R-I cells were treated with 0.2% DMSO, 10 μ M rifampicin, 10 μ M SPA70 or co-treated with 10 μ M rifampicin and 10 μ M SPA70 for 48 h. mRNA was quantified using RT-qPCR and normalized to the corresponding mean expression of 18S and TBP. Data is shown as mean fold change to DMSO-treated cells of three samples per group and individual experiments illustrated with dots. Statistically significant differences are illustrated with asterisks and daggers. ** p <0.01, *** p <0.001 compared to 10 μ M rifampicin treatment analyzed by one-way ANOVA with Dunnett's multiple comparisons test. † p <0.05 compared to value 1 (DMSO) analyzed by one sample t-test corrected by the method of Bonferroni.

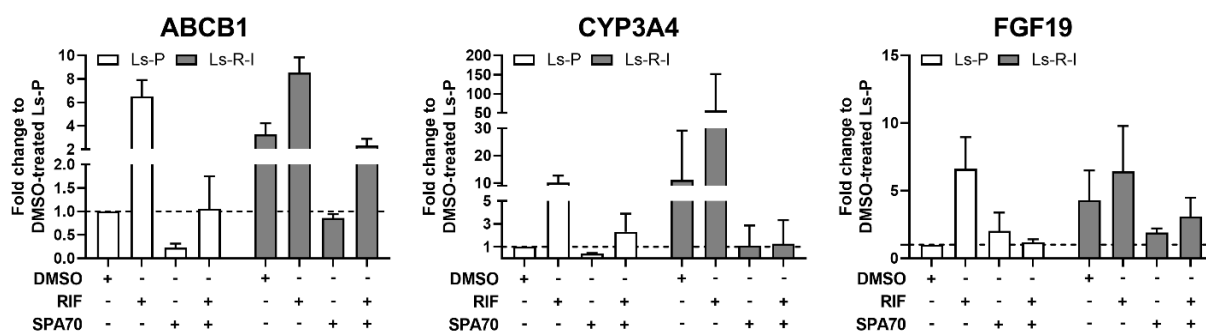


Figure 23. PXR antagonism reduces expression of induced genes in Ls-R-I cells to comparable levels as basal levels of Ls-P. Ls-P and Ls-R-I cells were treated with 0.2% DMSO, 10 μ M rifampicin, 10 μ M SPA70 or co-treated with 10 μ M rifampicin and 10 μ M SPA70 for 48 h. mRNA was quantified using RT-qPCR and normalized to the corresponding mean expression of 18S and TBP. Data is shown as mean fold change relative to DMSO-treated Ls-P cells (set as 1) of three samples per group.

4.7. Effect of PXR antagonism in irinotecan-resistant cells

Irinotecan resistance was accompanied with increased expression of several genes. Some of these potentially relevant genes for resistance appeared to be regulated by PXR, including ABCB1 and CYP3A4. Therefore, specific PXR antagonist SPA70 was utilized in aiming at to resensitize Ls-R-I cells to irinotecan. Cell viability of Ls-R-I cells was not reduced by SPA70 treatment (Fig. 24A), and as a result, IC₅₀ values in the absence or presence of SPA70 were comparable (Fig. 24B, Table 16).

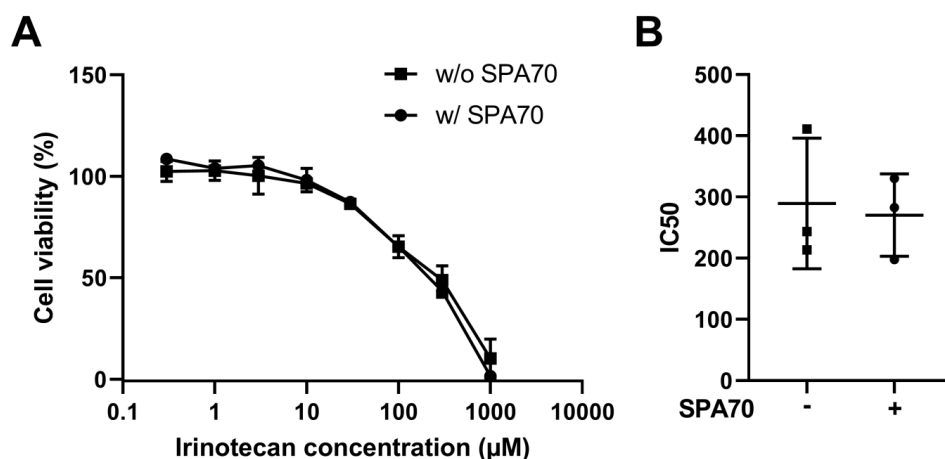


Figure 24. PXR antagonism does not resensitize Ls-R-I cells to irinotecan. (A) Ls-R-I cells showed comparable cell viabilities after treatment with and without PXR antagonist SPA70. Ls-R-I cells were pretreated for 72 h with 0.1% DMSO or 10 μ M SPA70 and then co-treated with increasing concentrations of irinotecan (0.3–1,000 μ M) in the presence or absence of 10 μ M SPA70 for 72 h. Cell viability in the presence of vehicle DMSO only was set as 100%. Data is expressed as mean cell viability \pm SD from three independent experiments with technical triplicates. (B) SPA70 treatment displayed no difference in IC₅₀ values of irinotecan in Ls-R-I cells. IC₅₀ values were calculated with nonlinear regression using GraphPadPrism (version 8.3.0). IC₅₀ is expressed as mean \pm SD from three independent experiments and individual experiments illustrated with dots. Statistical significances illustrated with asterisks, compared to the IC₅₀ value of DMSO-treated Ls-R-I, analyzed with paired t-test.

Table 16. Drug sensitivity IC₅₀ values of irinotecan in Ls-R-I cells without and with SPA70 co-treatment.

Treatment	Irinotecan: IC ₅₀ μM (95% CI)
w/o SPA70	268.3 (161.3–463.3)
w/ SPA70	261.3 (191.0–361.8)

Ls-R-I cells demonstrated cross-resistance towards paclitaxel, therefore, resensitization experiment was also conducted with SPA70. Compared to the DMSO-treated Ls-R-I cells, treatment with SPA70 increased the sensitivity (Fig. 25A) and consequently reduced the IC₅₀ of paclitaxel (Fig. 25B, Table 17). The IC₅₀ value of SPA70-treated cells was reduced to lower level than with parental LS174T cells, which was 3 nM. At the highest concentration (3,000 nM), however, still approximately 40% of the cells were viable, which is more than was with the parental cells at that concentration.

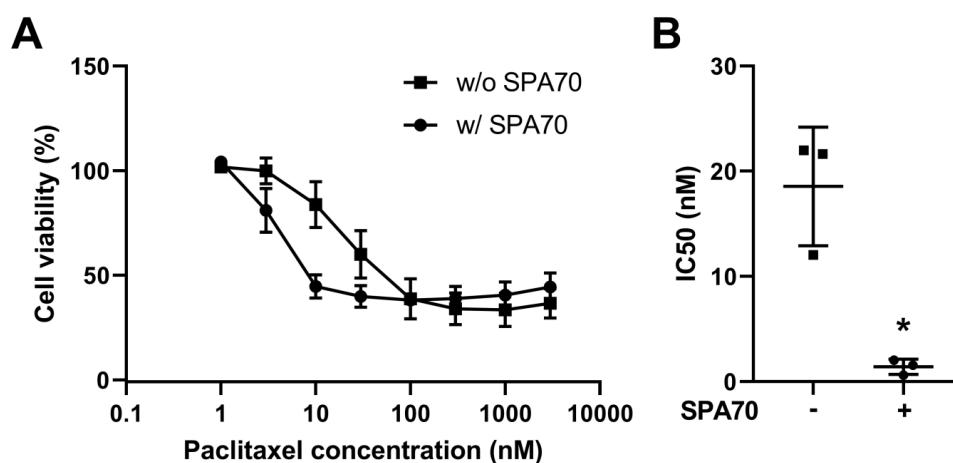


Figure 25. PXR antagonism resensitizes Ls-R-I cells to paclitaxel. (A) Ls-R-I cells showed reduced cell viability after co-treatment of paclitaxel with PXR antagonist SPA70. Ls-R-I cells were pretreated for 72 h with 0.1% DMSO or 10 μM SPA70 and then co-treated with increasing concentrations of paclitaxel (0.1–3,000 nM) in the presence or absence of 10 μM SPA70. Cell viability in the presence of vehicle DMSO only was set as 100%. Data is expressed as mean cell viability ±SD from three independent experiments with technical triplicates. (B) SPA70 treatment decreases IC₅₀ of paclitaxel in Ls-R-I cells. IC₅₀ values were calculated with nonlinear regression using GrapPadPrism (version 8.3.0). IC₅₀ is expressed as mean ±SD from three independent experiments and individual experiments illustrated with dots. Statistical significances illustrated with asterisks, **p*<0.05, compared to the IC₅₀ value of DMSO-treated Ls-R-I, analyzed with paired t-test.

Table 17. Drug sensitivity IC₅₀ values of paclitaxel in Ls-R-I cells without and with SPA70 co-treatment.

Treatment	Paclitaxel: IC ₅₀ nM (95% CI)
w/o SPA70	17.84 (10.6–29.7)
w/ SPA70	1.4 (0.48–2.8)

4.8. Identification of novel PXR antagonists

Identification of potential PXR antagonists started with an in silico screen of the Tübingen kinase inhibitor collection (TüKIC) compound library consisting of nearly 8,500 proprietary compounds (Pharmaceutical and Medicinal Chemistry, University of Tübingen). 90% of these compounds are protein kinase inhibitors, which represent an important group of molecularly targeted cancer drugs. Rest of these compounds consist of eicosanoid modulators. This compound collection was utilized because it contains a large set of unique compounds and these compounds have not been previously investigated in relation to their PXR modulation ability. In addition, potentially these compounds could elicit a dual function by inhibiting both kinases and PXR, therefore these compounds could be of special interest for the prevention of drug resistance in cancer chemotherapy. Altogether 15,000 structures (filtered, including all tautomers and stereoisomers) were computationally docked to PXR LBP using Glide (Schrödinger LLC) (Friesner et al., 2006, 2004; Halgren et al., 2004). The most promising compounds based on docking score and visual evaluation were subsequently evaluated with computationally more demanding Induced Fit Docking (IFD) (Farid et al., 2006; Sherman et al., 2006b, 2006a). Based on the IFD results, binding modes of selected compounds were evaluated with molecular dynamic simulations (hundreds of ns to μ s). Based on these molecular modelling results, 56 of the most promising compounds were selected for PXR transactivation assay. In silico screen is able to predict only possible binding of ligands to PXR LBP and not to differentiate agonists and antagonists. Therefore, we decided to evaluate these potential ligands by comparing PXR activation of these compounds (Fig. 26A) against their capacity to inhibit rifampicin-induced activation (Fig. 26B). We decided a threshold for compounds that would be selected for further testing: $\leq 50\%$ activation in both agonist and antagonist modes. Out of the 56 compounds, two (**2**, **12**) passed this threshold.

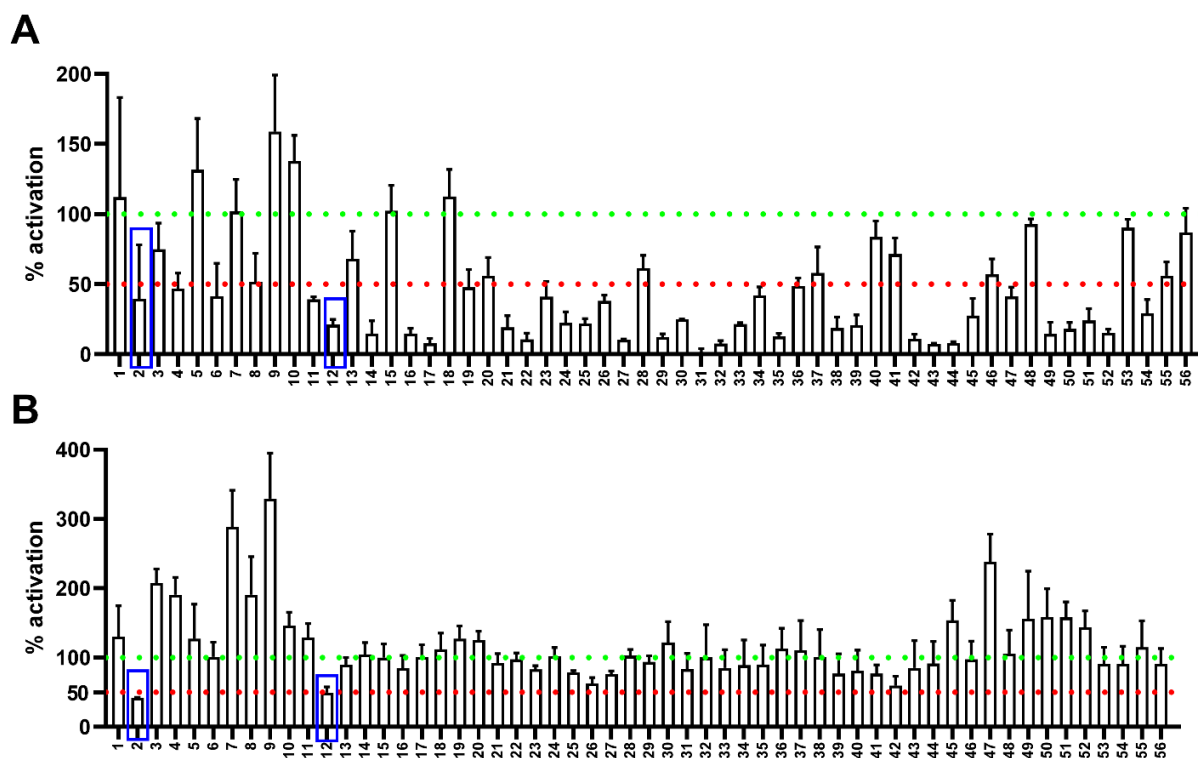


Figure 26. Effects of *in silico* screened TükIC compounds (A) alone or (B) in combination with 10 μ M rifampicin on PXR-mediated transactivation of CYP3A4 reporter gene. HepG2 cells with stable PXR expression were transiently transfected with CYP3A4 reporter gene, treated with 0.1% (A) or 0.2% (B) DMSO, 10 μ M rifampicin, 10 μ M test compounds or co-treated with 10 μ M rifampicin and 10 μ M test compounds. Luciferase activities were measured after 24 h treatment. Data is expressed as mean \pm SD % activation calculated according to (Zhu et al., 2004) from three independent experiments with technical triplicates. Fold induction achieved by 10 μ M rifampicin was set as 100%. Green and red dashed lines represent the 100% and 50% activation, respectively. Compounds that were selected for further testing are highlighted with blue rectangles.

Interestingly, these two compounds (**2**, **12**) appeared structurally similar. This motivated us to conduct a structural analogue search from the TükIC compound library against these two compounds with the aim to obtain the best coverage of structurally diverse representative set of analogues and understanding of structure-activity relationship (SAR) within this compound series. This resulted in identification of 30 structurally related additional potential ligands, which were tested in relation to their PXR-activation potential (Fig. 27A) and their capability to suppress rifampicin-induced PXR activation (Fig. 27B). From all these compounds, one compound (**73**) showed PXR antagonizing potential. Compared to compounds **2** and **12**, this compound showed weaker PXR activation and stronger suppression of rifampicin-induced PXR activation.

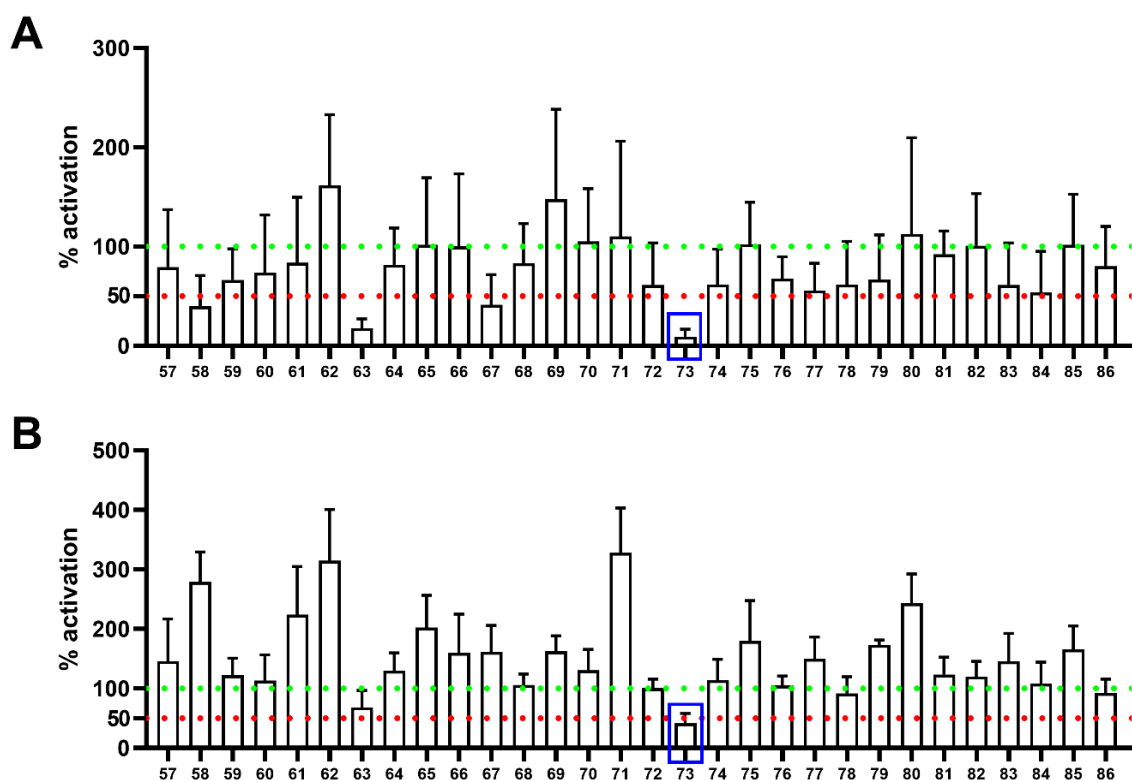


Figure 27. Effects of structural analogues of compounds 2 and 12 (A) alone or (B) in combination with rifampicin on PXR-mediated transactivation of CYP3A4 reporter gene. HepG2 cells with stable PXR expression were transiently transfected with CYP3A4 reporter gene, treated with 0.1% (A) or 0.2% (B) DMSO, 10 μ M rifampicin, 10 μ M of test compounds or co-treated with 10 μ M rifampicin and 10 μ M test compounds. Luciferase activities were measured after 24 h treatment. Data is expressed as mean \pm SD % activation calculated according to (Zhu et al., 2004) from three independent experiments with technical triplicates. Fold induction achieved by 10 μ M rifampicin was set as 100%. Green and red dashed lines represent the 100% and 50% activation, respectively. The compound that was selected for further testing is highlighted with blue rectangles.

Similarly, compound **73** was utilized in a subsequent structural analogue search. This time search was based on the activity data from previous rounds utilizing the information of beneficial and non-beneficial substituents. This search resulted in identification of additional 25 potential ligands. One of them (**100**) showed potential for PXR antagonism (Fig. 28). This compound displayed only 13% activation of PXR compared to rifampicin and suppressed by 70% the rifampicin-induced PXR activation. Surprisingly, testing identified also one potential PXR agonist (**109**) with high structural similarity to the identified potential antagonists.

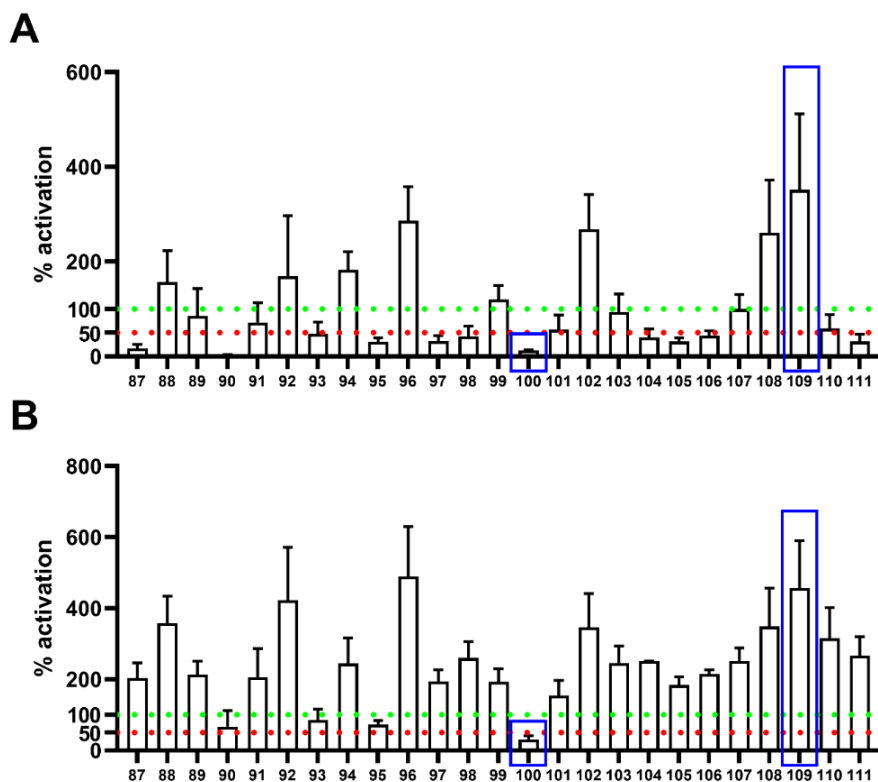


Figure 28. Effects of structural analogues of compound 73 (A) alone or (B) in combination with rifampicin on PXR-mediated transactivation of CYP3A4 reporter gene. HepG2 cells with stable PXR expression were transiently transfected with CYP3A4 reporter gene, treated with 0.1% (A) or 0.2% (B) DMSO, 10 μ M rifampicin, 10 μ M of test compound or co-treated with 10 μ M rifampicin and 10 μ M test compounds. Luciferase activities were measured after 24 h treatment. Data is expressed as mean \pm SD % activation calculated according to (Zhu et al., 2004) from three independent experiments with technical triplicates. Fold induction achieved by 10 μ M rifampicin was set as 100%. Green and red dashed lines represent the 100% and 50% activation, respectively. Compounds that were selected for further testing are highlighted with blue rectangles.

Overall, testing of selected compounds from TükIC library resulted in identification of four potential PXR antagonists with high structural similarity and a structurally highly similar potent full agonist (Fig. 29). All compounds contain benzosuberone moiety, two additional aromatic rings and an amide.

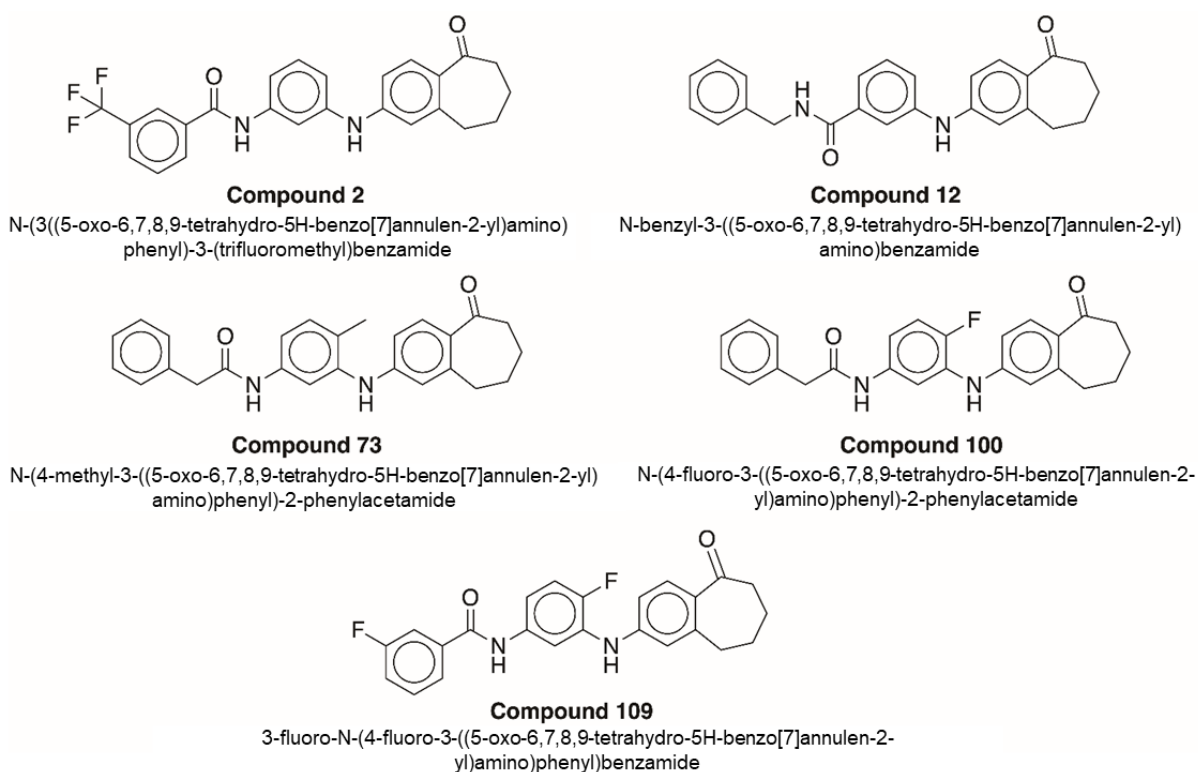


Figure 29. Structures of potential PXR ligands.

To confirm that antagonistic effects of these four potential antagonists (**2**, **12**, **73**, **100**) were not only rifampicin-specific, their ability to suppress SR12813-induced PXR activation was assessed. All of the compounds suppressed SR12813-induced PXR activation in a similar way as they suppressed rifampicin-induced activation, except compound **12**, which displayed only 30% reduction in SR12813-induced activation (Fig. 30). These results provided further support for the assumption that these compounds act as PXR antagonists.

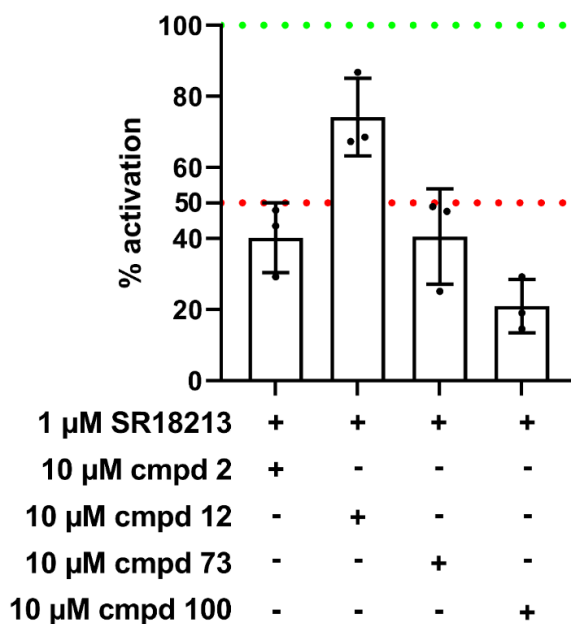


Figure 30. Effects of compounds 2, 12, 73 and 100 in combination with 1 μM SR18213 on PXR-mediated transactivation of CYP3A4 reporter gene. HepG2 cells with stable PXR expression were transiently transfected with CYP3A4 reporter gene, treated with 0.2% DMSO, and co-treated with 1 μM SR18213 and 10 μM test compounds. Luciferase activities were measured after 24 h treatment. Data is expressed as mean ±SD % activation calculated according to (Zhu et al., 2004) from three independent experiments with technical triplicates individual experiments illustrated with dots. Fold induction achieved by 1 μM SR12813 was set as 100%. Green and red dashed lines represent the 100% and 50% activation, respectively.

Next, cell toxicity of the four novel potential PXR antagonists and the structurally-related agonist was determined. Compounds **2**, **73**, **100** and **109** showed modest toxicity (cell viability >75%) at 10 μM, whereas compound **12** exhibited similar cell viability also at the highest tested concentration, which was 30 μM (Fig. 31). Therefore 30 μM for compound **12** and 10 μM for other test compounds were selected to be used as the highest concentrations in subsequent assays.

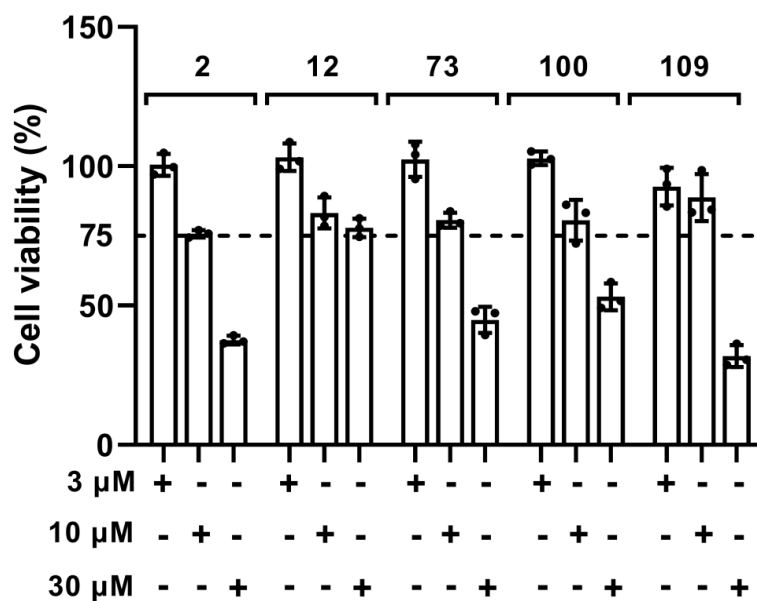


Figure 31. Cell viability of HepG2 cells following 24 h treatment with novel PXR ligands. HepG2 cells were seeded, and on following day treated with 0.1% DMSO, 3, 10 and 30 μM of test compounds. Cell viabilities were measured after 24 h incubation with treatments using CellTiter-Glo assay. Cell viability in the presence of vehicle DMSO only was set as 100%. Results are expressed as mean \pm SD from three independent experiments with technical triplicates and individual experiments illustrated with dots.

4.9. Concentration-response analysis of potential PXR antagonists

To assess the PXR inhibition potential of these four potential antagonists, reporter gene assays were conducted after co-treatment of cells with increasing concentrations of test compounds together with 10 μM rifampicin. The IC_{50} values with 95% confidence intervals for compounds **2**, **12**, **73** and **100** were 11.2 (7.7–17.2), 33.7 (20.2–61.6), 8.3 (6.1–11.7) and 2.8 (2.1–3.8) μM , respectively (Fig. 32). Based on this, compound **100** appears to be the most effective and potent antagonist of the four identified compounds.

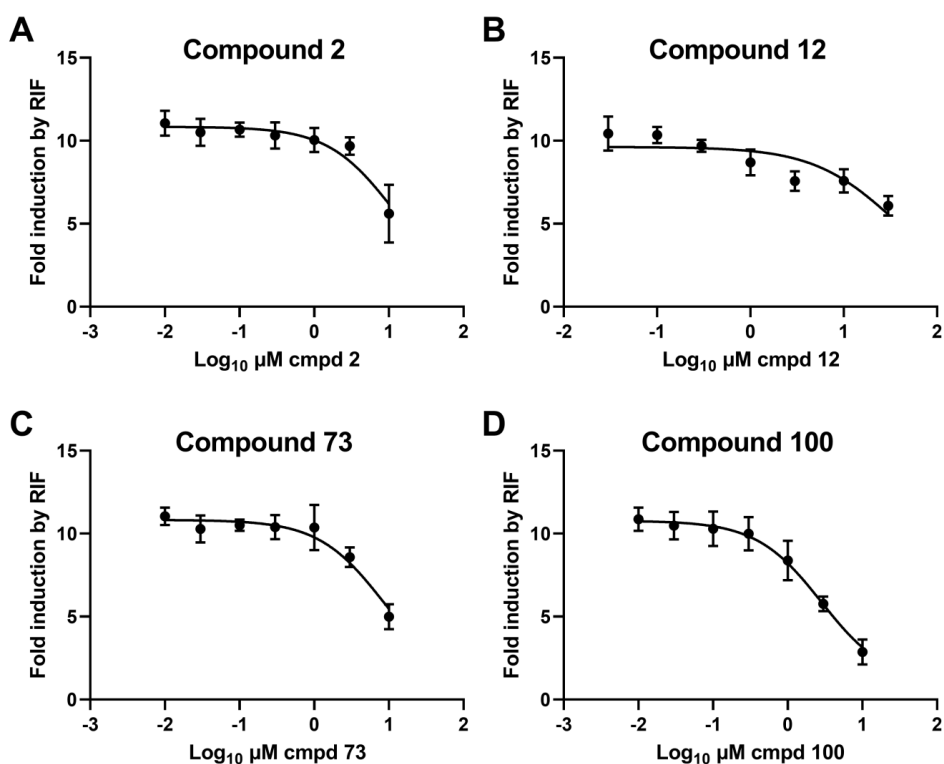


Figure 32. Determination of IC₅₀ values for compounds (A) 2, (B) 12, (C) 73 and (D) 100. HepG2 cells with stable PXR expression were transiently transfected with CYP3A4 reporter and co-treated with 10 μM rifampicin and increasing concentrations of test compounds. Luciferase activities were measured after 24 h treatment. Data is expressed as mean ±SD fold induction with respect to the DMSO-treated cells from three independent experiments with technical triplicates. IC₅₀ values calculated with nonlinear regression using formula with 3 parameters (constraint bottom =1) using GraphPadPrism (version 8.3.0).

As observed in initial testing, the potential PXR antagonists also appeared to display partial agonistic activity (Fig. 26A-28A). Therefore, concentration-response analyses were conducted and their EC₅₀ values were determined (Fig. 33). The maximal effect was low with compounds **2**, **73** and **100**, while compound **12** showed modest activation of PXR at the highest concentration. The EC₅₀ values with 95% confidence intervals for compounds **2**, **12**, **73** and **100** were 7.0 (1.2–?), 22.3 (8.8–110.1), 0.4 (0.2–0.9) and 0.2 (0.04–0.5) μM, respectively. The EC₅₀ value for the potential agonistic compound **109** was also determined, which was 29.2 μM (20.0–?) (Fig. 33E). Plateau, however, was not reached with all test compounds, because higher concentrations could not be used due to toxicity. For this reason, upper confidence limit could not be determined for compounds **2** and **109**.

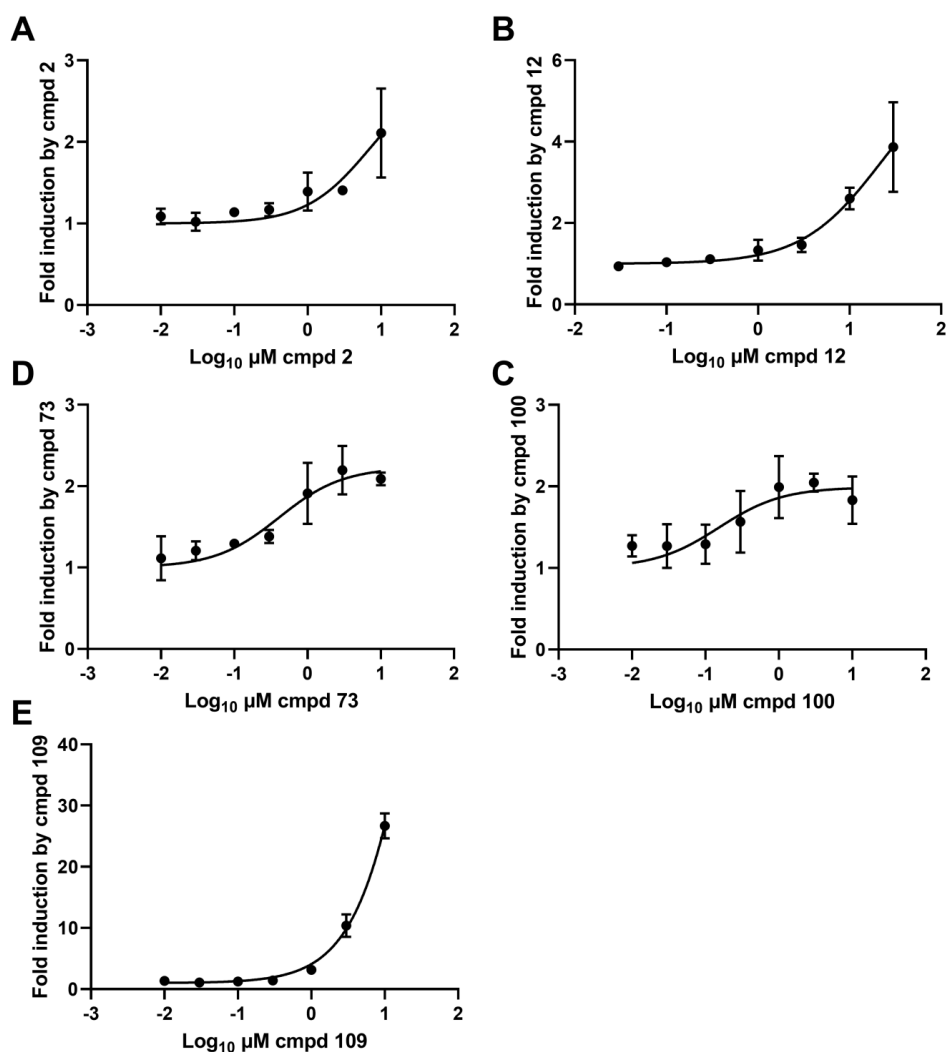


Figure 33. Concentration-response analysis of the compounds (A) 2, (B) 12, (C) 73, (D) 100 and (E) 109 demonstrating PXR agonism. HepG2 cells with stable PXR expression were transiently transfected with CYP3A4 reporter gene, treated with 0.1% DMSO, increasing concentrations of test compounds. Luciferase activities were measured after 24 h treatment. Data is expressed as mean \pm SD fold induction with respect to the DMSO-treated cells from three independent experiments with technical triplicates. EC_{50} values calculated with nonlinear regression using formula with 3 parameters (constraint bottom =1) using GraphPadPrism (version 8.3.0).

4.10. Mode of antagonism of potential PXR antagonists

To clarify the mechanism of PXR inhibition by these potential antagonists, the effect of test compounds with increasing concentrations to dose-response of rifampicin was assessed (Fig. 34). Increase in the concentration of test compounds increased the EC_{50} value of rifampicin, indicating that these compounds elicit competitive antagonism (Table 18).

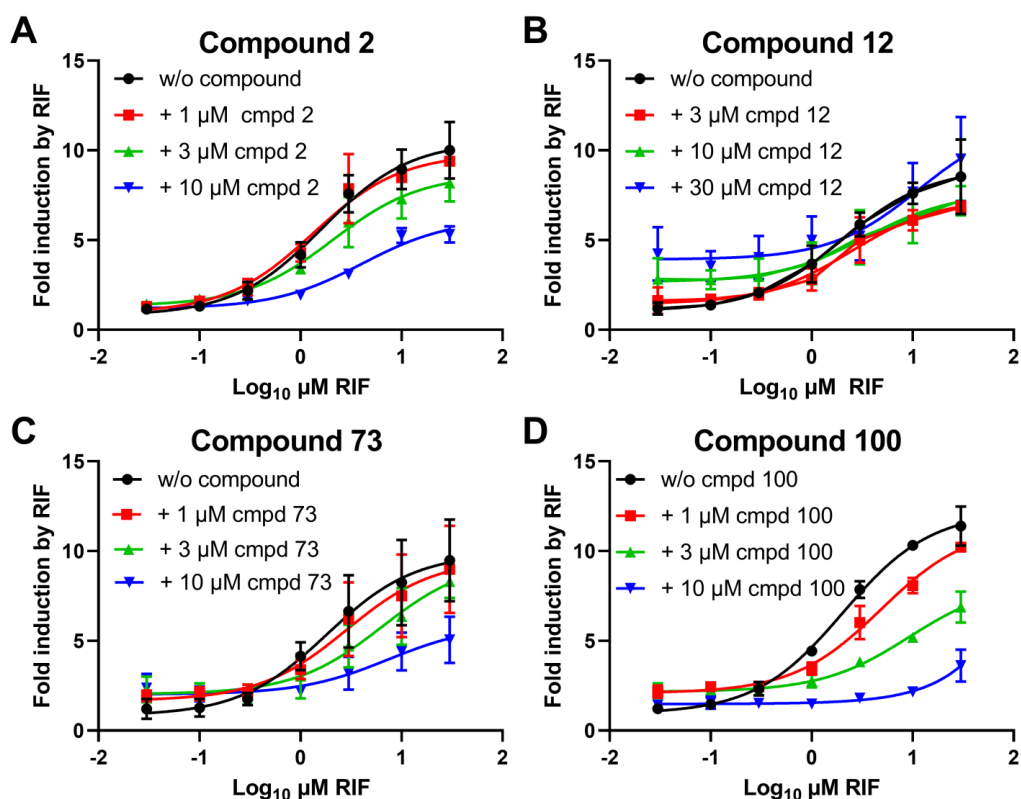


Figure 34. Effects of compounds 2 (A), 12 (B), 73 (C) and 100 (D) on the concentration-response curve of rifampicin. HepG2 cells with stable PXR expression were transiently transfected with CYP3A4 reporter gene, treated with increasing concentrations of rifampicin with or without fixed concentrations of test compounds. Luciferase activities were measured after 24 h treatment. Data is expressed as mean \pm SD fold induction with respect to the DMSO-treated cells from three independent experiments with technical triplicates.

Table 18. EC₅₀-values of rifampicin with co-treatments of compounds 2, 12, 73 and 100.

	EC ₅₀ μ M of RIF (95% CI)			
	Compound 2	Compound 12	Compound 73	Compound 100
w/o compound	1.6 (0.9–2.9)	2.0 (1.1–3.8)	1.8 (0.8–4.5)	2.0 (1.6–3.0)
+ 1 μ M / 3	1.3 (0.7–2.4)	2.5 (1.3–4.6)	2.9 (1.0–9.1)	4.8 (3.4–7.0)
+ 3 μ M / 10	2.1 (1.1–4.1)	3.4 (1.0–15.1)	6.4 (2.5–19.6)	9.3 (5.4–17.0)
+ 10 μ M / 30	4.1 (2.3–7.2)	11.4 (2.3–2543)	7.4 (2.0–47.7)	2850 (wide)

Fixed concentrations of 1–10 μ M of compounds 2, 73 and 100 and 3–30 μ M of compound 12 were used.

4.11. Binding of novel PXR ligands to PXR LBD

Ligand binding domain assembly assay can be utilized to identify both agonist and antagonists that bind to LBD of nuclear receptors (Pissios et al., 2000). All tested compounds induced PXR assembly of LBD, but not as strongly as rifampicin (Fig. 35). Compound 100 displayed the highest induction (13-fold) of test compounds, followed by compound 73 (7-fold). Compounds 12 and 109 showed similar level of induction, 5- and 4.0-fold, respectively. These results provided support for the assumption that these compounds bind to the PXR LBD.

Unfortunately, compound 2 could not be tested in this assay due to limited availability of this compound.

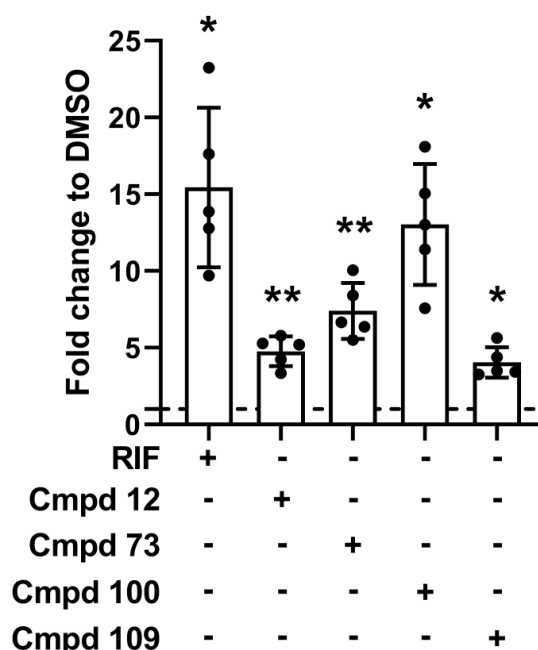


Figure 35. Novel PXR ligands induce PXR LBD assembly. HepG2 cells were transiently transfected with GL4-G5 reporter gene, GAL4-DBD/PXR-LBD(132-188) and VP16-AD/PXR-LBD(189-434) plasmids and treated on next day with 0.1% DMSO, 10 μ M rifampicin or 10 μ M test compounds. After 24 h firefly and Metridia luciferases were measured. Data is expressed as mean \pm SD fold induction with respect to the DMSO-treated cells from five independent experiments with technical triplicates and individual experiments illustrated with dots. Statistically significant differences are illustrated with asterisks. * p <0.05, ** p <0.01 compared to DMSO, which was set as 1 analyzed by one-sample t-test corrected by the method of Bonferroni.

To confirm that the newly identified PXR ligands bind to the ligand binding domain of PXR, the limited proteolytic digestion assay was performed. This assay can be utilized to study the direct binding of ligands to nuclear receptor's LBD (Lemaire et al. 2007). Ligands that bind directly to the LBD cause conformational changes, which hinder the accessibility of proteases to the protease cleavage sites. Known PXR agonist T0901317 was used as a positive control, which caused a limited proteolytic digestion pattern demonstrating binding to the LBD. Similarly, all of the novel PXR ligands resulted in protection of proteolytic fragments of the PXR LBD, even though the pattern was not exactly the same as with T0901317 (Fig. 36). The pattern can be distinct due to the different conformational changes induced by the ligand binding.

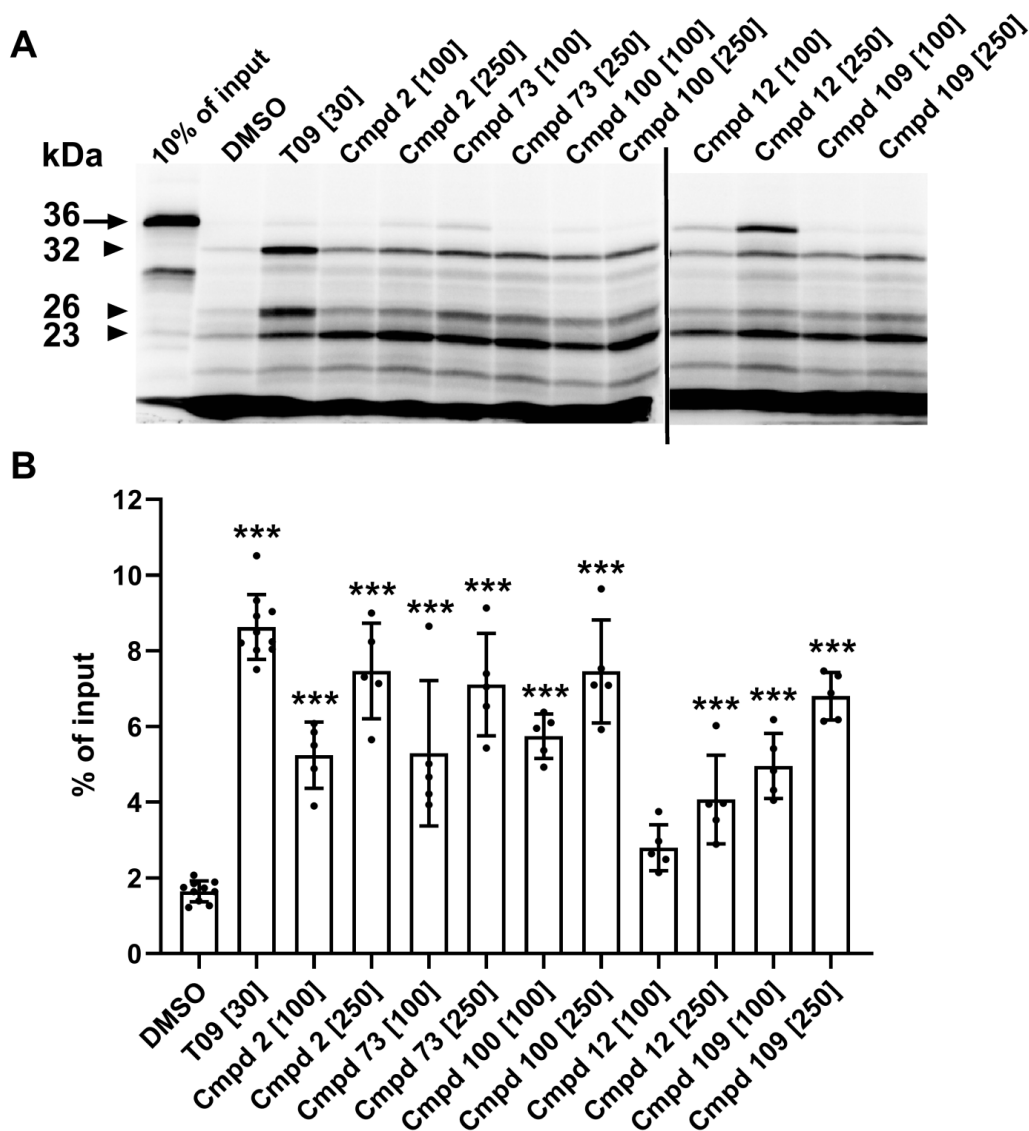


Figure 36. All novel PXR ligands bind directly to the PXR-LBD. Limited proteolytic digestion analysis was conducted by pre-incubating PXR-LBD with 100 μ M or 250 μ M test compounds, 30 μ M T0901317 (T09) or 2.5% DMSO. **(A)** Arrow shows 36 kDa input of PXR-LBD, and arrow heads show protected 32, 26 and 23 kDa fragments after limited proteolytic digest with trypsin. **(B)** Respective densitometric quantifications of the sum of the three protected fragments. Columns show mean \pm SD of five independent experiments and the individual experiments illustrated with dots calculated with respect to input. Statistically significant differences are illustrated with asterisks. *** p <0.001, compared to respective pre-incubations with DMSO analyzed by one-way ANOVA with Dunnett's multiple comparisons test.

4.12. Relevance of specific amino acids for ligand binding of potential PXR ligands

Previous studies (Banerjee et al., 2016; Ngan et al., 2009) and our docking pose analysis and molecular dynamic simulations with compound 100 suggest that the following amino acids are critical for ligand binding interactions: Q285, S247, H407, W299, Y306 and H327. Therefore, these amino acids were mutated to alanine and the relevance of these amino acids on the activation of PXR by the novel PXR ligands was investigated. In addition, constitutively active

LBP-filled triple mutant S208W/S247W/C284W (Wang et al., 2008) was included to assess, if the potential PXR ligands can still antagonize or activate PXR, even when the LBP is filled by mutation of selected amino acids to bulky tryptophan.

First, to assess the effect of these mutations on their protein expression in cells, HepG2 cells were transfected with these mutants and Western blot was performed with total protein extracts. PXR mutants were detected similarly as WT PXR at approximately 50 kDa (Fig. 37). Expression levels of the mutants were similar to wild-type PXR. Except H327A, which displayed slightly lower expression.

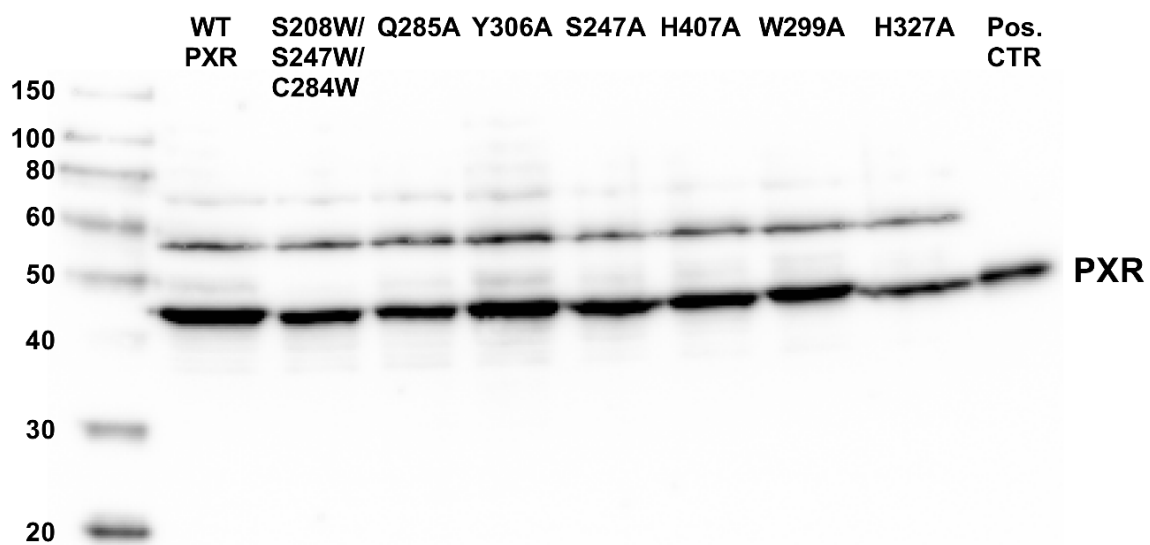


Figure 37. Transfected PXR mutants are expressed in HepG2 cells. PXR mutants were detected at similar size as wild-type PXR (WT PXR), at approximately 50 kDa. HepG2 cells were transfected using CaPO₄ and glycerol shock with plasmids encoding WT PXR, triple or single amino acid mutated PXR mutants. Two days later, Metiridia luciferase was measured, cells were harvested and total protein was extracted. Loaded protein amount was adjusted to the transfection efficiency measured with Metiridia luciferase activity. Western blot was performed using anti-PXR antibody. Positive control (Pos.CTR) was in vitro translated PXR protein.

To assess the constitutive or ligand-induced activities of the single PXR mutants, transfected cells were treated with rifampicin. Similar to WT PXR, mutants Q285A and W299A maintained their inducibility by rifampicin, whereas mutants S247A and H407A showed high basal constitutive activity, but they were not further inducible by rifampicin (Fig. 38). In contrast, mutant Y306A displayed neither constitutive nor rifampicin-induced activity.

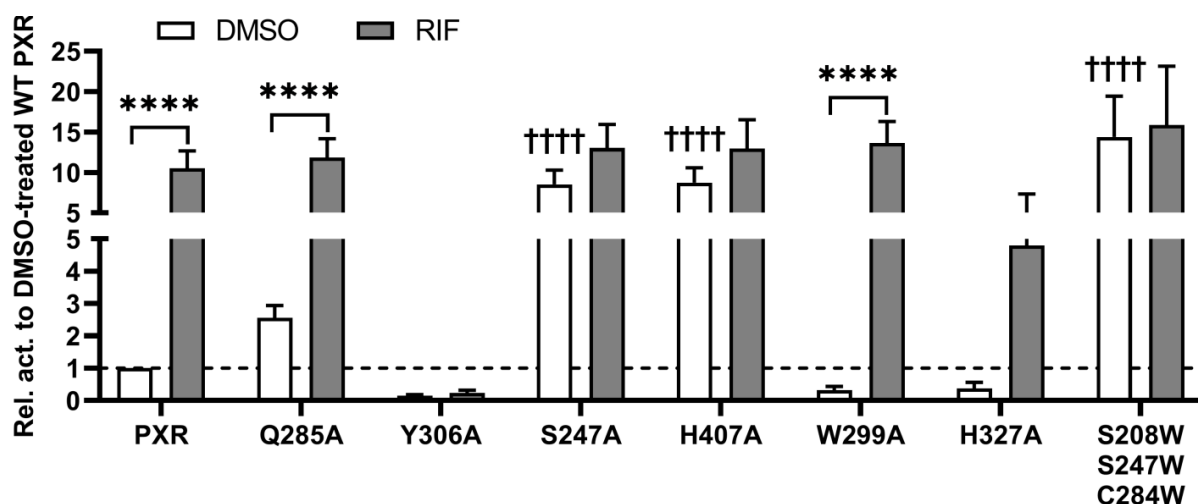


Figure 38. Constitutive or ligand-induced activity of single or triple amino acid mutated mutants compared to wild-type PXR. HepG2 cells were transiently transfected with expression plasmids encoding wild-type PXR (WT PXR) or indicated single or triple PXR mutants and treated with 0.1% DMSO or 10 μ M rifampicin. After 24 h firefly and Metridia luciferases were measured. Data is expressed as mean activity \pm SD relative to the DMSO-treated WT PXR from five independent experiments with technical triplicates. Statistically significant differences are illustrated with asterisks or daggers. **** p <0.0001 compared to DMSO-treated respective plasmid analyzed by two-way ANOVA with Sidak's multiple comparisons test. †††† p <0.0001 compared to DMSO-treated WT PXR analyzed by one-way ANOVA with Dunnett's multiple comparisons test.

To investigate the effect of the novel potential PXR antagonists and the structurally-related agonist (**109**) on activation of single or triple PXR mutants, cells transfected with these mutants where treated with the test compounds. Test compounds activated mutant Q285A quite similarly as WT PXR (Fig. 39). None of the test compounds activated mutant Y306A, which also displayed low basal activity compared to WT PXR (Fig. 38). The activity of constitutively active mutant S247A was inhibited by compounds **73** and **100**, whereas compound **109** further activated this mutant slightly. In contrast, compounds **73** and **100** were incapable to inhibit the constitutive active mutant H407A, whereas compounds **12** and **109** showed slight activation of this mutant. Compounds **73** and **100** displayed higher activation of mutant W299A compared to other mutants, whereas compound **12** activated this mutant only weakly. Mutant H327A was modestly activated by compounds **12** and **73**, whereas compounds **100** and **109** showed stronger activation. Generally, test compounds exhibited no effects on constitutively active triple mutant, besides compound **73**, which slightly inhibited the activity of this mutant and compound **109**, which weakly activated this mutant. Unfortunately, compound **2** could not be tested in this and subsequent assays due to limited availability of this compound.

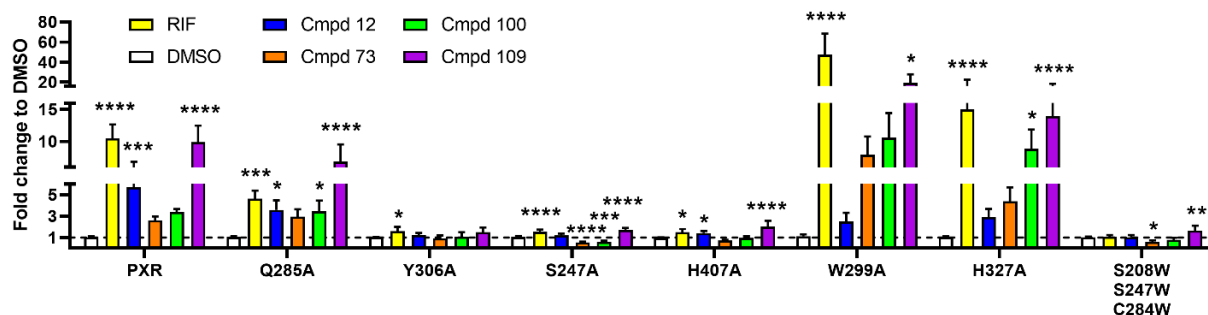


Figure 39. Ligand-induced effects on activation of single or triple amino acid mutated PXR mutants. HepG2 cells were transiently transfected with expression plasmids encoding wild-type PXR (WT PXR) or indicated single or triple PXR mutants and treated with 0.1% DMSO, 10 μ M rifampicin or 10 μ M test compounds. After 24 h firefly and Metridia luciferases were measured. Results are expressed as mean \pm SD fold induction with respect to the DMSO-treated respective plasmid from five independent experiments with technical triplicates. Statistically significant differences are illustrated with asterisks. * p <0.05, ** p <0.01, *** p <0.001, **** p <0.0001 compared to DMSO-treated respective cells within mutant group analyzed by one-way ANOVA with Dunnett's multiple comparisons test.

4.13. Effects of novel PXR ligands on coregulatory protein interactions with PXR

Ligand-dependent interactions of coregulatory proteins with PXR were investigated with mammalian two hybrid assays. Agonist compound **109** promoted the interaction of co-activator SRC1 with PXR, but not as strongly as rifampicin. In contrast, the potential PXR antagonists did not promote SRC1 recruitment; however, they impaired the rifampicin-induced interaction of SRC1 with PXR (Fig. 40A). The constitutive interaction of corepressor SMRT with PXR was reduced by rifampicin and in a similar way by the agonist compound **109**. Likewise, all three novel PXR antagonists impaired the constitutive interaction of PXR LBD with SMRT to same extent or even more as rifampicin (Fig. 40B). As both SRC1 and SMRT bind to the same AF-2 region (Pavek, 2016), it indicates that the potential antagonists distort the interactions for both coregulators in this region.

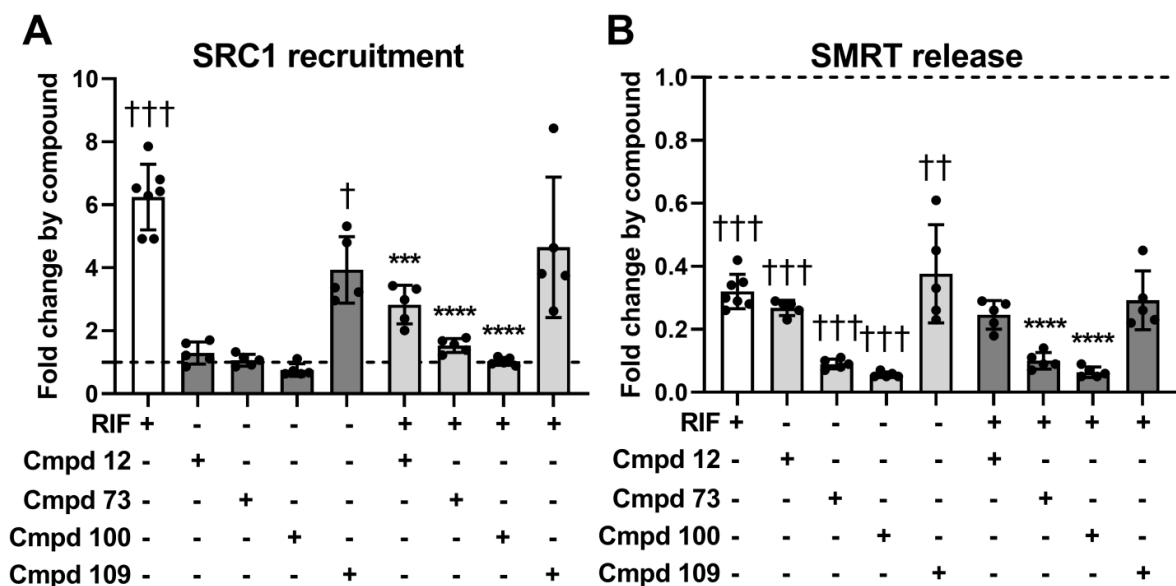


Figure 40. Effects of novel PXR ligands on coregulatory protein interactions with PXR. HepG2 cells were co-transfected with GL4-G5 reporter gene and expression plasmids encoding VP16-PXR-LBD(108-434) fusion protein and (A) GAL4-DBD-SRC1-RID or (B) GAL4-DBD-SMRT-RID and treated with 0.2% DMSO, 10 μ M test compounds alone or co-treated with 10 μ M rifampicin. Results are expressed as mean \pm SD fold induction with respect to the DMSO-treated cells from five independent experiments with technical triplicates and individual experiments illustrated with dots. Statistically significant differences are illustrated with asterisks or daggers. *** p <0.001, **** p <0.0001 co-treatments compared to 10 μ M rifampicin-treated cells analyzed by one-way ANOVA with Dunnett's multiple comparisons test. †† p <0.01, ††† p <0.001 single treatments compared to DMSO which was set as 1 analyzed by one sample t-test corrected by the method of Bonferroni.

4.14. Effects of novel PXR ligands on expression of endogenous PXR target genes

LS174T cells with high PXR expression were utilized to investigate whether the novel PXR ligands affect the PXR-mediated endogenous gene expression. Rifampicin treatment induced the expression of ABCB1 and CYP3A4, as expected, whereas CYP2B6 or AKR1B10 were not induced. Test compounds showed gene-specific effects. Compounds **73** and **100**, as single treatments, did not induce expression of ABCB1 (Fig. 41A). In addition, rifampicin-induced expression of ABCB1 was suppressed by compounds **73** and **100**. Not only single treatments of compounds **73** and **100**, but also co-treatments with rifampicin suppressed the basal expression level of CYP2B6 (Fig. 41B). In contrast, these compounds induced expression of CYP3A4; however, variability between samples was large (Fig. 41C). In contrast to compounds **73** and **100**, compound **12** showed no inhibition of rifampicin-induced gene expression (Fig. 41). Moreover, single treatment of compound **12** induced ABCB1 and CYP3A4 4-fold and 8-fold, respectively. Compound **12** exhibited also strong additive effect with rifampicin on expression of CYP3A4. Compound **109**, which was identified in the reporter

gene assays as a strong activator of PXR exhibited on average 17-fold induction of CYP3A4 with large variability, whereas ABCB1 and AKR1B10 were induced to lesser extent (Fig. 42).

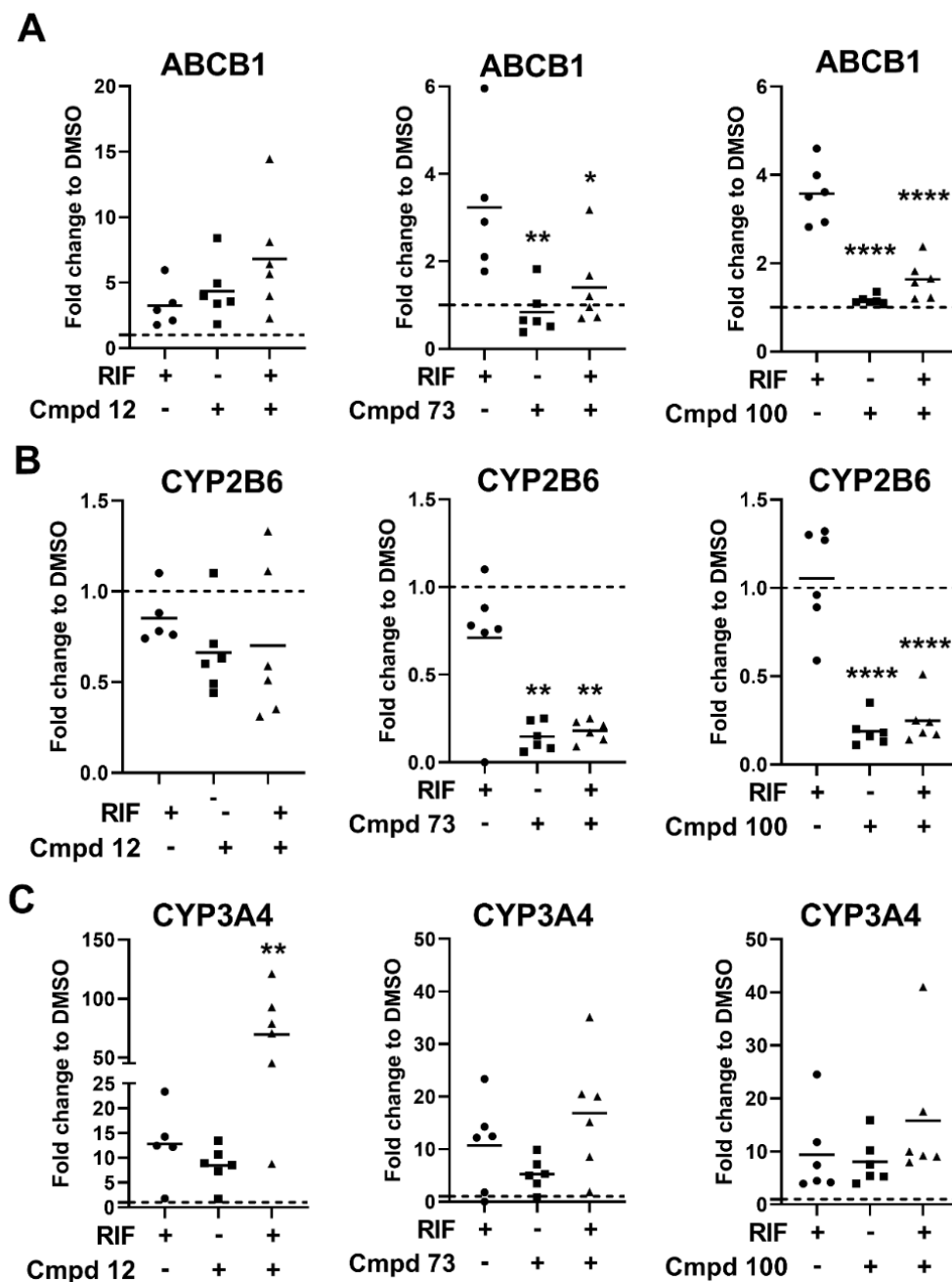


Figure 41. Effects of potential PXR antagonists on expression of endogenous PXR target gene expression. LS174T cells were treated with 0.2% DMSO, 10 μ M rifampicin, or 10 μ M test compounds or co-treated with 10 μ M rifampicin and 10 μ M test compounds for 72 h. mRNA of (A) ABCB1, (B) CYP2B6 and (C) CYP3A4 was quantified using RT-qPCR and normalized to the corresponding expression of 18S. Data is expressed as mean fold change with respect to the DMSO-treated cells, which was set as 1, from six independent experiments with technical triplicates and individual experiments illustrated with dots. Statistically significant differences are illustrated with asterisks. * p <0.05, **** p <0.0001 compared to 10 μ M rifampicin-treated cells analyzed by one-way ANOVA with Dunnett's multiple comparisons test.

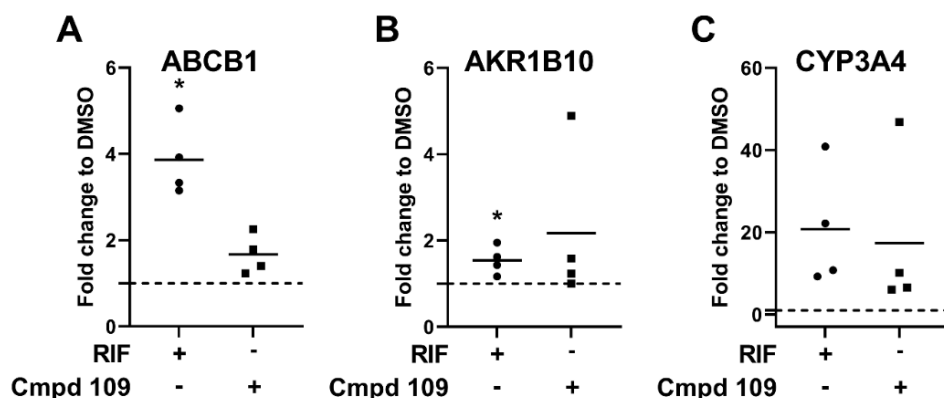


Figure 42. Effect of potential PXR agonist compound 109 on expression of endogenous PXR target genes. LS174T cells were treated with 0.1% DMSO, 10 μ M rifampicin or 10 μ M compound 109 for 48 h. mRNA of (A) ABCB1, (B) AKR1B10 and (C) CYP3A4 was quantified using RT-qPCR and normalized to the corresponding expression of 18S. Results are expressed as mean fold change with respect to the DMSO-treated cells, which was set as 1, from four independent experiments with technical triplicates and individual experiments illustrated with dots. Statistically significant differences are illustrated with asterisks. * p <0.05 compared to DMSO which was set as 1 analyzed by one sample t-test corrected by the method of Bonferroni.

4.15. Nuclear receptor selectivity of novel PXR ligands

To evaluate the specificity of these novel PXR ligands, we investigated their potential to activate or suppress the transactivation of constitutive androstane receptor (CAR) and vitamin D receptor (VDR). These two receptors were selected because of their close structural resemblance to PXR. PXR, CAR and VDR belong to the same nuclear receptor subfamily 1 group (NR11). Moreover, the sequence similarity between these receptors is for DBD and LBD 63-66% and 37-45%, respectively (Wu et al., 2013b). Two isoforms of CAR were included: constitutive active isoform 1 and ligand-induced isoform 3.

The constitutive activity of CAR1 was weakly suppressed by compound 73 (Fig. 43A), while CAR3 was not induced by any of the test compounds (Fig. 43B). In addition, none of the compounds displayed additive or inhibitory effect CITCO-induced CAR3 activity. Compounds 12 and 109 displayed weak activation of VDR, but for both compounds activation was less than 5% of $1\alpha,25(\text{OH})_2\text{D}_3$ -induced activation. None of the compounds showed additive or inhibitory effect on $1\alpha,25(\text{OH})_2\text{D}_3$ -induced activity (Fig. 43C). This suggests that these compounds exhibit selectivity towards PXR among this group of nuclear receptors.

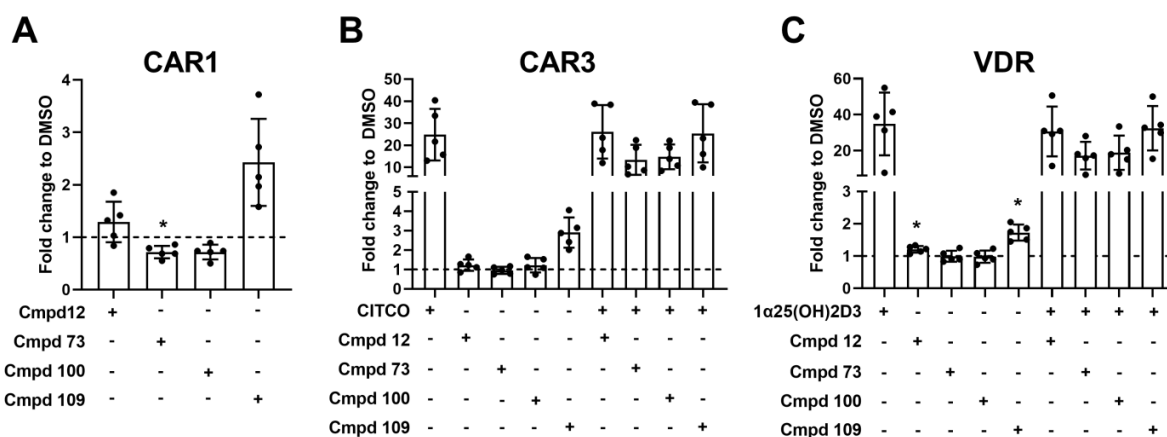


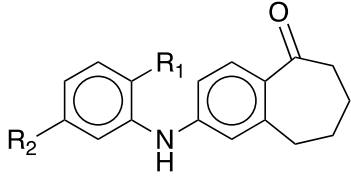
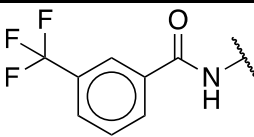
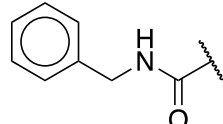
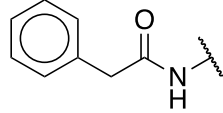
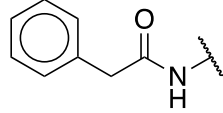
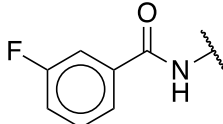
Figure 43. Nuclear receptor selectivity of potential PXR ligands. HepG2 cells were transiently transfected with CYP3A4 reporter gene and expression plasmids encoding (A) CAR1 and (B) CAR3 or direct repeat (DR3)₃ reporter gene and expression plasmid encoding (C) VDR. Then, cells were treated with 0.2% DMSO, 10 μM CITCO, 1 μM 1α,25(OH)₂D₃ or co-treated with test compounds. After 24 h firefly and Metridia luciferase were measured. Data is expressed as mean ±SD fold induction with respect to the DMSO-treated cells from five independent experiments with technical triplicates and individual experiments illustrated with dots. Statistically significant differences are illustrated with asterisks. **p*<0.05 single treatments of test compounds compared to DMSO-treated cells set as 1 analyzed by one sample t-test corrected by the method of Bonferroni and co-treatments compared to (B) 10 μM CITCO or (C) 1 μM 1α25(OH)₂D₃ analyzed by one-way ANOVA with Dunnett's multiple comparisons test.

4.16. Structure-activity relationship (SAR) analysis

All these novel PXR ligands share a common molecular scaffold (Table 19). Subtle differences in the molecular structures appear to impact greatly to the PXR activation and inhibition ability of these compounds. Clear structure-activity relationship (SAR) trends are evident within this compound series. Size of the R₁ substituent in the middle ring appears to correlate with the antagonistic activity. In this position, the two most potent antagonists (**73**, **100**) contain sterically larger substituent (CH₃, F), whereas a smaller hydrogen is present with the other antagonists (**2**, **12**). In R₂ position, all compounds have a proximal lipophilic aromatic group (benzyl or phenyl), which is linked to the scaffold with an amide bond. Moreover, the increased flexibility of the benzyl group could be beneficial for the antagonistic effect. Length of the R₂ substituent is detrimental to the activity. The shortest compound (**109**) shows the highest activation of PXR, whereas compounds with longer structures are the best antagonists (**73**, **100**). Similar to compound **109**, compound **2** has phenyl amide group at the R₂ position. In compound **2**, however, the aromatic ring contains an additional CF₃ group, which increases considerably the sterical size of this substituent. Compound **12** is similar in length compared to compounds **73** and **100**, but it contains an inverted amide. This inversion, besides the hydrogen substituent in R₁, could reduce the antagonistic activity of compound **12**. Of note,

the activities of these compounds are measured in cells; therefore, it is somewhat ambiguous to what extent these observations are related to the direct binding affinity or to the induced conformational changes of PXR upon ligand binding.

Table 19. Common molecular scaffold and distinct substituents of novel PXR ligands.

Compound No.	R ¹	R ²	IC ₅₀ (95% CI)
			
2			11.2 (7.7–17.2)
12			33.7 (20.2–61.0)
73			8.3 (6.1–11.7)
100			2.8 (2.1–3.8)
			EC ₅₀ (95% CI)
109			29.2 (20.0–?)

4.17. Inhibitory effects of compounds 100 and 109 on kinases

Several kinases have been shown to phosphorylate PXR and consequently affect the transcriptional activity of PXR (Table 20). In general, phosphorylation of PXR has been shown to inhibit PXR activity and repress the expression of PXR target genes in human cell models, with the exception of JNK (Lichti-Kaiser et al., 2009; Lin et al., 2008; Pondugula et al., 2009).

Table 20. PXR phosphorylating kinases.

Kinase	Effect on gene expression	Reference
CDK1	-	Lichti-Kaiser et al., 2009
CDK2	↓ (human)	Lin et al., 2008
CDK5	↓ (human)	Dong et al., 2010
CK2	-	Lichti-Kaiser et al., 2009

GSK3	-	Lichti-Kaiser et al., 2009
JNK	↑ (human)	Taneja et al., 2018
PKA	↑ (mouse)	Ding and Staudinger, 2005a
PKA	↑ (mouse)	Lichti-Kaiser et al., 2009
PKA	↓ (human, rat)	Lichti-Kaiser et al., 2009
PKC	↓ (mouse)	Ding and Staudinger, 2005b
P70 S6K	-	Lichti-Kaiser et al., 2009
P70 S6K	↓ (human)	Pondugula et al., 2009

Compounds **100** and **109** were tested with two concentrations against 335 kinases. All the kinases that are known to phosphorylate PXR were included in the selected panel. Compound **100** at 10 μ M inhibited at least by 50% five kinases (Table 21). In addition, one of them (RAF1) was also inhibited by 86% at 1 μ M. Compound **109** not only inhibited eight different kinases at least by 50% at concentration of 10 μ M, but it also inhibited four of these at 1 μ M concentration. These results indicate that the inhibitory effect on PXR by compound **100** is not simply due to inhibition of PXR phosphorylation, as PKA inhibition should result in activation and not inhibition of PXR.

Table 21. Kinases inhibited \geq 50% by compounds 100 and 109.

		Compound 100		Compound 109	
		10 μ M	1 μ M	10 μ M	1 μ M
Kinase		Residual activity (%)			
BRAF		25	58	39	67
CK1-delta		106	110	15	23
CK1-epsilon		117	107	15	79
CK1-gamma3		105	101	32	79
MAPKAPK3		50	109	65	98
p38 alpha		73	78	4	17
p38 beta		50	71	2	3
PKA		21	97	49	86
RAF1		3	14	12	36

5. Discussion

5.1. Mechanism of resistance in cisplatin- and irinotecan-resistant cells

Long-term treatment of LS174T cells with cisplatin and irinotecan resulted in development of acquired cancer drug resistance. Compared to parental (Ls-P) cells, cisplatin-resistant (Ls-R-C) and irinotecan-resistant (Ls-R-I) cells were 6- and 78-fold more resistant, respectively. These cells proved to maintain the resistance phenotype after long-term treatment without the drug and also after a freeze/thaw cycle, thus demonstrating the stability of the phenotype. Parental LS174T cells were cultured for the same time as drug-selected cells to reduce the effects related to culture duration. Some variability, however, was observed with the cancer drug cytotoxicity, which affected the determined IC₅₀ values. First, the IC₅₀ values of cisplatin cytotoxicity of Ls-P and Ls-R-C cells after freeze/thaw test were approximately 2-fold higher than in other determinations. These results may be explained by some technical differences between the experiment settings, such as distinct cisplatin stocks. Furthermore, the IC₅₀ values of cisplatin and irinotecan cytotoxicity of Ls-R-C and Ls-R-I cells respectively, were determined to be higher after the long-term stability and freeze thaw stability experiments compared to the IC₅₀ value, which was determined directly after the end of the selection period. A possible explanation for this might be that resistant cells were cultured in drug-containing medium until the start of each the long-term and freeze/thaw stability experiment and until all the necessary repetitions of these experiments were completed, which took several weeks. Therefore, these cells could have continued acquiring resistance compared to the earlier determination of IC₅₀ after selection.

Both Ls-R-C and Ls-R-I cells were generated by continuous treatment and drug concentrations were increased in a stepwise manner. Thus, these cells can be defined as high-level laboratory models, which try to elucidate the possible resistance mechanisms (McDermott et al., 2014). In contrast to these models, the clinically relevant resistance models are usually generated using pulse treatment and lower doses (McDermott et al., 2014). These clinically relevant resistance models typically exhibit two to five-fold increases in IC₅₀ value. The disadvantage of this model type is that it can be challenging to detect subtle molecular alterations. Therefore, the aim here was to develop high-level laboratory models, where the resulting alterations can be detected with more confidence. The highest concentration that was used to generate Ls-R-C and Ls-R-I cells were 30 μ M and 40 μ M, respectively. The clinical maximum plasma concentration after single dose of cisplatin (100 mg/m²) or liposomal cisplatin (125mg/m²) has been observed to be in both cases approximately 20 μ M (Himmelstein et al., 1981;

Stathopoulos et al., 2005). Reflected to this data, the highest concentration of cisplatin used for Ls-R-C cells is close to the clinical concentrations. Furthermore, compared to the Ls-P cells, Ls-R-C cells were 6-fold more resistant, which is close to the clinically relevant models. In contrast, the dose of 125 mg/m² irinotecan administered to cancer patients has led to a maximum plasma concentration of approximately 3 μM (FDA, 2004; Schaaf et al., 2006). Therefore, the highest concentration used for generation of Ls-R-I cells was 10-fold higher than the clinical concentrations, which perhaps also reflects the observed high resistance (78-fold). The plasma concentration, however, cannot be directly correlated to the concentration of drug inside tumor. Given the above, the Ls-R-C model might reflect more the clinical situation than the Ls-R-I model.

Ls-R-C and Ls-R-I cells were cultured in 2D as a monolayer on a cell culture dish. Cell models cultured in 2D lack the proper cell-cell and cell-extracellular environment interactions (reviewed in Kapałczyńska et al., 2018). For this reason, the possible alterations in cancer cell microenvironment due to resistance in Ls-R-C or Ls-R-I cells could not be similarly observed as it would appear in 3D cell cultures, which resemble more the *in vivo* situation of tumor. 3D cultured cells have also been observed to be initially more resistant to cancer drugs when compared to same cells cultured in 2D (Breslin and O'Driscoll, 2016; Liu et al., 2018a; Souza et al., 2018). Due to this high intrinsic resistance, development of acquired resistance models could be challenging in 3D cultures. Instead, these 3D cultured models could be more suitable to investigate intrinsic drug resistance of tumors. It would be also interesting to compare the intrinsic cisplatin or irinotecan resistance of 3D cultured LS174T cells to our acquired resistance cell models. Development of acquired resistance typically takes several months as was demonstrated with Ls-R-C and Ls-R-I cells. Long-term culture in 3D is more difficult to perform than in 2D (Kapałczyńska et al., 2018). Therefore, generation of acquired cancer drug resistance in 3D culture is most likely demanding. Although, the 2D cultured Ls-R-C and Ls-R-I cells do not perfectly resemble the situation *in vivo*, these cell models should be sufficient to fulfill our aim to investigate the molecular mechanisms and the role of PXR in acquired cancer drug resistance.

Cisplatin resistance has been associated with altered DNA repair and decreased accumulation of cisplatin due to reduced uptake of cisplatin into cells, enhanced efflux and increased detoxification of cisplatin (reviewed in Amable, 2016). Altered DNA repair in cisplatin resistance has been linked to increased expression of the DNA repair gene ERCC1. Previous studies have demonstrated that low ERCC1 expression enhances cisplatin toxicity (Arora et

al., 2010; Bai et al., 2012). The here observed increased expression of ERCC1 in Ls-R-C cells corroborates these earlier findings. Cisplatin has also been shown to induce the expression of GADD45A, which is also involved in DNA repair and suppression of this gene has enhanced the cytotoxicity of cisplatin (Liu et al., 2018b; Smith et al., 2000). Accordingly, GADD45A was also upregulated in Ls-R-C cells. These findings support the association of altered DNA repair with cisplatin resistance.

SLC31A1 acts as an uptake transporter for cisplatin (Ishida et al., 2002; Song et al., 2004), while SLC31A2 induces the cleavage of SLC31A1 (Öhrvik et al., 2016). Accordingly, decreased expression of SLC31A1 and increased expression of SLC31A2 has been observed to attribute to reduced cellular uptake of cisplatin and thus cisplatin resistance (Ishida et al., 2002; Lee et al., 2011; Zisowsky et al., 2007). Our results of downregulated SLC31A1 and upregulated SLC31A2 in Ls-R-C cells are in accordance with these previous findings and provide further support for the association of reduced uptake of cisplatin with cisplatin resistance.

Enhanced efflux of cisplatin has been associated with increased expression of ABCC2 (Liedert et al., 2003, Wakamatsu et al. 2007) and ATP7A/B transporters (Inoue et al., 2010; Li et al., 2016; Samimi et al., 2004a). All these genes were upregulated in Ls-R-C cells, except ATP7B. This can be explained by the fact that ATP7B is solely expressed in liver, while ATP7A is expressed in several tissues (Samimi et al., 2004a). Therefore, our results are in line with those of previous studies and confirm the relevance of increased cisplatin efflux as mechanism of cisplatin resistance. In addition, other efflux transporters, including ABCB11, ABCC1/3 and ABGG2 were also upregulated in Ls-R-C, whereas ABCB1 was extremely downregulated. Cisplatin itself is not a substrate for ABCB1, but many other cancer drugs are, including doxorubicin, irinotecan and paclitaxel (Pan et al., 2016). Hence, it could conceivably be hypothesized that in cisplatin-resistant tumors the simultaneously administered cancer drugs, which are ABCB1 substrates would not be transported out of the cancer cells. Instead, these drugs could maintain their efficacy in cisplatin-resistant cancer cells. This hypothesis is supported by the lack of cross-resistance of irinotecan in Ls-R-C cells as these cells were as sensitive to irinotecan as Ls-P cells.

Finally, enhanced cisplatin inactivation by glutathione S-transferases has been linked to cisplatin resistance (De Luca et al., 2019; Zou et al., 2019). In contrast to these previous findings, GSTP1 was downregulated in Ls-R-C cells, while GSTA1 displayed comparable

levels as in Ls-P cells. Therefore, cisplatin inactivation by these enzymes appears irrelevant for cisplatin resistance in LS174T cells.

Given the above, enhanced DNA repair and decreased cisplatin accumulation by enhanced efflux and reduced uptake, explain probably to a large extent cisplatin resistance in Ls-R-C cells. Other genes, however, also displayed altered expression. Admittedly, not all of these changes are likely relevant for the cisplatin resistance, such as upregulated proapoptotic gene BBC3 or downregulated antiapoptotic BCL2, because these changes do not improve cell survival and thereby do not enhance cancer drug resistance. Additional mechanisms for cisplatin resistance could include altered control of apoptosis and survival balance because cisplatin-resistant cells showed increased expression of BCL2L1 and CDKN1A. BCL2L1 is an antiapoptotic protein that is, for example, involved in resistance against anthracyclines (Marin et al., 2010). CDKN1A is not only the effect mediator of p53 and a negative regulator of the cell cycle but also can suppress apoptosis; therefore, it can mediate oncogenic functions (Abbas and Dutta, 2009). Ls-R-C cells showed reduced expression of CYP1A2, SLC10A2 and SLCO2B1, which are not known to metabolize or transport cisplatin. Therefore, the relevance of these genes to cisplatin resistance would need further investigations. In addition to gene-related changes, Ls-R-C cells grew much slower than Ls-P cells. This can partially also explain cisplatin resistance, as Petitperez et al. (2013) have demonstrated with SN38-resistant colorectal cancer cells.

Irinotecan resistance has been previously associated with increased drug efflux, reduced expression of its molecular target topoisomerase 1 (TOP1) or mutations in TOP1 and with altered activation of apoptosis and survival pathways (reviewed in Holohan et al., 2013; Pan et al., 2016). These mechanisms are here supported by several detected gene expression changes in the Ls-R-I cells. First, irinotecan is a substrate of ABCB1 and increased expression of this multidrug efflux transporter has been observed in irinotecan-resistant cells (Choi et al., 2015; Iyer et al., 2002; Luo et al., 2002). Accordingly, ABCB1 was upregulated in Ls-R-I cells, which supports the association of increased efflux with irinotecan resistance. In contrast, the expression of ABCG2 was not increased in Ls-R-I cells. This finding is contradictory to previous studies, which have demonstrated increased expression of ABCG2 in SN38- and irinotecan-resistant breast, cervical and colon cancer cells (Candeil et al., 2004; Choi et al., 2015; Jandu et al., 2016; Takara et al., 2009). This contradiction could be explained by the difference in cell lines as these earlier studies have used other cell lines than LS174T.

Second, irinotecan and its active metabolite SN38 target directly TOP1 (Kawato et al., 1991). In this study, Ls-R-I cells showed reduced levels of TOP1, which is in line with earlier studies conducted with SN38- and irinotecan-resistant cancer cells (Jandu et al., 2016; Kanzawa et al., 1990). Reduced TOP1 levels could obviously decrease the efficacy of SN38. Therefore, this finding provides confirmation for the assumption of reduced target level as a relevant mechanism of irinotecan resistance.

Similar to Ls-R-C cells, Ls-R-I cells exhibited increased expression of BCL2L1 and CDKN1A. These results reflect the findings of Choi et al. 2015, who also detected higher expression of CDKN1A in irinotecan-resistant cells. Ls-R-I cells showed also increased expression of EGFR and FGF19. These results are in accordance with earlier studies, which demonstrated increased expression of EGFR in SN38-resistant cells (Petitprez and Larsen, 2013). In addition, FGF19 activation has been shown to enhance cell growth, migration and invasion of colorectal cancer cells via PXR-dependent manner (Wang et al., 2011). Therefore, these results further support the idea of altered apoptosis and survival pathways as putative irinotecan resistance mechanisms in LS174T cells.

Similarly as in Ls-R-C cells, Ls-R-I cells showed also increased expression of GADD45A, which is involved in DNA repair (Liu et al., 2018b). Therefore, enhanced DNA repair could be a novel additional mechanism in irinotecan resistance in LS174T cells. Finally, irinotecan is metabolized to inactive metabolites by CYP3A4 (Haaz et al., 1998; Santos et al., 2000). CYP3A4 was highly induced in Ls-R-I cells, which could also contribute to the irinotecan resistance.

Interestingly, compared to Ls-P cells Ls-R-I cells showed higher expression of CXCR4. This receptor and its ligand CXCL12 has been connected with multiple tumor progressive functions, including angiogenesis, metastasis and invasion, growth and survival and drug resistance (reviewed in Domanska et al., 2013). Accordingly, CXCR4 expression has been associated with poorer survival of cancer patients (Li et al., 2014; Zhao et al., 2015). CXCR4 overexpression was previously observed in cisplatin-, gefitinib- and oxaliplatin-resistant cancer cell lines (Huang et al., 2016; Jung et al., 2013; Li et al., 2014). Activated CXCL12/CXCR4 axis could, therefore, also be involved in irinotecan resistance in LS174T cells. In addition, CXCR4 has been identified as one of the cancer stem cell markers (Hermann et al., 2007). Interestingly, other colon cancer stem cell markers, such as ALDH1A1 and OLFM4 (Planque et al., 2016), were not overexpressed in Ls-R-I cells. In contrast, these genes were downregulated.

Other gene expression changes were also observed, which are probably not contributing to irinotecan resistance, because these changes would not aid in developing the resistance. For instance, UGT1A1 and UGT1A9 were slightly downregulated and not upregulated as could be expected based on their function. These enzymes metabolize SN38 to inactive metabolites (Gagné et al., 2002; Iyer et al., 1998). In accordance with earlier studies (Jandu et al., 2016; Kanzawa et al., 1990; Petitprez et al., 2013), Ls-R-I cells grew slightly slower than Ls-P cells. Therefore, reduced growth rate could also partially explain the irinotecan resistance in LS174T cells. Finally, all of these above mentioned changes were not considerably large, even though the fold resistance to Ls-P cells was; therefore it seems reasonable that irinotecan resistance is not due to one single mechanism, but moreover it could be caused by a combination of several mechanisms.

This work has several limitations. First, not all possible genes associated with cancer drug resistance were investigated. We used here a targeted approach investigating only genes associated with selected mechanisms of cancer drug resistance. Therefore, there could be additional genes that might be part of cisplatin or irinotecan resistance, which were not found here. In addition, appearance of mutations was not disclosed here, which could be relevant for function of certain genes. For instance, mutations in TOP1, which reduced the activity of this enzyme, have been observed in SN38-resistant cells (Arakawa et al., 2006). In addition, the changes in mRNA expression were not confirmed on the protein level. For this reason, only relative expression changes larger than 1.5-fold or smaller than 0.75 were included. It has been previously demonstrated that 1.5-fold change in mRNA can be detected also in protein level (Jeske et al., 2017). In general, the correlation between mRNA and protein expression has been demonstrated to be poor (reviewed in de Souza Abreu et al., 2009). Transcriptional changes explain around 40% of the protein level variance, whereas approximately 60% of the difference could be due to other changes than transcriptional, such as regulation of translation and degradation of protein. However, genes that show differential mRNA expression due to an experimental condition, such as treatment, demonstrate remarkably higher correlation between mRNA and protein than genes that are not differentially expressed (Koussounadis et al., 2015). This gives evidence for the assumption that differentially expressed mRNA is also biologically meaningful (Koussounadis et al., 2015). Both resistant cells exhibited several alterations in gene expression that could be assumed to be observed similarly at protein level. However, the relevance of these alterations for function of the protein and moreover the biological relevance would require further investigations. Relevance of each gene for cisplatin or irinotecan

resistance could be confirmed in further experiments by knocking down individual genes and assessing the effect on drug resistance. Although the effect of single gene to overall resistance is probably small, as several drug resistance related alterations were observed here.

5.2. Role of PXR-dependent regulation on gene expression of cisplatin- and irinotecan-resistant cells

In Ls-R-C cells, none of the measured genes, except ABCB1 and ABCB11 were affected by the treatment with prototypical PXR agonist rifampicin or PXR specific antagonist SPA70. This is perhaps surprising, as cisplatin has been shown to activate PXR in several cell lines (Masuyama et al., 2016, 2005). Interestingly, short term (72 h) treatment with cisplatin induced the expression of established PXR target genes, ABCB1 and CYP3A4 (Fig. 7), whereas selection with cisplatin (long-term treatment) elucidated opposite results: reduced expression of ABCB1 and comparable expression of CYP3A4 compared to the Ls-P cells. Moreover, PXR mRNA and protein expressions were reduced in Ls-R-C cells compared to parental cells. In accordance with this, Yasuda et al. (2019) observed reduced PXR mRNA levels in HepG2 cells after treatment with 25 μ M cisplatin. Cisplatin appears to be a PXR activator, at least in short-term, but in long-term other pathways are probably activated that lead to downregulation of these PXR target genes that were induced in short-term, probably by reducing PXR expression itself. Given the above, PXR seems not to be involved in acquired cisplatin resistance in LS174T cells; instead, other signaling pathways are activated, which are relevant for the cisplatin resistance.

In contrast to Ls-R-C cells, in Ls-R-I cells, PXR appears to be at least partially involved in drug resistance. Rifampicin induced and SPA70 suppressed some of the possibly relevant genes, such as multidrug efflux transporter ABCB1 and irinotecan metabolizing enzyme CYP3A4. Similarly, PXR activation and inhibition appeared to affect slightly FGF19 expression. FGF19 has been previously shown to enhance cellular growth and migration in LS174T cells in a PXR-dependent manner (Wang et al., 2011). Moreover, PXR antagonism reduced the induced expression of these genes in Ls-R-I cells back to nearly the same levels as basal levels in Ls-P. Given the above, PXR seems to regulate at least partly the gene expression changes in Ls-R-I cells.

Ls-R-C showed no cross-resistance towards irinotecan, while Ls-R-I cells exhibited slight cross-resistance towards cisplatin. This may be explained by the fact that only few of the

investigated cancer drug resistance-associated genes were similarly expressed in these cells. These results indicate that in these cells the resistance is caused by distinct mechanisms.

PXR splice variant called sPXR has been proposed to have tumor suppressing effects due the dominant negative effect it has towards functional PXR (Breuker et al., 2014). Both Ls-R-C and Ls-R-I cells exhibited similar levels of PXR1 and sPXR as Ls-P cells. Therefore, alternative splicing of PXR leading to reduced level of tumor suppressive sPXR or increased levels of tumor promoting PXR1 cannot explain the observed cisplatin or irinotecan resistance.

5.3. Resensitization of drug-resistant cancer cells by PXR antagonism

Because our findings indicate that PXR does not regulate the genes involved in cisplatin resistance of LS174T cells, we assumed that these cells would not be resensitized to cisplatin with PXR antagonism. Recently, Yasuda et al. (2019) have demonstrated resensitization of cisplatin-resistant liver cancer HepG2 cells with PXR antagonist leflunomide. In contrast to liver cancer cells, we used here colorectal cancer LS174T cells. In these distinct cell lines, different genes could be involved in the cisplatin resistance. Unfortunately, no gene expression analysis was conducted in the earlier study by Yasuda et al. (2019). Moreover, leflunomide is not a very potent PXR antagonist (Ekins et al., 2008) and it has been shown to even elicit PXR activation at lower doses than that were used in resensitization (Ratajewski et al., 2015). Moreover, PXR antagonism by leflunomide is an off-target effect of the drug. Leflunomide is used as an immunosuppressant for the treatment of arthritis because it blocks dihydroorotate dehydrogenase, which is necessary for multiplication of lymphocytes (EMA, 2014). Therefore, it is possible that some other than PXR-mediated pathways could have caused the increased caspase-3 activity observed by Yasuda et al. (2019). In addition, the end point of resensitization in this previous study was increased caspase-3 activity and not a phenotypic change in overall cell viability. Therefore, it is not comprehensively proven that leflunomide decreased per se the cell viability of resistant cells, because only caspase-3 activity was assessed instead of actual cell viability. In the gene expression analysis of Ls-R-C cells contradictory changes of apoptosis regulating genes were observed, such as upregulated proapoptotic gene BBC3 and downregulated antiapoptotic gene BCL2. It should also be kept in mind that caspases have been shown to affect cellular growth and inhibit necrosis, therefore pure caspase activation cannot be automatically related to the amount of cell death (Hardwick and Soane, 2013). Overall, in LS174T cells other than PXR regulated pathways appear to be involved in the acquired cisplatin resistance. Consequently, in these cells PXR antagonism would probably not be beneficial in reducing the cisplatin resistance.

Even though some genes, participating in irinotecan resistance in Ls-R-I cells proved to be regulated by PXR, antagonizing PXR with SPA70 did not resensitize Ls-R-I cells to irinotecan. Possible explanation for this is that to resensitize cells back towards irinotecan, it is not sufficient to suppress solely the few genes, such as ABCB1 and CYP3A4, which were regulated by PXR. Other than these PXR-activated pathways are at least as important for the resistance, including apoptosis and proliferation pathways. It could be concluded that irinotecan resistance is a complex phenomenon consisting of activation of several pathways and suppressing solely one of these is not enough to resensitize irinotecan-resistant LS174T cells.

Ls-R-I cells displayed increased expression of ABCB1 and CYP3A4, which have been demonstrated to be relevant for paclitaxel resistance (Hendrikx et al., 2013; Vaidyanathan et al., 2016). Accordingly, Ls-R-I cells showed cross-resistance towards paclitaxel. Moreover, treatment of Ls-R-I cells with PXR antagonist resensitized cells towards paclitaxel. The cell viability was, however, still approximately 40% at the highest paclitaxel concentration in resensitized Ls-R-I cells, which was slightly higher than the cell viability of Ls-P cells at that concentration. This can affect to the calculation of IC_{50} value. Higher paclitaxel concentrations could not be used due to solubility problems. Nevertheless, paclitaxel resistance appears to be more dependent on PXR-regulated genes; therefore, PXR antagonism was beneficial in reducing paclitaxel resistance. In general, it seems that PXR antagonism could be suggested as a useful approach to attenuate cancer drug resistance only, if the resistance is mostly dependent on PXR-regulated genes. Furthermore, even if the compound that results in drug resistance, activates PXR, it is not necessarily possible to resensitize cells with a PXR antagonist, if other than PXR-regulated pathways are also activated and have impact on the development of drug resistance.

5.4. Identification of novel PXR antagonists and their mechanism of action

Combination of in silico, cellular and biochemical assays resulted in identification of five novel PXR ligands with high structural similarity. Based on their effects on reporter gene assays four of them were identified as PXR antagonists and one as a full agonist. Unfortunately, one of the antagonists (compound **2**) could not be characterized thoroughly because of limited availability of this compound.

With increasing concentrations, all four potential antagonists shifted the rifampicin concentration-response curve to the right hand, thereby increasing the EC_{50} of rifampicin, which suggests that these compounds are competitive antagonists. The maximum effect by

rifampicin (E_{max}) appears to decline with higher concentrations of novel antagonists, especially with compounds **73** and **100**, which could indicate additional non-competitive antagonism. However, higher concentrations of rifampicin could not be used and therefore the plateau of the effect was not reached and this possible decrease in E_{max} could not be confirmed unequivocally.

Competitive antagonists compete with the agonist in binding to the LBP and hinder the binding of the agonist. The binding of these novel ligands to PXR LBD was demonstrated to occur in vitro with limited proteolytic digestion assay and also in cells with LBD assembly assay. In addition, the results from the reporter gene assay using LBP-filled triple mutant suggests that these compounds bind to the LBP as the high constitutive activity of this mutant was not reduced. Only compound **73** showed also weak inhibition of constitutive active LBP-filled triple mutant. Therefore, it cannot be totally ruled out that this compound could additionally also bind outside the LBP. Similarly, coumestrol and pimecrolimus have been previously demonstrated not only bind into PXR LBP, but also additionally outside LBP (Burk et al., 2018; Wang et al., 2008).

Specific ligand-induced effects were investigated utilizing single amino acid PXR mutants. None of the compounds activated mutants Y306A, S247A or H407A. Y306A appears to be a non-inducible mutant, whereas S247A and H407A showed high constitutive activity, but were not further induced by ligands. Generally, the activation pattern of these compounds was similar: rifampicin caused the highest induction, followed by compound **109** and **12**. Compounds **73** and **100** demonstrated typically the lowest activation of PXR mutants. Few exceptions existed. First, compound **12** displayed lowest induction of mutants W299A and H327A. Therefore, these amino acids may be important for the PXR activating interactions of compound **12**. Second, compounds **73** and **100** activated mutant W299A more strongly than the other mutants, acting as agonists for this mutant. Interestingly, similar behavior has been demonstrated previously with SPA70, which acts as an antagonist of wild-type PXR, but is an agonist for W299A (Huber et al., 2020). Molecular dynamic simulations suggested that SPA70 affects the position of helix 12 in the AF-2 region in W299A differently as in wild-type PXR. Compound **100** displayed also strong activation of H327A compared to the weak activation of wild-type PXR.

The newly identified antagonists impaired the rifampicin-induced interaction of coactivator SRC1 with PXR. This has been demonstrated previously with other PXR antagonists such as ketoconazole, pazopanib, pimecrolimus and sulforaphane (Burk et al., 2018; Huang et al.,

2007; Zhou et al., 2007). On the other hand, these novel antagonists also impaired the constitutive interaction of PXR with corepressor SMRT. Similar effects have been previously observed with ketoconazole, pazopanib and pimecrolimus (Burk et al., 2018; Huang et al., 2007). In contrast, enhanced interaction of PXR with SMRT has been shown only with SPA70 (Lin et al., 2017). Ultimately, these novel PXR antagonists inhibit PXR activation by compromising the coactivator interactions.

Based on the mechanism, two classes of nuclear receptor antagonism have been proposed earlier (Chai et al., 2020). These two classes, active and passive antagonism, were first demonstrated with estrogen receptors (Shiau et al., 2002). Active antagonists contain typically bulky substituents that disturb the AF-2 region physically, whereas passive antagonists change position of helix 12 to obstruct AF-2 surface usually via lack of appropriate interactions in the LBP (Kojetin and Burris, 2013). Active antagonists have shown also to enhance interactions of nuclear receptor with corepressors, while passive antagonists prevents the binding of both corepressors and coactivators (Schoch et al., 2010). Given the above, the novel PXR antagonists identified in this work could be classified as passive antagonists.

The here executed combination of distinct assays proved to be important to confirm the effects of these compounds on PXR, because cellular assays identified four of these compounds as antagonists and one as a strong full agonist. In contrast to reporter gene assays, one of the potential antagonists (**12**) induced endogenous PXR target gene expression in LS174T cells as strongly as rifampicin and did not suppress the rifampicin-induced expression. Interestingly, other two antagonists (**73**, **100**) displayed gene-specific effects on endogenous PXR target gene expression. Similarly, as compound **12**, compounds **73** and **100** induced the expression of CYP3A4 and did not suppress the rifampicin-induced expression. In contrast, compounds **73** and **100** did not induce the expression of ABCB1 and repressed strongly the rifampicin-induced expression. Likewise, the basal expression of CYP2B6 was reduced by these compounds. Due to these results, it could be argued that compounds **73** and **100** are selective PXR modulators instead of being simple PXR antagonists. Interestingly, the newly identified PXR agonist (**109**) displayed weaker induction of ABCB1 compared to rifampicin, while the CYP3A4 induction was comparable between compound **109** and rifampicin.

PXR, CAR and VDR belong to the same group I of nuclear receptor subfamily 1 (NR1I) and exhibit sequence similarity (Wu et al., 2013b). CAR3 differs from CAR1 by a five amino acid insertion in the LBD (Auerbach et al., 2005). Despite this insertion, CAR1 and CAR3 are still predicted to contain similar LBP's (Auerbach et al., 2003). CAR3 is, however, ligand-induced

transcription factor and needs presence of RXR for the maximal ligand-induced activity, while CAR1 is constitutively active variant (Auerbach et al., 2005). Compound **73** act as a very weak inverse agonist on constitutive active CAR1, while other PXR ligands showed no effects on CAR1 activity. None of the compounds influenced CAR3 activity. Compounds **12** and **109** activated very weakly VDR, whereas compounds **73** and **100** had no effect on VDR activity. Overall, these novel PXR ligands appear to be PXR selective among the nuclear receptor NR11 group, because the effects observed on CAR1 and VDR were very weak and may not be biologically meaningful. It is, however, possible that these compounds could exhibit stronger receptor-dependent effects on some other nuclear receptors.

Several kinases have been shown to phosphorylate PXR, and as a result to affect the transcriptional activity of PXR (Ding and Staudinger, 2005a, 2005b; Lichti-Kaiser et al., 2009; Lin et al., 2008; Pondugula et al., 2009). Therefore, compounds **100** and **109** were tested for their potential to inhibit a panel of 335 wild-type kinases. Compound **100** and compound **109** inhibited at least by 50% five and eight kinases, respectively. Among the inhibited kinases, only protein kinase A (PKA) has been demonstrated to phosphorylate PXR (Ding and Staudinger, 2005a; Lichti-Kaiser et al., 2009). In humans, PXR phosphorylation by PKA repressed the transcriptional activity (Lichti-Kaiser et al., 2009). Inhibition of PKA by compound **100** and **109** should, therefore increase the transcriptional activity of PXR, which, for compound **100**, is the opposite of what was observed. Thus, the inhibitory effects on PXR of compound **100** are most likely not due to inhibition of PXR phosphorylation. The inhibition of PKA by compound **100** could, however, explain the partial agonism, which was observed in reporter gene assays and in the induction of endogenous CYP3A4. Especially because this compound was not able to recruit coactivators, which is a typical function for agonists. Inhibition of PKA could also contribute to the PXR activation effects observed with compound **109**. Thus, compound **109** could induce the transcriptional activity of PXR not only via direct binding to PXR but also by inhibition of PKA.

Development of small molecule inhibitors for PXR has proven challenging due to the large and flexible ligand binding pocket, which binds promiscuous ligands (Staudinger, 2019). The majority of compounds that bind to PXR activates the receptor, which also hinders the design of antagonists (Chai et al., 2020). Moreover, subtle structural changes impact greatly on the PXR activation or inhibition potential as has been observed with PXR antagonist SPA70 and PXR agonist SBJ7, which differ only by one methyl group and in the location of a methoxy group (Lin et al., 2017). Similarly, subtle structural changes in the here newly identified PXR

ligands affected the PXR activation and inhibition potential. In addition to small molecule inhibitors, other approaches for PXR inhibition can be pursued as well. PROteolysis TArgeting Chimeras (PROTAC) are small molecules that comprise two functionalities linked together: one that binds to E3 ubiquitin ligase and other that binds to the targeted protein (Flanagan and Neklesa, 2019). The close distance of these functionalities results in the target protein ubiquitination and subsequent degradation. Typically over 90% of the expressed target protein is degraded, therefore the mechanism of inhibition differs greatly from traditional small molecule antagonists (Flanagan and Neklesa, 2019). In addition, PROTACs can also inhibit constitutive active nuclear receptors. In contrast, small molecule antagonists usually inhibit only the agonist-induced activity of nuclear receptor (Chai et al., 2020). Another approach for reducing the target protein expression would be oligonucleotide-based drugs, such as antisense oligonucleotides and small interfering RNAs (siRNA) (Bennett and Swayze, 2010). Common hindrance for utilizing any of these approaches is the limited number of developed compounds. Not only is the number of PXR antagonists small, but also no therapeutic PROTACs or oligonucleotide-based drugs targeting PXR have been published to date. Antisense oligonucleotides and siRNAs against PXR have only been utilized in PXR-related research to study for instance gene functions (Chen et al., 2016; Jeske et al., 2017; Zucchini et al., 2005). However, PROTACs and oligonucleotide-based therapeutics against androgen or estrogen receptor have been investigated in clinical trials (NCT02144051; NCT03300505; NCT04072952). In addition, both PROTACs and oligonucleotide-based therapeutics can elicit off-target effects, which could lead to reduced expression of other than the target protein (Bennett and Swayze, 2010; Moreau et al., 2020). Ideal small molecule inhibitor should also show selectivity towards PXR or at least antagonize PXR at lower concentrations than non-desired targets. This has been demonstrated with SPA70 (Lin et al., 2017). PXR is involved in variety of physiological functions, therefore the total abolishment of PXR could elucidate harmful effects. PXR is not a traditional target in cancer therapy, because it has not been classified as a typical mutated driver gene in cancers (Dietlein et al., 2020). In addition, based on the data on the Human Protein Atlas, even though PXR shows increased expression in certain cancers, including colorectal, liver, pancreas and stomach cancers, it has not shown clear prognostic value [(Uhlen et al., 2017), <http://www.proteinatlas.org>]. Although, Dong et al. (2017) observed association with PXR expression and decreased survival of colorectal cancer patients. It could thus be suggested that selective modulation by PXR antagonism and not total PXR ablation could be more sensible in attenuating cancer drug resistance so that only those PXR-mediated effects that are relevant for resistance would be reduced, such as efflux

of cancer drugs by ABCB1. In contrast, for instance, androgen receptor and the signaling pathways activated by this nuclear receptor are the driving forces in prostate cancer and thereby the main target to block in the treatment of this disease (reviewed in Wadosky and Koochekpour, 2016). Therefore, utilizing PROTACs or oligonucleotide-based therapeutics in the treatment of prostate cancer is much more reasonable.

PXR antagonists would not be used as a monotherapy in the treatment of cancer, but rather as part of the cancer drug regimen. Alternatively, a multitarget approach, where cancer drugs themselves would act also as PXR antagonists could be beneficial. Several cancer drugs have shown to activate PXR, such as tamoxifen, paclitaxel and sorafenib (Harmsen et al., 2013, 2010), but only few cancer drugs have demonstrated PXR antagonism, including belinostat and pazopanib (Abbott et al., 2019; Burk et al., 2018). Here, our newly identified PXR antagonist, compound **100**, inhibited potently the kinase activity of RAF-kinases, especially the activity of c-RAF, which is encoded by the proto-oncogene RAF1. These RAF-kinases are important downstream effectors in the mitogen-activated protein kinase (MAPK) pathway (reviewed in Khazak et al., 2007). Activation of MAPK pathway has been shown to promote tumor growth by enhancing cell proliferation, angiogenesis and vasculogenesis. The c-RAF has been demonstrated to be vital for the development of Kras-mutated non-small cell lung cancer in mice, where its abrogation has reduced the tumor growth (Blasco et al., 2011; Sanclemente et al., 2018). In addition, simultaneous inhibition of EGFR and c-RAF has shown in mice to stop the progression of certain Kras-mutated pancreatic ductal adenocarcinomas (Blasco et al., 2019). Increased expression of c-RAF was also associated with decreased survival of ovarian cancer patients (McPhillips et al., 2006). A few multikinase inhibitors targeting as well c-RAF have granted marketing authorization, such as sorafenib and regorafenib (EMA, 2019b, 2013). But no specific c-RAF kinase inhibitors are yet clinically available.

Selective PXR modulation by small molecule compounds considering the variety of PXR-regulated functions could be a beneficial approach to reduce cancer drug resistance. However, selective PXR modulator would not be sufficient as monotherapy, but should be combined with cancer drugs that potentially develop resistance via PXR-regulated genes. Alternatively, a novel approach would be bifunctional ligands, such as here identified the novel PXR antagonizing kinase inhibitor. Investigation of possible drug-drug interactions via PXR activation are part of mandatory testing for marketing authorization approval (EMA, 2012). Therefore, in the cancer drug development it may be a useful strategy to not only prioritize those drug candidates that have no effect on PXR, but also to monitor compounds for PXR

inhibition. Ultimately, more knowledge is required from all approaches targeting PXR in the context of cancer drug resistance.

6. Conclusions

This work shows that long-term continuous treatment of cisplatin and irinotecan results in acquired drug resistance. The selected cells displayed for the most part distinct gene expression alterations. Several genes that previously have been shown to be associated with cisplatin and irinotecan resistance were altered in their expression. However, also a few novel gene expression changes were observed that could contribute to cisplatin and/or irinotecan resistance. For instance, Ls-R-C cells showed increased expression of antiapoptotic gene BCL2L1. CDKN1A was also upregulated in these cells, which can elicit apoptosis suppressing functions. Ls-R-I cells exhibited increased expression of GADD45A, which is involved in DNA repair. These results suggest, that in addition to the previously described resistance mechanisms associated with cisplatin or irinotecan resistance, reduced apoptosis and enhanced DNA repair could be additional mechanisms. These selected resistant cells exhibited no remarkable cross-resistance towards the respective other drug. However, irinotecan-resistant cells exhibited considerable cross-resistance towards paclitaxel, which is likely due to the PXR-dependent increased expression of ABCB1 and CYP3A4. These proteins are involved in the efflux transport and metabolism of paclitaxel. Cisplatin- and irinotecan-resistant cells differ also in their response to PXR activation and inhibition. None of the relevant genes regarding drug resistance were affected by PXR activation or inhibition in cisplatin-resistant cells, whereas in irinotecan-resistant cells some of these genes, including ABCB1 and CYP3A4, were suppressed by treatment with a PXR antagonist. Therefore, PXR appears not to play a role in cisplatin resistance, while in irinotecan-resistant cells PXR has at least some role. However, other pathways contribute also greatly to irinotecan resistance, as was indicated by the failed resensitization towards irinotecan of irinotecan-resistant cells by treatment with the PXR antagonist. In contrast, co-treatment of irinotecan-resistant cells with PXR antagonist reduced the paclitaxel resistance. This suggests that PXR could have a relevant role in paclitaxel resistance. To summarize, PXR antagonism can be a beneficial approach to resensitize drug-resistant cancer cells, however, only if the resistance is caused predominantly by PXR-dependent gene expression changes. It is not a general approach, even not for all cells, which are resistant to PXR-activating drugs, as further cancer drug resistance mechanisms may be more important than PXR activation.

Combination of *in silico* methods and cellular assays resulted in the identification of four novel PXR antagonists and one full agonist with high structural similarity from TüKIC compound library. Further characterization revealed that these four antagonists appeared to function as competitive antagonists with partial agonist activity. In addition, these compounds impaired the rifampicin-induced interaction of PXR with coactivator SRC1; therefore, they could be classified also as passive antagonists. Finally, compounds were tested with respect to their effect on expression of endogenous PXR target genes. Compounds exhibited distinct gene-specific effects. Interestingly, compounds **73** and **100** suppressed the rifampicin-induced expression of ABCB1, while they induced the expression of CYP3A4. This suggests that these compounds could be selective PXR modulators. Compound **12** showed no PXR inhibition activity, while it induced the expression of ABCB1 and CYP3A4, demonstrating similar effects as the compound **109**, which was in the reporter gene assays identified as a pure agonist. All these ligands share high structural similarity. Therefore, it can be concluded that subtle changes in structures of PXR ligands can have great impact on the activation or inhibition of PXR.

Cancer drug resistance is often a major hindrance for successful cancer therapy. Currently, only few options exist for prevention or overcoming cancer drug resistance (reviewed in Aleksakhina et al., 2019). First, patients can be given sequential therapy, meaning that they are treated with another cancer drug that do not share the resistance mechanism with the first drug. For instance, breast cancer patients, which develop resistance against aromatase inhibitors, can be given sequential therapy with estrogen receptor degrader (Ward et al., 2020). In addition, imatinib-resistant chronic myeloid leukemia can be treated with dasatinib or nilotinib, which are effective against the imatinib-resistant mutations (Ward et al., 2020). Second, a commonly used option to prevent cancer drug resistance is to use combination therapy to inhibit different signaling pathways or different targets on the same signaling pathway (Aleksakhina et al., 2019). Combination of BRAF and MEK inhibitors are commonly utilized in the treatment of melanoma (Ward et al., 2020). Finally, adaptive therapy using low or intermittent dosing instead of typically used highest tolerated doses of chemotherapeutics, has been investigated to evade cancer drug resistance (Aleksakhina et al., 2019). This approach, however, is still in experimental stage and not a standard regimen in contrast to the two previous approaches, which are routinely used. In addition, sequential and combinatorial therapy affects for the most part only mutation-associated resistance mechanisms and not the general cancer drug resistance mechanism, such as increased efflux. Efforts to attenuate cancer drug resistance occurring via these general mechanisms, have been for the most part focused on inhibition of ABC

transporters, especially ABCB1 (reviewed in Robey et al., 2018). Unfortunately, these inhibitors have not been proven to reduce cancer drug resistance clinically in cancer patients.

Due to the putative role of PXR in cancer drug resistance and tumor progression, PXR antagonism has been proposed as a potential approach to overcome drug resistance. Earlier studies have shown that PXR antagonism increases the potency of cytotoxic drugs in cancer cells (Abbott et al., 2019; Lin et al., 2017). However, it is not comprehensively proven that PXR antagonism could resensitize drug-resistant cancer cells. Despite, Yasuda et al. (2019) demonstrated increased caspase-3 activation in leflunomide-treated cisplatin-resistant liver cancer cells. To the best of our knowledge this work here demonstrates for the first time that PXR antagonism can be used to reduce drug resistance in drug-resistant colorectal cancer cells. However, this approach appears to be beneficial only if the drug resistance is primarily dependent on PXR-regulated genes, as it appears to be with paclitaxel but not with irinotecan. Irinotecan resistance instead could be suggested to be a complex phenomenon consisting of activation of several pathways.

The limited number of available PXR antagonists further presents an obstacle for using the PXR antagonism as a potential approach to overcome cancer drug resistance. To the best of our knowledge, this work presents first time a compound with dual function of inhibiting both PXR and RAF-kinases. Utilizing this type of bifunctional ligands besides combinatorial therapy of chemotherapeutic and PXR antagonist could provide further options in the field of cancer therapy. The novel antagonists identified in this work could be used as a starting point for developing more efficient PXR antagonists or selective PXR modulators that could be utilized as part of cancer treatment. Further optimization could be done to increase the potency for PXR inhibition, while not losing the potent inhibition of RAF-kinases, which could be beneficial in the treatment of certain cancers. Cancer drug resistance is context- and drug-dependent so that it will not be overcome by one approach. Therefore, further studies about the drug-related mechanisms and different approaches are required in the future.

7. Declaration of collaboration

Molecular modelling including preparation of PXR conformations, screening, structural analogue searches and molecular dynamic simulations were conducted by Dr. Tatu Pantsar (University of Tübingen) and M.Sc. Azam Rashidian (University Hospital Tübingen).

Kinome profiling was performed by ProQinase GmbH (Freiburg, Germany).

Limited proteolytic digestion assay was conducted with the help of Dr. Oliver Burk (Dr. Margarete Fischer-Bosch Institute for Clinical Pharmacology).

8. References

- Abbas, T., Dutta, A., 2009. p21 in cancer: intricate networks and multiple activities. *Nat. Rev. Cancer* 9, 400–414. <https://doi.org/10.1038/nrc2657>
- Abbott, K.L., Chaudhury, C.S., Chandran, et al. A., et al., 2019. Belinostat, at its clinically relevant concentrations, inhibits rifampicin-induced CYP3A4 and MDR1 gene expression. *Mol. Pharmacol.* 95, 324–334. <https://doi.org/10.1124/mol.118.114587>
- Aleksakhina, S.N., Kashyap, A., Imyanitov, E.N., 2019. Mechanisms of acquired tumor drug resistance. *Biochim. Biophys. Acta Rev. Cancer* 1872, 188310. <https://doi.org/10.1016/j.bbcan.2019.188310>
- Al-Salman, F., Plant, N., 2012. Non-coplanar polychlorinated biphenyls (PCBs) are direct agonists for the human pregnane-X receptor and constitutive androstane receptor, and activate target gene expression in a tissue-specific manner. *Toxicol. Appl. Pharmacol.* 263, 7–13. <https://doi.org/10.1016/j.taap.2012.05.016>
- Alt, F.W., Kellems, R.E., Bertino, J.R., Schimke, R.T., 1978. Selective multiplication of dihydrofolate reductase genes in methotrexate-resistant variants of cultured murine cells. *J. Biol. Chem.* 253, 1357–1370.
- Amable, L., 2016. Cisplatin resistance and opportunities for precision medicine. *Pharmacol. Res.* 106, 27–36. <https://doi.org/10.1016/j.phrs.2016.01.001>
- Arakawa, Y., Suzuki, H., Saito, S., Yamada, H., 2006. Novel missense mutation of the DNA topoisomerase I gene in SN-38-resistant DLD-1 cells. *Mol. Cancer Ther.* 5, 502–508. <https://doi.org/10.1158/1535-7163.MCT-05-0246>
- Arnold, K.A., Eichelbaum, M., Burk, O., 2004. Alternative splicing affects the function and tissue-specific expression of the human constitutive androstane receptor. *Nucl. Recept.* 2, 1. <https://doi.org/10.1186/1478-1336-2-1>
- Arora, S., Kothandapani, A., Tillison, K., Kalman-Maltese, V., Patrick, S.M., 2010. Downregulation of XPF-ERCC1 enhances cisplatin efficacy in cancer cells. *DNA Repair* 9, 745–753. <https://doi.org/10.1016/j.dnarep.2010.03.010>
- Auerbach, S.S., Ramsden, R., Stoner, M.A., Verlinde, C., Hassett, C., Omiecinski, C.J., 2003. Alternatively spliced isoforms of the human constitutive androstane receptor. *Nucleic Acids Res.* 31, 3194–3207.
- Auerbach, S.S., Stoner, M.A., Su, S., Omiecinski, C.J., 2005. Retinoid X receptor-alpha-dependent transactivation by a naturally occurring structural variant of human constitutive androstane receptor (NR1I3). *Mol. Pharmacol.* 68, 1239–1253. <https://doi.org/10.1124/mol.105.013417>
- Bai, Z., Wang, Y., Zhe, H., He, J., Hai, P., 2012. ERCC1 mRNA levels can predict the response to cisplatin-based concurrent chemoradiotherapy of locally advanced cervical squamous cell carcinoma. *Radiat. Oncol. Lond. Engl.* 7, 221. <https://doi.org/10.1186/1748-717X-7-221>
- Banerjee, M., Chai, S.C., Wu, J., Robbins, D., Chen, T., 2016. Tryptophan 299 is a conserved residue of human pregnane X receptor critical for the functional consequence of ligand binding. *Biochem. Pharmacol.* 104, 131–138. <https://doi.org/10.1016/j.bcp.2016.02.009>
- Banerjee, M., Chen, T., 2014. Thiazide-like diuretic drug metolazone activates human pregnane X receptor to induce cytochrome 3A4 and multidrug-resistance protein 1. *Biochem. Pharmacol.* 92, 389–402. <https://doi.org/10.1016/j.bcp.2014.08.025>
- Basseville, A., Preisser, L., de Carné Trécesson, S., et al., 2011. Irinotecan induces steroid and xenobiotic receptor (SXR) signaling to detoxification pathway in colon cancer cells. *Mol. Cancer* 10, 80. <https://doi.org/10.1186/1476-4598-10-80>
- Bennett, C.F., Swayze, E.E., 2010. RNA targeting therapeutics: molecular mechanisms of antisense oligonucleotides as a therapeutic platform. *Annu. Rev. Pharmacol. Toxicol.* 50, 259–293. <https://doi.org/10.1146/annurev.pharmtox.010909.105654>
- Benson, E.A., Eadon, M.T., Desta, Z., et al., 2016. Rifampin regulation of drug transporters gene expression and the association of microRNAs in human hepatocytes. *Front. Pharmacol.* 7, 111. <https://doi.org/10.3389/fphar.2016.00111>
- Berthier, A., Oger, F., Gheeraert, C., et al., 2012. The novel antibacterial compound walrycin A induces human PXR transcriptional activity. *Toxicol. Sci.* 127, 225–235. <https://doi.org/10.1093/toxsci/kfs073>
- Bertilsson, G., Heidrich, J., Svensson, K., et al., 1998. Identification of a human nuclear receptor defines a new signaling pathway for CYP3A induction. *Proc. Natl. Acad. Sci.* 95, 12208–12213. <https://doi.org/10.1073/pnas.95.21.12208>
- Bhalla, S., Ozalp, C., Fang, S., Xiang, L., Kemper, J.K., 2004. Ligand-activated pregnane X receptor interferes with HNF-4 signaling by targeting a common coactivator PGC-1alpha. Functional implications in

- hepatic cholesterol and glucose metabolism. *J. Biol. Chem.* 279, 45139–45147.
<https://doi.org/10.1074/jbc.M405423200>
- Bitter, A., Rümmele, P., Klein, K., et al., 2015. Pregnane X receptor activation and silencing promote steatosis of human hepatic cells by distinct lipogenic mechanisms. *Arch. Toxicol.* 89, 2089–2103.
<https://doi.org/10.1007/s00204-014-1348-x>
- Blasco, M.T., Navas, C., Martín-Serrano, G., et al., 2019. Complete regression of advanced pancreatic ductal adenocarcinomas upon combined inhibition of EGFR and C-RAF. *Cancer Cell* 35, 573–587.e6.
<https://doi.org/10.1016/j.ccell.2019.03.002>
- Blasco, R.B., Francoz, S., Santamaría, D., et al., 2011. c-Raf, but not B-Raf, is essential for development of K-Ras oncogene driven non-small cell lung carcinoma. *Cancer Cell* 19, 652–663.
<https://doi.org/10.1016/j.ccr.2011.04.002>
- Blumberg, B., Sabbagh, W., Juguilon, H., et al., 1998. SXR, a novel steroid and xenobioticsensing nuclear receptor. *Genes Dev.* 12, 3195–3205.
- Bray, F., Ferlay, J., Soerjomataram, I., Siegel, R.L., Torre, L.A., Jemal, A., 2018. Global cancer statistics 2018: GLOBOCAN estimates of incidence and mortality worldwide for 36 cancers in 185 countries. *CA. Cancer J. Clin.* 68, 394–424. <https://doi.org/10.3322/caac.21492>
- Breslin, S., O’Driscoll, L., 2016. The relevance of using 3D cell cultures, in addition to 2D monolayer cultures, when evaluating breast cancer drug sensitivity and resistance. *Oncotarget* 7, 45745–45756.
<https://doi.org/10.18632/oncotarget.9935>
- Breuker, C., Planque, C., Rajabi, F., et al., 2014. Characterization of a novel PXR isoform with potential dominant-negative properties. *J. Hepatol.* 61, 609–616. <https://doi.org/10.1016/j.jhep.2014.04.030>
- Brewer, C.T., Chen, T., 2016. PXR variants: the impact on drug metabolism and therapeutic responses. *Acta Pharm. Sin. B* 6, 441–449. <https://doi.org/10.1016/j.apsb.2016.07.002>
- Burk, O., Arnold, K.A., Nussler, A.K., et al., 2005. Antimalarial artemisinin drugs induce cytochrome P450 and MDR1 expression by activation of xenosensors pregnane X receptor and constitutive androstane receptor. *Mol. Pharmacol.* 67, 1954–1965. <https://doi.org/10.1124/mol.104.009019>
- Burk, O., Kuzikov, M., Kronenberger, T., et al., 2018. Identification of approved drugs as potent inhibitors of pregnane X receptor activation with differential receptor interaction profiles. *Arch. Toxicol.* 92, 1435–1451. <https://doi.org/10.1007/s00204-018-2165-4>
- Burk, O., Tegude, H., Koch, I., et al., 2002. Molecular mechanisms of polymorphic CYP3A7 expression in adult human liver and intestine. *J. Biol. Chem.* 277, 24280–24288. <https://doi.org/10.1074/jbc.M202345200>
- Candeil, L., Gourdiér, I., Peyron, D., et al., 2004. ABCG2 overexpression in colon cancer cells resistant to SN38 and in irinotecan-treated metastases. *Int. J. Cancer* 109, 848–854. <https://doi.org/10.1002/ijc.20032>
- Carazo, A., Hyrsova, L., Dusek, J., et al., 2017. Acetylated deoxycholic (DCA) and cholic (CA) acids are potent ligands of pregnane X (PXR) receptor. *Toxicol. Lett.* 265, 86–96.
<https://doi.org/10.1016/j.toxlet.2016.11.013>
- Cave, M.C., Clair, H.B., Hardesty, J.E., et al., 2016. Nuclear receptors and nonalcoholic fatty liver disease. *Biochim. Biophys. Acta* 1859, 1083–1099. <https://doi.org/10.1016/j.bbagr.2016.03.002>
- Chai, S.C., Wright, W.C., Chen, T., 2020. Strategies for developing pregnane X receptor antagonists: Implications from metabolism to cancer. *Med. Res. Rev.* 40, 1061–1083.
<https://doi.org/10.1002/med.21648>
- Chen, Y., Huang, W., Chen, F., et al., 2016. Pregnane X receptors regulate CYP2C8 and P-glycoprotein to impact on the resistance of NSCLC cells to Taxol. *Cancer Med.* 5, 3564–3571.
<https://doi.org/10.1002/cam4.960>
- Chen, Y., Tang, Y., Chen, S., Nie, D., 2009. Regulation of drug resistance by human pregnane X receptor in breast cancer. *Cancer Biol. Ther.* 8, 1265–1272. <https://doi.org/10.4161/cbt.8.13.8696>
- Chen, Y., Tang, Y., Robbins, G.T., Nie, D., 2010. Camptothecin attenuates cytochrome P450 3A4 induction by blocking the activation of human pregnane X receptor. *J. Pharmacol. Exp. Ther.* 334, 999–1008. <https://doi.org/10.1124/jpet.110.168294>
- Chen, Y., Tang, Y., Wang, M.-T., Zeng, S., Nie, D., 2007. Human pregnane X receptor and resistance to chemotherapy in prostate cancer. *Cancer Res.* 67, 10361–10367. <https://doi.org/10.1158/0008-5472.CAN-06-4758>
- Choi, S.H., Hong, H.K., Cho, Y.B., Lee, W.Y., Yoo, H.Y., 2015. Identification of Sestrin3 Involved in the In vitro Resistance of Colorectal Cancer Cells to Irinotecan. *PLoS One* 10, e0126830.
<https://doi.org/10.1371/journal.pone.0126830>
- Cresteil, T., Monsarrat, B., Alvinerie, P., Tréluyer, J.M., Vieira, I., Wright, M., 1994. Taxol metabolism by human liver microsomes: identification of cytochrome P450 isozymes involved in its biotransformation. *Cancer Res.* 54, 386–392.

- De Luca, A., Parker, L.J., Ang, W.H., et al., 2019. A structure-based mechanism of cisplatin resistance mediated by glutathione transferase P1-1. *Proc. Natl. Acad. Sci. U. S. A.* 116, 13943–13951. <https://doi.org/10.1073/pnas.1903297116>
- de Souza Abreu, R., Penalva, L.O., Marcotte, E.M., Vogel, C., 2009. Global signatures of protein and mRNA expression levels. *Mol. Biosyst.* 5, 1512–1526. <https://doi.org/10.1039/b908315d>
- Deng, R., Xu, C., Chen, X., et al., 2014. Resveratrol suppresses the inducible expression of CYP3A4 through the pregnane X receptor. *J. Pharmacol. Sci.* 126, 146–154. <https://doi.org/10.1254/jphs.14132fp>
- Deuring, J.J., Li, M., Cao, W., et al., 2019. Pregnane X receptor activation constrains mucosal NF- κ B activity in active inflammatory bowel disease. *PloS One* 14, e0221924. <https://doi.org/10.1371/journal.pone.0221924>
- di Masi, A., De Marinis, E., Ascenzi, P., Marino, M., 2009. Nuclear receptors CAR and PXR: Molecular, functional, and biomedical aspects. *Mol. Aspects Med.* 30, 297–343. <https://doi.org/10.1016/j.mam.2009.04.002>
- Dietlein, F., Weghorn, D., Taylor-Weiner, A., et al., 2020. Identification of cancer driver genes based on nucleotide context. *Nat. Genet.* 52, 208–218. <https://doi.org/10.1038/s41588-019-0572-y>
- Ding, X., Staudinger, J.L., 2005a. Induction of drug metabolism by forskolin: the role of the pregnane X receptor and the protein kinase a signal transduction pathway. *J. Pharmacol. Exp. Ther.* 312, 849–856. <https://doi.org/10.1124/jpet.104.076331>
- Ding, X., Staudinger, J.L., 2005b. Repression of PXR-mediated induction of hepatic CYP3A gene expression by protein kinase C. *Biochem. Pharmacol.* 69, 867–873. <https://doi.org/10.1016/j.bcp.2004.11.025>
- Dohse, M., Scharenberg, C., Shukla, S., et al., 2010. Comparison of ATP-binding cassette transporter interactions with the tyrosine kinase inhibitors imatinib, nilotinib, and dasatinib. *Drug Metab. Dispos. Biol. Fate Chem.* 38, 1371–1380. <https://doi.org/10.1124/dmd.109.031302>
- Domanska, U.M., Kruijzinga, R.C., Nagengast, W.B., et al., 2013. A review on CXCR4/CXCL12 axis in oncology: no place to hide. *Eur. J. Cancer Oxf. Engl.* 1990 49, 219–230. <https://doi.org/10.1016/j.ejca.2012.05.005>
- Dong, H., Lin, W., Wu, J., Chen, T., 2010. Flavonoids activate pregnane x receptor-mediated CYP3A4 gene expression by inhibiting cyclin-dependent kinases in HepG2 liver carcinoma cells. *BMC Biochem.* 11, 23. <https://doi.org/10.1186/1471-2091-11-23>
- Dong, Y., Wang, Z., Xie, G.-F., et al., 2017. Pregnane X receptor is associated with unfavorable survival and induces chemotherapeutic resistance by transcriptional activating multidrug resistance-related protein 3 in colorectal cancer. *Mol. Cancer* 16, 71. <https://doi.org/10.1186/s12943-017-0641-8>
- Dotzlaw, H., Leygue, E., Watson, P., Murphy, L.C., 1999. The human orphan receptor PXR messenger RNA is expressed in both normal and neoplastic breast tissue. *Clin. Cancer Res. Off. J. Am. Assoc. Cancer Res.* 5, 2103–2107.
- Ekins, S., Kholodovych, V., Ai, N., et al., 2008. Computational discovery of novel low micromolar human pregnane X receptor antagonists. *Mol. Pharmacol.* 74, 662–672. <https://doi.org/10.1124/mol.108.049437>
- EMA, 2019a. Sprycel EPAR Medicine overview. Accessed 25.06.2020. Available from <https://www.ema.europa.eu>
- EMA, 2019b. Nexavar: Summary of product characteristics. Accessed 18.11.2020. Available from <https://www.ema.europa.eu>
- EMA, 2018. Tasigna EPAR Summary review for the public. Accessed 25.06.2020. Available from <https://www.ema.europa.eu>
- EMA, 2014. Arava EPAR Summary for the public. Accessed 21.10.2020. Available from <https://www.ema.europa.eu>
- EMA, 2012. Guideline on the investigation of drug interactions. Accessed 21.10.2020. Available from <https://www.ema.europa.eu>
- EMA, E., 2013. Stivarga Assessment Report. Accessed 27.06.2020. Available from <https://www.ema.europa.eu>
- Eurostat, 2016. Causes and occurrence of deaths in EU. Accessed 27.04.2020. Available from <https://ec.europa.eu/eurostat>
- Farid, R., Day, T., Friesner, R.A., Pearlstein, R.A., 2006. New insights about HERG blockade obtained from protein modeling, potential energy mapping, and docking studies. *Bioorg. Med. Chem.* 14, 3160–3173. <https://doi.org/10.1016/j.bmc.2005.12.032>
- FDA, 2014. Beleodaq/belinostat Summary review. Accessed 09.02.2020. Available from <https://www.fda.gov/drugs>
- FDA, 2004. Camptosar Biopharm review. Accessed 09.02.2020. Available from <https://www.fda.gov/drugs>
- Flanagan, J.J., Neklesa, T.K., 2019. Targeting Nuclear Receptors with PROTAC degraders. *Mol. Cell. Endocrinol.* 493, 110452. <https://doi.org/10.1016/j.mce.2019.110452>

- Frank, C., Makkonen, H., Dunlop, T.W., Matilainen, M., Väisänen, S., Carlberg, C., 2005. Identification of pregnane X receptor binding sites in the regulatory regions of genes involved in bile acid homeostasis. *J. Mol. Biol.* 346, 505–519. <https://doi.org/10.1016/j.jmb.2004.12.003>
- Friesner, R.A., Banks, J.L., Murphy, R.B., et al., 2004. Glide: a new approach for rapid, accurate docking and scoring. 1. Method and assessment of docking accuracy. *J. Med. Chem.* 47, 1739–1749. <https://doi.org/10.1021/jm0306430>
- Friesner, R.A., Murphy, R.B., Repasky, M.P., et al., 2006. Extra precision glide: docking and scoring incorporating a model of hydrophobic enclosure for protein-ligand complexes. *J. Med. Chem.* 49, 6177–6196. <https://doi.org/10.1021/jm051256o>
- Fujita, D., Saito, Y., Nakanishi, T., Tamai, I., 2016. Organic Anion Transporting Polypeptide (OATP)2B1 Contributes to Gastrointestinal Toxicity of Anticancer Drug SN-38, Active Metabolite of Irinotecan Hydrochloride. *Drug Metab. Dispos. Biol. Fate Chem.* 44, 1–7. <https://doi.org/10.1124/dmd.115.066712>
- Gagné, J.-F., Montminy, V., Belanger, P., Journault, K., Gaucher, G., Guillemette, C., 2002. Common human UGT1A polymorphisms and the altered metabolism of irinotecan active metabolite 7-ethyl-10-hydroxycamptothecin (SN-38). *Mol. Pharmacol.* 62, 608–617. <https://doi.org/10.1124/mol.62.3.608>
- Galadari, S., Rahman, A., Pallichankandy, S., Thayyullathil, F., 2017. Reactive oxygen species and cancer paradox: To promote or to suppress? *Free Radic. Biol. Med.* 104, 144–164. <https://doi.org/10.1016/j.freeradbiomed.2017.01.004>
- Garcia, M., Thirouard, L., Sedès, L., et al., 2018. Nuclear Receptor Metabolism of Bile Acids and Xenobiotics: A Coordinated Detoxification System with Impact on Health and Diseases. *Int. J. Mol. Sci.* 19. <https://doi.org/10.3390/ijms19113630>
- Gardner-Stephen, D., Heydel, J.-M., Goyal, A., et al., 2004. Human PXR variants and their differential effects on the regulation of human UDP-glucuronosyltransferase gene expression. *Drug Metab. Dispos. Biol. Fate Chem.* 32, 340–347. <https://doi.org/10.1124/dmd.32.3.340>
- Geick, A., Eichelbaum, M., Burk, O., 2001. Nuclear receptor response elements mediate induction of intestinal MDR1 by rifampin. *J. Biol. Chem.* 276, 14581–14587. <https://doi.org/10.1074/jbc.M010173200>
- Gong, H., Singh, S.V., Singh, S.P., et al., 2006. Orphan nuclear receptor pregnane X receptor sensitizes oxidative stress responses in transgenic mice and cancerous cells. *Mol. Endocrinol. Baltim. Md* 20, 279–290. <https://doi.org/10.1210/me.2005-0205>
- Goodwin, B., Gauthier, K.C., Umetani, M., et al., 2003. Identification of bile acid precursors as endogenous ligands for the nuclear xenobiotic pregnane X receptor. *Proc. Natl. Acad. Sci. U. S. A.* 100, 223–228. <https://doi.org/10.1073/pnas.0237082100>
- Goodwin, B., Hodgson, E., Liddle, C., 1999. The orphan human pregnane X receptor mediates the transcriptional activation of CYP3A4 by rifampicin through a distal enhancer module. *Mol. Pharmacol.* 56, 1329–1339. <https://doi.org/10.1124/mol.56.6.1329>
- Gotoh, S., Negishi, M., 2015. Statin-activated nuclear receptor PXR promotes SGK2 dephosphorylation by scaffolding PP2C to induce hepatic gluconeogenesis. *Sci. Rep.* 5, 14076. <https://doi.org/10.1038/srep14076>
- Gotoh, S., Negishi, M., 2014. Serum- and Glucocorticoid-Regulated Kinase 2 Determines Drug-Activated Pregnane X Receptor to Induce Gluconeogenesis in Human Liver Cells. *J. Pharmacol. Exp. Ther.* 348, 131–140. <https://doi.org/10.1124/jpet.113.209379>
- Gupta, D., Venkatesh, M., Wang, H., et al., 2008. Expanding the roles for pregnane X receptor in cancer: proliferation and drug resistance in ovarian cancer. *Clin. Cancer Res. Off. J. Am. Assoc. Cancer Res.* 14, 5332–5340. <https://doi.org/10.1158/1078-0432.CCR-08-1033>
- Haaz, M.C., Rivory, L., Riché, C., Vernillet, L., Robert, J., 1998. Metabolism of irinotecan (CPT-11) by human hepatic microsomes: participation of cytochrome P-450 3A and drug interactions. *Cancer Res.* 58, 468–472.
- Hakkola, J., Rysä, J., Hukkanen, J., 2016. Regulation of hepatic energy metabolism by the nuclear receptor PXR. *Biochim. Biophys. Acta* 1859, 1072–1082. <https://doi.org/10.1016/j.bbagr.2016.03.012>
- Halgren, T.A., Murphy, R.B., Friesner, R.A., et al., 2004. Glide: a new approach for rapid, accurate docking and scoring. 2. Enrichment factors in database screening. *J. Med. Chem.* 47, 1750–1759. <https://doi.org/10.1021/jm030644s>
- Hardwick, J.M., Soane, L., 2013. Multiple functions of BCL-2 family proteins. *Cold Spring Harb. Perspect. Biol.* 5. <https://doi.org/10.1101/cshperspect.a008722>
- Harmsen, S., Meijerman, I., Beijnen, J.H., Schellens, J.H.M., 2009. Nuclear receptor mediated induction of cytochrome P450 3A4 by anticancer drugs: a key role for the pregnane X receptor. *Cancer Chemother. Pharmacol.* 64, 35–43. <https://doi.org/10.1007/s00280-008-0842-3>

- Harmsen, S., Meijerman, I., Febus, C.L., Maas-Bakker, R.F., Beijnen, J.H., Schellens, J.H.M., 2010. PXR-mediated induction of P-glycoprotein by anticancer drugs in a human colon adenocarcinoma-derived cell line. *Cancer Chemother. Pharmacol.* 66, 765–771. <https://doi.org/10.1007/s00280-009-1221-4>
- Harmsen, S., Meijerman, I., Maas-Bakker, R.F., Beijnen, J.H., Schellens, J.H.M., 2013. PXR-mediated P-glycoprotein induction by small molecule tyrosine kinase inhibitors. *Eur. J. Pharm. Sci. Off. J. Eur. Fed. Pharm. Sci.* 48, 644–649. <https://doi.org/10.1016/j.ejps.2012.12.019>
- He, J., Gao, J., Xu, M., et al., 2013. PXR ablation alleviates diet-induced and genetic obesity and insulin resistance in mice. *Diabetes* 62, 1876–1887. <https://doi.org/10.2337/db12-1039>
- Healan-Greenberg, C., Waring, J.F., Kempf, D.J., Blomme, E.A.G., Tirona, R.G., Kim, R.B., 2008. A human immunodeficiency virus protease inhibitor is a novel functional inhibitor of human pregnane X receptor. *Drug Metab. Dispos. Biol. Fate Chem.* 36, 500–507. <https://doi.org/10.1124/dmd.107.019547>
- Hendriks, J.J.M.A., Lagas, J.S., Rosing, H., Schellens, J.H.M., Beijnen, J.H., Schinkel, A.H., 2013. P-glycoprotein and cytochrome P450 3A act together in restricting the oral bioavailability of paclitaxel. *Int. J. Cancer* 132, 2439–2447. <https://doi.org/10.1002/ijc.27912>
- Hermann, P.C., Huber, S.L., Herrler, T., et al., 2007. Distinct populations of cancer stem cells determine tumor growth and metastatic activity in human pancreatic cancer. *Cell Stem Cell* 1, 313–323. <https://doi.org/10.1016/j.stem.2007.06.002>
- Herraez, E., Gonzalez-Sanchez, E., Vaquero, J., et al., 2012. Cisplatin-induced chemoresistance in colon cancer cells involves FXR-dependent and FXR-independent up-regulation of ABC proteins. *Mol. Pharm.* 9, 2565–2576. <https://doi.org/10.1021/mp300178a>
- Himmelstein, K.J., Patton, T.F., Belt, R.J., Taylor, S., Repta, A.J., Sternson, L.A., 1981. Clinical kinetics on intact cisplatin and some related species. *Clin. Pharmacol. Ther.* 29, 658–664. <https://doi.org/10.1038/clpt.1981.91>
- Hoffart, E., Ghebregiorghis, L., Nussler, A.K., et al., 2012. Effects of atorvastatin metabolites on induction of drug-metabolizing enzymes and membrane transporters through human pregnane X receptor. *Br. J. Pharmacol.* 165, 1595–1608. <https://doi.org/10.1111/j.1476-5381.2011.01665.x>
- Holohan, C., Van Schaeybroeck, S., Longley, D.B., Johnston, P.G., 2013. Cancer drug resistance: an evolving paradigm. *Nat. Rev. Cancer* 13, 714–726. <https://doi.org/10.1038/nrc3599>
- Holzer, A.K., Howell, S.B., 2006. The internalization and degradation of human copper transporter 1 following cisplatin exposure. *Cancer Res.* 66, 10944–10952. <https://doi.org/10.1158/0008-5472.CAN-06-1710>
- Hrycay, E.G., Bandiera, S.M., 2015. Involvement of Cytochrome P450 in Reactive Oxygen Species Formation and Cancer. *Adv. Pharmacol. San Diego Calif* 74, 35–84. <https://doi.org/10.1016/bs.apha.2015.03.003>
- Huang, H., Wang, H., Sinz, M., et al., 2007. Inhibition of drug metabolism by blocking the activation of nuclear receptors by ketoconazole. *Oncogene* 26, 258–268. <https://doi.org/10.1038/sj.onc.1209788>
- Huang, W.-S., Hsieh, M.-C., Huang, C.-Y., et al., 2016. The association of CXC receptor 4 mediated signaling pathway with oxaliplatin-resistant human colorectal cancer cells. *PLoS One* 11, e0159927. <https://doi.org/10.1371/journal.pone.0159927>
- Huber, A.D., Wright, W.C., Lin, W., et al., 2020. Mutation of a single amino acid of pregnane X receptor switches an antagonist to agonist by altering AF-2 helix positioning. *Cell. Mol. Life Sci. CMLS.* <https://doi.org/10.1007/s00018-020-03505-y>
- Humerickhouse, R., Lohrbach, K., Li, L., Bosron, W.F., Dolan, M.E., 2000. Characterization of CPT-11 hydrolysis by human liver carboxylesterase isoforms hCE-1 and hCE-2. *Cancer Res.* 60, 1189–1192.
- Hustert, E., Zibat, A., Presecan-Siedel, E., et al., 2001. Natural protein variants of pregnane X receptor with altered transactivation activity toward CYP3A4. *Drug Metab. Dispos. Biol. Fate Chem.* 29, 1454–1459.
- Inoue, Y., Matsumoto, H., Yamada, S., et al., 2010. Association of ATP7A expression and in vitro sensitivity to cisplatin in non-small cell lung cancer. *Oncol. Lett.* 1, 837–840. <https://doi.org/10.3892/ol.00000147>
- Ishida, S., Lee, J., Thiele, D.J., Herskowitz, I., 2002. Uptake of the anticancer drug cisplatin mediated by the copper transporter Ctr1 in yeast and mammals. *Proc. Natl. Acad. Sci. U. S. A.* 99, 14298–14302. <https://doi.org/10.1073/pnas.162491399>
- Ishida, S., McCormick, F., Smith-McCune, K., Hanahan, D., 2010. Enhancing tumor-specific uptake of the anticancer drug cisplatin with a copper chelator. *Cancer Cell* 17, 574–583. <https://doi.org/10.1016/j.ccr.2010.04.011>
- Iusuf, D., Ludwig, M., Elbatsh, A., et al., 2014. OATP1A/1B transporters affect irinotecan and SN-38 pharmacokinetics and carboxylesterase expression in knockout and humanized transgenic mice. *Mol. Cancer Ther.* 13, 492–503. <https://doi.org/10.1158/1535-7163.MCT-13-0541>
- Iyer, L., King, C.D., Whittington, P.F., et al., 1998. Genetic predisposition to the metabolism of irinotecan (CPT-11). Role of uridine diphosphate glucuronosyltransferase isoform 1A1 in the glucuronidation of its active metabolite (SN-38) in human liver microsomes. *J. Clin. Invest.* 101, 847–854. <https://doi.org/10.1172/JC1915>

- Iyer, L., Ramírez, J., Shepard, D.R., et al., 2002. Biliary transport of irinotecan and metabolites in normal and P-glycoprotein-deficient mice. *Cancer Chemother. Pharmacol.* 49, 336–341. <https://doi.org/10.1007/s00280-001-0420-4>
- Jandu, H., Aluzaitė, K., Fogh, L., et al., 2016. Molecular characterization of irinotecan (SN-38) resistant human breast cancer cell lines. *BMC Cancer* 16, 34. <https://doi.org/10.1186/s12885-016-2071-1>
- Januchowski, R., Zawierucha, P., Andrzejewska, M., Ruciński, M., Zabel, M., 2013. Microarray-based detection and expression analysis of ABC and SLC transporters in drug-resistant ovarian cancer cell lines. *Biomed. Pharmacother. Biomedicine Pharmacother.* 67, 240–245. <https://doi.org/10.1016/j.biopha.2012.11.011>
- Jensen, N.F., Stenvang, J., Beck, M.K., et al., 2015. Establishment and characterization of models of chemotherapy resistance in colorectal cancer: Towards a predictive signature of chemoresistance. *Mol. Oncol.* 9, 1169–1185. <https://doi.org/10.1016/j.molonc.2015.02.008>
- Jeske, J., Bitter, A., Thasler, W.E., Weiss, T.S., Schwab, M., Burk, O., 2017. Ligand-dependent and -independent regulation of human hepatic sphingomyelin phosphodiesterase acid-like 3A expression by pregnane X receptor and crosstalk with liver X receptor. *Biochem. Pharmacol.* 136, 122–135. <https://doi.org/10.1016/j.bcp.2017.04.013>
- Jones, S.A., Moore, L.B., Shenk, J.L., et al., 2000. The pregnane X receptor: a promiscuous xenobiotic receptor that has diverged during evolution. *Mol. Endocrinol. Baltim. Md* 14, 27–39. <https://doi.org/10.1210/mend.14.1.0409>
- Jung, M.-J., Rho, J.-K., Kim, Y.-M., et al., 2013. Upregulation of CXCR4 is functionally crucial for maintenance of stemness in drug-resistant non-small cell lung cancer cells. *Oncogene* 32, 209–221. <https://doi.org/10.1038/onc.2012.37>
- Kandel, B.A., Thomas, M., Winter, S., et al., 2016. Genomewide comparison of the inducible transcriptomes of nuclear receptors CAR, PXR and PPAR α in primary human hepatocytes. *Biochim. Biophys. Acta* 1859, 1218–1227. <https://doi.org/10.1016/j.bbagr.2016.03.007>
- Kanzawa, F., Sugimoto, Y., Minato, K., et al., 1990. Establishment of a camptothecin analogue (CPT-11)-resistant cell line of human non-small cell lung cancer: characterization and mechanism of resistance. *Cancer Res.* 50, 5919–5924.
- Kapałczyńska, M., Kolenda, T., Przybyła, W., et al., 2018. 2D and 3D cell cultures – a comparison of different types of cancer cell cultures. *Arch. Med. Sci. AMS* 14, 910–919. <https://doi.org/10.5114/aoms.2016.63743>
- Kawato, Y., Aonuma, M., Hirota, Y., Kuga, H., Sato, K., 1991. Intracellular roles of SN-38, a metabolite of the camptothecin derivative CPT-11, in the antitumor effect of CPT-11. *Cancer Res.* 51, 4187–4191.
- Khazak, V., Astsaturov, I., Serebriiskii, I.G., Golemis, E.A., 2007. Selective Raf Inhibition in Cancer Therapy. *Expert Opin. Ther. Targets* 11, 1587–1609. <https://doi.org/10.1517/14728222.11.12.1587>
- Kliwer, S.A., Moore, J.T., Wade, L., et al., 1998. An orphan nuclear receptor activated by pregnanes defines a novel steroid signaling pathway. *Cell* 92, 73–82. [https://doi.org/10.1016/s0092-8674\(00\)80900-9](https://doi.org/10.1016/s0092-8674(00)80900-9)
- Kodama, S., Koike, C., Negishi, M., Yamamoto, Y., 2004. Nuclear receptors CAR and PXR cross talk with FOXO1 to regulate genes that encode drug-metabolizing and gluconeogenic enzymes. *Mol. Cell. Biol.* 24, 7931–7940. <https://doi.org/10.1128/MCB.24.18.7931-7940.2004>
- Kodama, S., Moore, R., Yamamoto, Y., Negishi, M., 2007. Human nuclear pregnane X receptor cross-talk with CREB to repress cAMP activation of the glucose-6-phosphatase gene. *Biochem. J.* 407, 373–381. <https://doi.org/10.1042/BJ20070481>
- Kodama, S., Negishi, M., 2011. Pregnane X receptor PXR activates the GADD45beta gene, eliciting the p38 MAPK signal and cell migration. *J. Biol. Chem.* 286, 3570–3578. <https://doi.org/10.1074/jbc.M110.179812>
- Kojetin, D.J., Burris, T.P., 2013. Small Molecule Modulation of Nuclear Receptor Conformational Dynamics: Implications for Function and Drug Discovery. *Mol. Pharmacol.* 83, 1–8. <https://doi.org/10.1124/mol.112.079285>
- Kothandapani, A., Sawant, A., Dangeti, V.S.M.N., Sobol, R.W., Patrick, S.M., 2013. Epistatic role of base excision repair and mismatch repair pathways in mediating cisplatin cytotoxicity. *Nucleic Acids Res.* 41, 7332–7343. <https://doi.org/10.1093/nar/gkt479>
- Koussounadis, A., Langdon, S.P., Um, I.H., Harrison, D.J., Smith, V.A., 2015. Relationship between differentially expressed mRNA and mRNA-protein correlations in a xenograft model system. *Sci. Rep.* 5, 10775. <https://doi.org/10.1038/srep10775>
- Krasowski, M.D., Yasuda, K., Hagey, L.R., Schuetz, E.G., 2005. Evolution of the Pregnane X Receptor: Adaptation to Cross-Species Differences in Biliary Bile Salts. *Mol. Endocrinol.* 19, 1720–1739. <https://doi.org/10.1210/me.2004-0427>

- Krausova, L., Stejskalova, L., Wang, H., et al., 2011. Metformin suppresses pregnane X receptor (PXR)-regulated transactivation of CYP3A4 gene. *Biochem. Pharmacol.* 82, 1771–1780. <https://doi.org/10.1016/j.bcp.2011.08.023>
- Lage, H., Christmann, M., Kern, M.A., et al., 1999. Expression of DNA repair proteins hMSH2, hMSH6, hMLH1, O6-methylguanine-DNA methyltransferase and N-methylpurine-DNA glycosylase in melanoma cells with acquired drug resistance. *Int. J. Cancer* 80, 744–750. [https://doi.org/10.1002/\(sici\)1097-0215\(19990301\)80:5<744::aid-ijc19>3.0.co;2-5](https://doi.org/10.1002/(sici)1097-0215(19990301)80:5<744::aid-ijc19>3.0.co;2-5)
- Lamba, V., Yasuda, K., Lamba, J.K., et al., 2004. PXR (NR1I2): splice variants in human tissues, including brain, and identification of neurosteroids and nicotine as PXR activators. *Toxicol. Appl. Pharmacol.* 199, 251–265. <https://doi.org/10.1016/j.taap.2003.12.027>
- Lee, Y.-Y., Choi, C.H., Do, I.-G., et al., 2011. Prognostic value of the copper transporters, CTR1 and CTR2, in patients with ovarian carcinoma receiving platinum-based chemotherapy. *Gynecol. Oncol.* 122, 361–365. <https://doi.org/10.1016/j.ygyno.2011.04.025>
- Lehmann, J.M., McKee, D.D., Watson, M.A., Willson, T.M., Moore, J.T., Kliewer, S.A., 1998. The human orphan nuclear receptor PXR is activated by compounds that regulate CYP3A4 gene expression and cause drug interactions. *J. Clin. Invest.* 102, 1016–1023. <https://doi.org/10.1172/JCI3703>
- Lemaire, G., Benod, C., Nahoum, V., et al., 2007. Discovery of a highly active ligand of human pregnane x receptor: a case study from pharmacophore modeling and virtual screening to “in vivo” biological activity. *Mol. Pharmacol.* 72, 572–581. <https://doi.org/10.1124/mol.106.033415>
- Lemaire, G., de Sousa, G., Rahmani, R., 2004. A PXR reporter gene assay in a stable cell culture system: CYP3A4 and CYP2B6 induction by pesticides. *Biochem. Pharmacol.* 68, 2347–2358. <https://doi.org/10.1016/j.bcp.2004.07.041>
- Li, J., Jiang, K., Qiu, X., et al., 2014. Overexpression of CXCR4 is significantly associated with cisplatin-based chemotherapy resistance and can be a prognostic factor in epithelial ovarian cancer. *BMB Rep.* 47, 33–38. <https://doi.org/10.5483/bmbrep.2014.47.1.069>
- Li, L., Li, H., Garzel, B., et al., 2015. SLC13A5 is a novel transcriptional target of the pregnane X receptor and sensitizes drug-induced steatosis in human liver. *Mol. Pharmacol.* 87, 674–682. <https://doi.org/10.1124/mol.114.097287>
- Li, Q., Gardner, K., Zhang, L., Tsang, B., Bostick-Bruton, F., Reed, E., 1998. Cisplatin induction of ERCC-1 mRNA expression in A2780/CP70 human ovarian cancer cells. *J. Biol. Chem.* 273, 23419–23425. <https://doi.org/10.1074/jbc.273.36.23419>
- Li, T., Chiang, J.Y.L., 2013. Nuclear receptors in bile acid metabolism. *Drug Metab. Rev.* 45, 145–155. <https://doi.org/10.3109/03602532.2012.740048>
- Li, T., Chiang, J.Y.L., 2005. Mechanism of rifampicin and pregnane X receptor inhibition of human cholesterol 7 alpha-hydroxylase gene transcription. *Am. J. Physiol. Gastrointest. Liver Physiol.* 288, G74-84. <https://doi.org/10.1152/ajpgi.00258.2004>
- Li, Z.-H., Zheng, R., Chen, J.-T., Jia, J., Qiu, M., 2016. The role of copper transporter ATP7A in platinum-resistance of esophageal squamous cell cancer (ESCC). *J. Cancer* 7, 2085–2092. <https://doi.org/10.7150/jca.16117>
- Lichti-Kaiser, K., Xu, C., Staudinger, J.L., 2009. Cyclic AMP-dependent protein kinase signaling modulates pregnane x receptor activity in a species-specific manner. *J. Biol. Chem.* 284, 6639–6649. <https://doi.org/10.1074/jbc.M807426200>
- Liedert, B., Materna, V., Schadendorf, D., Thomale, J., Lage, H., 2003. Overexpression of cMOAT (MRP2/ABCC2) is associated with decreased formation of platinum-DNA adducts and decreased G2-arrest in melanoma cells resistant to cisplatin. *J. Invest. Dermatol.* 121, 172–176. <https://doi.org/10.1046/j.1523-1747.2003.12313.x>
- Lim, Y.-P., Cheng, C.-H., Chen, W.-C., et al., 2015. Allyl isothiocyanate (AITC) inhibits pregnane X receptor (PXR) and constitutive androstane receptor (CAR) activation and protects against acetaminophen- and amiodarone-induced cytotoxicity. *Arch. Toxicol.* 89, 57–72. <https://doi.org/10.1007/s00204-014-1230-x>
- Lim, Y.-P., Ma, C.-Y., Liu, C.-L., et al., 2012. Sesamin: A Naturally Occurring Lignan Inhibits CYP3A4 by Antagonizing the Pregnane X Receptor Activation. *Evid.-Based Complement. Altern. Med. ECAM* 2012, 242810. <https://doi.org/10.1155/2012/242810>
- Lin, W., Wang, Y.-M., Chai, S.C., et al., 2017. SPA70 is a potent antagonist of human pregnane X receptor. *Nat. Commun.* 8, 741. <https://doi.org/10.1038/s41467-017-00780-5>
- Lin, W., Wu, J., Dong, H., Bouck, D., Zeng, F.-Y., Chen, T., 2008. Cyclin-dependent kinase 2 negatively regulates human pregnane X receptor-mediated CYP3A4 gene expression in HepG2 liver carcinoma cells. *J. Biol. Chem.* 283, 30650–30657. <https://doi.org/10.1074/jbc.M806132200>

- Lin, Y.S., Yasuda, K., Assem, M., et al., 2009. The major human pregnane X receptor (PXR) splice variant, PXR.2, exhibits significantly diminished ligand-activated transcriptional regulation. *Drug Metab. Dispos.* 37, 1295–1304. <https://doi.org/10.1124/dmd.108.025213>
- Linev, A.J., Ivanov, H.J., Zhelyazkov, I.G., Ivanova, H., Goranova-Marinova, V.S., Stoyanova, V.K., 2018. Mutations associated with imatinib mesylate resistance - Review. *Folia Med. (Plovdiv)* 60, 617–623. <https://doi.org/10.2478/folmed-2018-0030>
- Ling, Z., Shu, N., Xu, P., et al., 2016. Involvement of pregnane X receptor in the impaired glucose utilization induced by atorvastatin in hepatocytes. *Biochem. Pharmacol.* 100, 98–111. <https://doi.org/10.1016/j.bcp.2015.11.023>
- Liu, C.-L., Lim, Y.-P., Hu, M.-L., 2012. Fucoxanthin attenuates rifampin-induced cytochrome P450 3A4 (CYP3A4) and multiple drug resistance 1 (MDR1) gene expression through pregnane X receptor (PXR)-mediated pathways in human hepatoma HepG2 and colon adenocarcinoma LS174T cells. *Mar. Drugs* 10, 242–257. <https://doi.org/10.3390/md10010242>
- Liu, Q., Zhang, Z., Liu, Y., et al., 2018a. Cancer cells growing on perfused 3D collagen model produced higher reactive oxygen species level and were more resistant to cisplatin compared to the 2D model. *J. Appl. Biomater. Funct. Mater.* 16, 144–150. <https://doi.org/10.1177/2280800018764763>
- Liu, J., Jiang, G., Mao, P., et al., 2018b. Down-regulation of GADD45A enhances chemosensitivity in melanoma. *Sci. Rep.* 8, 4111. <https://doi.org/10.1038/s41598-018-22484-6>
- Livak, K.J., Schmittgen, T.D., 2001. Analysis of relative gene expression data using real-time quantitative PCR and the 2(-Delta Delta C(T)) Method. *Methods San Diego Calif* 25, 402–408. <https://doi.org/10.1006/meth.2001.1262>
- Luckert, C., Braeuning, A., Lampen, A., Hessel-Pras, S., 2018. PXR: Structure-specific activation by hepatotoxic pyrrolizidine alkaloids. *Chem. Biol. Interact.* 288, 38–48. <https://doi.org/10.1016/j.cbi.2018.04.017>
- Luo, F.R., Paranjpe, P.V., Guo, A., Rubin, E., Sinko, P., 2002. Intestinal transport of irinotecan in Caco-2 cells and MDCK II cells overexpressing efflux transporters Pgp, cMOAT, and MRP1. *Drug Metab. Dispos. Biol. Fate Chem.* 30, 763–770. <https://doi.org/10.1124/dmd.30.7.763>
- Lv, Y., Zhao, S., Han, J., Zheng, L., Yang, Z., Zhao, L., 2015. Hypoxia-inducible factor-1 α induces multidrug resistance protein in colon cancer. *OncoTargets Ther.* 8, 1941–1948. <https://doi.org/10.2147/OTT.S82835>
- Maglich, J.M., Parks, D.J., Moore, L.B., et al., 2003. Identification of a novel human constitutive androstane receptor (CAR) agonist and its use in the identification of CAR target genes. *J. Biol. Chem.* 278, 17277–17283. <https://doi.org/10.1074/jbc.M300138200>
- Marin, J.J.G., Briz, O., Herraiz, E., et al., 2018. Molecular bases of the poor response of liver cancer to chemotherapy. *Clin. Res. Hepatol. Gastroenterol.* 42, 182–192. <https://doi.org/10.1016/j.clinre.2017.12.006>
- Marin, J.J.G., Romero, M.R., Briz, O., 2010. Molecular bases of liver cancer refractoriness to pharmacological treatment. *Curr. Med. Chem.* 17, 709–740. <https://doi.org/10.2174/092986710790514462>
- Martin, P., Riley, R., Back, D.J., Owen, A., 2008. Comparison of the induction profile for drug disposition proteins by typical nuclear receptor activators in human hepatic and intestinal cells. *Br. J. Pharmacol.* 153, 805–819. <https://doi.org/10.1038/sj.bjp.0707601>
- Masuyama, H., Nakamura, K., Nobumoto, E., Hiramatsu, Y., 2016. Inhibition of pregnane X receptor pathway contributes to the cell growth inhibition and apoptosis of anticancer agents in ovarian cancer cells. *Int. J. Oncol.* 49, 1211–1220. <https://doi.org/10.3892/ijo.2016.3611>
- Masuyama, H., Nakatsukasa, H., Takamoto, N., Hiramatsu, Y., 2007. Down-regulation of pregnane X receptor contributes to cell growth inhibition and apoptosis by anticancer agents in endometrial cancer cells. *Mol. Pharmacol.* 72, 1045–1053. <https://doi.org/10.1124/mol.107.037937>
- Masuyama, H., Suwaki, N., Tateishi, Y., Nakatsukasa, H., Segawa, T., Hiramatsu, Y., 2005. The pregnane X receptor regulates gene expression in a ligand- and promoter-selective fashion. *Mol. Endocrinol. Baltim. Md* 19, 1170–1180. <https://doi.org/10.1210/me.2004-0434>
- Mathäs, M., Burk, O., Qiu, H., et al., 2012. Evolutionary history and functional characterization of the amphibian xenosensor CAR. *Mol. Endocrinol. Baltim. Md* 26, 14–26. <https://doi.org/10.1210/me.2011-1235>
- Mazaira, G.I., Zgajnar, N.R., Lotufo, C.M., et al., 2018. The nuclear receptor field: A historical overview and future challenges. *Nucl. Recept. Res.* 5. <https://doi.org/10.11131/2018/101320>
- McDermott, M., Eustace, A.J., Busschots, S., et al., 2014. In vitro development of chemotherapy and targeted therapy drug-resistant cancer cell lines: A practical guide with case studies. *Front. Oncol.* 4, 40. <https://doi.org/10.3389/fonc.2014.00040>

- McPhillips, F., Mullen, P., MacLeod, K.G., et al., 2006. Raf-1 is the predominant Raf isoform that mediates growth factor-stimulated growth in ovarian cancer cells. *Carcinogenesis* 27, 729–739. <https://doi.org/10.1093/carcin/bgi289>
- Miki, Y., Suzuki, T., Tazawa, C., Blumberg, B., Sasano, H., 2005. Steroid and xenobiotic receptor (SXR), cytochrome P450 3A4 and multidrug resistance gene 1 in human adult and fetal tissues. *Mol. Cell. Endocrinol.* 231, 75–85. <https://doi.org/10.1016/j.mce.2004.12.005>
- Min, L., Chen, Q., He, S., Liu, S., Ma, Y., 2012. Hypoxia-induced increases in A549/CDDP cell drug resistance are reversed by RNA interference of HIF-1 α expression. *Mol. Med. Rep.* 5, 228–232. <https://doi.org/10.3892/mmr.2011.604>
- Mnif, W., Pascussi, J.-M., Pillon, A., et al., 2007. Estrogens and antiestrogens activate hPXR. *Toxicol. Lett.* 170, 19–29. <https://doi.org/10.1016/j.toxlet.2006.11.016>
- Mooiman, K.D., Maas-Bakker, R.F., Moret, E.E., Beijnen, J.H., Schellens, J.H.M., Meijerman, I., 2013. Milk thistle's active components silybin and isosilybin: novel inhibitors of PXR-mediated CYP3A4 induction. *Drug Metab. Dispos. Biol. Fate Chem.* 41, 1494–1504. <https://doi.org/10.1124/dmd.113.050971>
- Moore, L. B., Parks, D.J., Jones, S.A., et al., 2000a. Orphan nuclear receptors constitutive androstane receptor and pregnane X receptor share xenobiotic and steroid ligands. *J. Biol. Chem.* 275, 15122–15127. <https://doi.org/10.1074/jbc.M001215200>
- Moore, L. B., Goodwin, B., Jones, S.A., 2000b. St. John's wort induces hepatic drug metabolism through activation of the pregnane X receptor. *Proc. Natl. Acad. Sci. U. S. A.* 97, 7500–7502.
- Moreau, A., T r uel, C., Beylot, M., et al., 2009. A novel pregnane X receptor and S14-mediated lipogenic pathway in human hepatocyte. *Hepatology* 49, 2068–2079. <https://doi.org/10.1002/hep.22907>
- Moreau, K., Coen, M., Zhang, A.X., et al., 2020. Proteolysis-targeting chimeras in drug development: A safety perspective. *Br. J. Pharmacol.* 177, 1709–1718. <https://doi.org/10.1111/bph.15014>
- Moscovitz, J.E., Kalgutkar, A.S., Nulick, K., et al., 2018. Establishing transcriptional signatures to differentiate PXR-, CAR-, and AhR-mediated regulation of drug metabolism and transport genes in cryopreserved human hepatocytes. *J. Pharmacol. Exp. Ther.* 365, 262–271. <https://doi.org/10.1124/jpet.117.247296>
- Mu, Y., Zhang, J., Zhang, S., et al., 2006. Traditional Chinese medicines Wu Wei Zi (*Schisandra chinensis* Baill) and Gan Cao (*Glycyrrhiza uralensis* Fisch) activate pregnane X receptor and increase warfarin clearance in rats. *J. Pharmacol. Exp. Ther.* 316, 1369–1377. <https://doi.org/10.1124/jpet.105.094342>
- Nakamura, K., Moore, R., Negishi, M., Sueyoshi, T., 2007. Nuclear pregnane X receptor cross-talk with FoxA2 to mediate drug-induced regulation of lipid metabolism in fasting mouse liver. *J. Biol. Chem.* 282, 9768–9776. <https://doi.org/10.1074/jbc.M610072200>
- Nakatomi, K., Yoshikawa, M., Oka, M., et al., 2001. Transport of 7-ethyl-10-hydroxycamptothecin (SN-38) by breast cancer resistance protein ABCG2 in human lung cancer cells. *Biochem. Biophys. Res. Commun.* 288, 827–832. <https://doi.org/10.1006/bbrc.2001.5850>
- Naspinski, C., Gu, X., Zhou, G.-D., Mertens-Talcott, S.U., Donnelly, K.C., Tian, Y., 2008. Pregnane X receptor protects HepG2 cells from BaP-induced DNA damage. *Toxicol. Sci. Off. J. Soc. Toxicol.* 104, 67–73. <https://doi.org/10.1093/toxsci/kfn058>
- NCT02144051, Phase I open label dose escalation study to investigate the safety & pharmacokinetics of AZD5312 in patients with androgen receptor tumors. Accessed 10.20.2020. Available from <https://clinicaltrials.gov/>
- NCT03300505, ARRx in combination with enzalutamide in metastatic castration resistant prostate cancer. Accessed 10.20.2020. Available from <https://clinicaltrials.gov/>
- NCT04072952, Clinical trial of ARV-471 in patients with ER+/HER2- locally advanced or metastatic breast cancer (mBC). Accessed 10.20.2020. Available from <https://clinicaltrials.gov/>
- N mcov -F rstov , V., Kopperov , D., Baluřikov , K., et al., 2016. Characterization of acquired paclitaxel resistance of breast cancer cells and involvement of ABC transporters. *Toxicol. Appl. Pharmacol.* 310, 215–228. <https://doi.org/10.1016/j.taap.2016.09.020>
- Ngan, C.-H., Beglov, D., Rudnitskaya, A.N., Kozakov, D., Waxman, D.J., Vajda, S., 2009. The structural basis of pregnane X receptor binding promiscuity. *Biochemistry* 48, 11572–11581. <https://doi.org/10.1021/bi901578n>
- Nishimura, T., Newkirk, K., Sessions, R.B., et al., 1996. Immunohistochemical staining for glutathione S-transferase predicts response to platinum-based chemotherapy in head and neck cancer. *Clin. Cancer Res. Off. J. Am. Assoc. Cancer Res.* 2, 1859–1865.
- Niu, Y., Wang, Z., Huang, H., et al., 2014. Activated pregnane X receptor inhibits cervical cancer cell proliferation and tumorigenicity by inducing G2/M cell-cycle arrest. *Cancer Lett.* 347, 88–97. <https://doi.org/10.1016/j.canlet.2014.01.026>

- Öhrvik, H., Logeman, B., Turk, B., Reinheckel, T., Thiele, D.J., 2016. Cathepsin protease controls copper and cisplatin accumulation via cleavage of the Ctr1 metal-binding ectodomain. *J. Biol. Chem.* 291, 13905–13916. <https://doi.org/10.1074/jbc.M116.731281>
- Olinga, P., Elferink, M.G.L., Draaisma, A.L., et al., 2008. Coordinated induction of drug transporters and phase I and II metabolism in human liver slices. *Eur. J. Pharm. Sci. Off. J. Eur. Fed. Pharm. Sci.* 33, 380–389. <https://doi.org/10.1016/j.ejps.2008.01.008>
- Ouyang, N., Ke, S., Eagleton, N., et al., 2010. Pregnane X receptor suppresses proliferation and tumorigenicity of colon cancer cells. *Br. J. Cancer* 102, 1753–1761. <https://doi.org/10.1038/sj.bjc.6605677>
- Pan, S.-T., Li, Z.-L., He, Z.-X., Qiu, J.-X., Zhou, S.-F., 2016. Molecular mechanisms for tumour resistance to chemotherapy. *Clin. Exp. Pharmacol. Physiol.* 43, 723–737. <https://doi.org/10.1111/1440-1681.12581>
- Pavek, P., 2016. Pregnane X Receptor (PXR)-Mediated Gene Repression and Cross-Talk of PXR with Other Nuclear Receptors via Coactivator Interactions. *Front. Pharmacol.* 7. <https://doi.org/10.3389/fphar.2016.00456>
- Persson, K.P., Ekehed, S., Otter, C., et al., 2006. Evaluation of human liver slices and reporter gene assays as systems for predicting the cytochrome p450 induction potential of drugs in vivo in humans. *Pharm. Res.* 23, 56–69. <https://doi.org/10.1007/s11095-005-8812-5>
- Petitprez, A., Larsen, A.K., 2013. Irinotecan resistance is accompanied by upregulation of EGFR and Src signaling in human cancer models. *Curr. Pharm. Des.* 19, 958–964.
- Petitprez, A., Poindessous, V., Ouaret, D., et al., 2013. Acquired irinotecan resistance is accompanied by stable modifications of cell cycle dynamics independent of MSI status. *Int. J. Oncol.* 42, 1644–1653. <https://doi.org/10.3892/ijco.2013.1868>
- Pfrunder, A., Gutmann, H., Beglinger, C., Drewe, J., 2003. Gene expression of CYP3A4, ABC-transporters (MDR1 and MRP1-MRP5) and hPXR in three different human colon carcinoma cell lines. *J. Pharm. Pharmacol.* 55, 59–66. <https://doi.org/10.1111/j.2042-7158.2003.tb02434.x>
- Piedade, R., Traub, S., Bitter, A., et al., 2015. Carboxymefloquine, the major metabolite of the antimalarial drug mefloquine, induces drug-metabolizing enzyme and transporter expression by activation of pregnane X receptor. *Antimicrob. Agents Chemother.* 59, 96–104. <https://doi.org/10.1128/AAC.04140-14>
- Pissios, P., Tzamelis, I., Kushner, P., Moore, D.D., 2000. Dynamic stabilization of nuclear receptor ligand binding domains by hormone or corepressor binding. *Mol. Cell* 6, 245–253. [https://doi.org/10.1016/s1097-2765\(00\)00026-5](https://doi.org/10.1016/s1097-2765(00)00026-5)
- Planque, C., Rajabi, F., Grillet, F., et al., 2016. Pregnane X-receptor promotes stem cell-mediated colon cancer relapse. *Oncotarget* 7, 56558–56573. <https://doi.org/10.18632/oncotarget.10646>
- Pondugula, S.R., Brimer-Cline, C., Wu, J., Schuetz, E.G., Tyagi, R.K., Chen, T., 2009. A phosphomimetic mutation at threonine-57 abolishes transactivation activity and alters nuclear localization pattern of human pregnane x receptor. *Drug Metab. Dispos. Biol. Fate Chem.* 37, 719–730. <https://doi.org/10.1124/dmd.108.024695>
- Pondugula, S.R., Pavek, P., Mani, S., 2016. Pregnane X receptor and cancer: Context-specificity is key. *Nucl. Recept. Res.* 3. <https://doi.org/10.11131/2016/101198>
- Prakash, C., Zuniga, B., Song, C.S., et al., 2015. Nuclear receptors in drug metabolism, drug response and drug interactions. *Nucl. Recept. Res.* 2. <https://doi.org/10.11131/2015/101178>
- Ratajewski, M., Grzelak, I., Wiśniewska, K., et al., 2015. Screening of a chemical library reveals novel PXR-activating pharmacologic compounds. *Toxicol. Lett.* 232, 193–202. <https://doi.org/10.1016/j.toxlet.2014.10.009>
- Raynal, C., Pascussi, J.-M., Leguelinel, G., et al., 2010. Pregnane X Receptor (PXR) expression in colorectal cancer cells restricts irinotecan chemosensitivity through enhanced SN-38 glucuronidation. *Mol. Cancer* 9, 46. <https://doi.org/10.1186/1476-4598-9-46>
- Robbins, D., Cherian, M., Wu, J., Chen, T., 2016. Human pregnane X receptor compromises the function of p53 and promotes malignant transformation. *Cell Death Discov.* 2, 16023. <https://doi.org/10.1038/cddiscovery.2016.23>
- Robey, R.W., Pluchino, K.M., Hall, M.D., Fojo, A.T., Bates, S.E., Gottesman, M.M., 2018. Revisiting the role of ABC transporters in multidrug-resistant cancer. *Nat. Rev. Cancer* 18, 452–464. <https://doi.org/10.1038/s41568-018-0005-8>
- Rysä, J., Buler, M., Savolainen, M.J., Ruskoaho, H., Hakkola, J., Hukkanen, J., 2013. Pregnane X receptor agonists impair postprandial glucose tolerance. *Clin. Pharmacol. Ther.* 93, 556–563. <https://doi.org/10.1038/clpt.2013.48>
- Saburi, Y., Nakagawa, M., Ono, M., et al., 1989. Increased expression of glutathione S-transferase gene in cis-diamminedichloroplatinum(II)-resistant variants of a Chinese hamster ovary cell line. *Cancer Res.* 49, 7020–7025.

- Samimi, G., Katano, K., Holzer, A.K., Safaei, R., Howell, S.B., 2004a. Modulation of the cellular pharmacology of cisplatin and its analogs by the copper exporters ATP7A and ATP7B. *Mol. Pharmacol.* 66, 25–32. <https://doi.org/10.1124/mol.66.1.25>
- Samimi, G., Safaei, R., Katano, K., et al., 2004b. Increased expression of the copper efflux transporter ATP7A mediates resistance to cisplatin, carboplatin, and oxaliplatin in ovarian cancer cells. *Clin. Cancer Res. Off. J. Am. Assoc. Cancer Res.* 10, 4661–4669. <https://doi.org/10.1158/1078-0432.CCR-04-0137>
- Sanclemente, M., Francoz, S., Esteban-Burgos, L., et al., 2018. c-RAF ablation induces regression of advanced Kras/Trp53 mutant lung adenocarcinomas by a mechanism independent of MAPK signaling. *Cancer Cell* 33, 217–228.e4. <https://doi.org/10.1016/j.ccell.2017.12.014>
- Santos, A., Zanetta, S., Cresteil, T., et al., 2000. Metabolism of irinotecan (CPT-11) by CYP3A4 and CYP3A5 in humans. *Clin. Cancer Res. Off. J. Am. Assoc. Cancer Res.* 6, 2012–2020.
- Saxena, M., Stephens, M.A., Pathak, H., Rangarajan, A., 2011. Transcription factors that mediate epithelial-mesenchymal transition lead to multidrug resistance by upregulating ABC transporters. *Cell Death Dis.* 2, e179. <https://doi.org/10.1038/cddis.2011.61>
- Schaaf, L.J., Hammond, L.A., Tipping, S.J., et al., 2006. Phase I and pharmacokinetic study of intravenous irinotecan in refractory solid tumor patients with hepatic dysfunction. *Clin. Cancer Res. Off. J. Am. Assoc. Cancer Res.* 12, 3782–3791. <https://doi.org/10.1158/1078-0432.CCR-05-2152>
- Schoch, G.A., D'Arcy, B., Stihle, M., et al., 2010. Molecular switch in the glucocorticoid receptor: Active and passive antagonist conformations. *J. Mol. Biol.* 395, 568–577. <https://doi.org/10.1016/j.jmb.2009.11.011>
- Shehu, A.I., Lu, J., Wang, P., et al., 2019. Pregnane X receptor activation potentiates ritonavir hepatotoxicity [WWW Document]. <https://doi.org/10.1172/JCI128274>
- Sherman, W., Beard, H.S., Farid, R., 2006a. Use of an induced fit receptor structure in virtual screening. *Chem. Biol. Drug Des.* 67, 83–84. <https://doi.org/10.1111/j.1747-0285.2005.00327.x>
- Sherman, W., Day, T., Jacobson, M.P., Friesner, R.A., Farid, R., 2006b. Novel procedure for modeling ligand/receptor induced fit effects. *J. Med. Chem.* 49, 534–553. <https://doi.org/10.1021/jm050540c>
- Shi, Z., Tiwari, A.K., Shukla, S., et al., 2009. Inhibiting the function of ABCB1 and ABCG2 by the EGFR tyrosine kinase inhibitor AG1478. *Biochem. Pharmacol.* 77, 781–793. <https://doi.org/10.1016/j.bcp.2008.11.007>
- Shiau, A.K., Barstad, D., Radek, J.T., et al., 2002. Structural characterization of a subtype-selective ligand reveals a novel mode of estrogen receptor antagonism. *Nat. Struct. Biol.* 9, 359–364. <https://doi.org/10.1038/nsb787>
- Siegel, R.L., Miller, K.D., Jemal, A., 2019. Cancer statistics, 2019. *CA. Cancer J. Clin.* 69, 7–34. <https://doi.org/10.3322/caac.21551>
- Smith, M.L., Ford, J.M., Hollander, M.C., et al., 2000. p53-mediated DNA repair responses to UV radiation: studies of mouse cells lacking p53, p21, and/or gadd45 genes. *Mol. Cell. Biol.* 20, 3705–3714. <https://doi.org/10.1128/mcb.20.10.3705-3714.2000>
- Song, I.-S., Savaraj, N., Siddik, Z.H., et al., 2004. Role of human copper transporter Ctr1 in the transport of platinum-based antitumor agents in cisplatin-sensitive and cisplatin-resistant cells. *Mol. Cancer Ther.* 3, 1543–1549.
- Souza, A.G., Silva, I.B.B., Campos-Fernandez, E., et al., 2018. Comparative assay of 2D and 3D cell culture models: Proliferation, gene expression and anticancer drug response. *Curr. Pharm. Des.* 24, 1689–1694. <https://doi.org/10.2174/1381612824666180404152304>
- Sparreboom, A., van Asperen, J., Mayer, U., et al., 1997. Limited oral bioavailability and active epithelial excretion of paclitaxel (Taxol) caused by P-glycoprotein in the intestine. *Proc. Natl. Acad. Sci. U. S. A.* 94, 2031–2035. <https://doi.org/10.1073/pnas.94.5.2031>
- Stage, T.B., Damkier, P., Christensen, M.M.H., Nielsen, L.B.-K., Højlund, K., Brøsen, K., 2016. Impaired glucose tolerance in healthy men treated with St. John's Wort. *Basic Clin. Pharmacol. Toxicol.* 118, 219–224. <https://doi.org/10.1111/bcpt.12486>
- Stathopoulos, G.P., Boulikas, T., Vougiouka, M., et al., 2005. Pharmacokinetics and adverse reactions of a new liposomal cisplatin (Lipoplatin): phase I study. *Oncol. Rep.* 13, 589–595.
- Staudinger, J.L., 2019. Clinical applications of small molecule inhibitors of Pregnane X receptor. *Mol. Cell. Endocrinol.* 485, 61–71. <https://doi.org/10.1016/j.mce.2019.02.002>
- Staudinger, J.L., Goodwin, B., Jones, S.A., et al., 2001. The nuclear receptor PXR is a lithocholic acid sensor that protects against liver toxicity. *Proc. Natl. Acad. Sci. U. S. A.* 98, 3369–3374. <https://doi.org/10.1073/pnas.051551698>
- Staudinger, J.L., Woody, S., Sun, M., Cui, W., 2013. Nuclear-receptor-mediated regulation of drug- and bile-acid-transporter proteins in gut and liver. *Drug Metab. Rev.* 45, 48–59. <https://doi.org/10.3109/03602532.2012.748793>

- Sundqvist, A., Bengoechea-Alonso, M.T., Ye, X., et al., 2005. Control of lipid metabolism by phosphorylation-dependent degradation of the SREBP family of transcription factors by SCF(Fbw7). *Cell Metab.* 1, 379–391. <https://doi.org/10.1016/j.cmet.2005.04.010>
- Synold, T.W., Dussault, I., Forman, B.M., 2001. The orphan nuclear receptor SXR coordinately regulates drug metabolism and efflux. *Nat. Med.* 7, 584–590. <https://doi.org/10.1038/87912>
- Takara, K., Kitada, N., Yoshikawa, E., et al., 2009. Molecular changes to HeLa cells on continuous exposure to SN-38, an active metabolite of irinotecan hydrochloride. *Cancer Lett.* 278, 88–96. <https://doi.org/10.1016/j.canlet.2008.12.033>
- Takara, K., Obata, Y., Yoshikawa, E., et al., 2006. Molecular changes to HeLa cells on continuous exposure to cisplatin or paclitaxel. *Cancer Chemother. Pharmacol.* 58, 785–793. <https://doi.org/10.1007/s00280-006-0226-5>
- Takeda, M., Mizokami, A., Mamiya, K., et al., 2007. The establishment of two paclitaxel-resistant prostate cancer cell lines and the mechanisms of paclitaxel resistance with two cell lines. *The Prostate* 67, 955–967. <https://doi.org/10.1002/pros.20581>
- Taneja, G., Chu, C., Maturu, P., Moorthy, B., Ghose, R., 2018. Role of c-Jun-N-Terminal Kinase in Pregnane X Receptor-Mediated Induction of Human Cytochrome P4503A4 In Vitro. *Drug Metab. Dispos. Biol. Fate Chem.* 46, 397–404. <https://doi.org/10.1124/dmd.117.079160>
- Taniguchi, R., Kumai, T., Matsumoto, N., et al., 2005. Utilization of human liver microsomes to explain individual differences in paclitaxel metabolism by CYP2C8 and CYP3A4. *J. Pharmacol. Sci.* 97, 83–90. <https://doi.org/10.1254/jphs.fp0040603>
- Teixeira, C., Reed, J.C., Pratt, M.A., 1995. Estrogen promotes chemotherapeutic drug resistance by a mechanism involving Bcl-2 proto-oncogene expression in human breast cancer cells. *Cancer Res.* 55, 3902–3907.
- Tian, Q., Zhang, J., Tan, T.M.C., et al., 2005. Human multidrug resistance associated protein 4 confers resistance to camptothecins. *Pharm. Res.* 22, 1837–1853. <https://doi.org/10.1007/s11095-005-7595-z>
- Uhlen, M., Zhang, C., Lee, S., et al., 2017. A pathology atlas of the human cancer transcriptome. *Science* 357. <https://doi.org/10.1126/science.aan2507>
- Uniprot, 2020a. O060809 (PRA10_HUMAN). Accessed 20.07.2020. Available from <https://www.uniprot.org/uniprot/O60809>
- Uniprot, 2020b. Q5VTA0 (PRA17_HUMAN). Accessed 20.07.2020. Available from <https://www.uniprot.org/uniprot/Q5VTA0>
- Vaidyanathan, A., Sawers, L., Gannon, A.-L., et al., 2016. ABCB1 (MDR1) induction defines a common resistance mechanism in paclitaxel- and olaparib-resistant ovarian cancer cells. *Br. J. Cancer* 115, 431–441. <https://doi.org/10.1038/bjc.2016.203>
- Vaquero, J., Briz, O., Herraez, E., Muntané, J., Marin, J.J.G., 2013. Activation of the nuclear receptor FXR enhances hepatocyte chemoprotection and liver tumor chemoresistance against genotoxic compounds. *Biochim. Biophys. Acta* 1833, 2212–2219. <https://doi.org/10.1016/j.bbamcr.2013.05.006>
- Verma, S., Tabb, M.M., Blumberg, B., 2009. Activation of the steroid and xenobiotic receptor, SXR, induces apoptosis in breast cancer cells. *BMC Cancer* 9, 3. <https://doi.org/10.1186/1471-2407-9-3>
- Wadosky, K.M., Koochekpour, S., 2016. Molecular mechanisms underlying resistance to androgen deprivation therapy in prostate cancer. *Oncotarget* 7, 64447–64470. <https://doi.org/10.18632/oncotarget.10901>
- Wakamatsu, T., Nakahashi, Y., Hachimine, D., Seki, T., Okazaki, K., 2007. The combination of glycyrrhizin and lamivudine can reverse the cisplatin resistance in hepatocellular carcinoma cells through inhibition of multidrug resistance-associated proteins. *Int. J. Oncol.* 31, 1465–1472.
- Wang, H., Huang, H., Li, H., et al., 2007. Activated pregnenolone X-receptor is a target for ketoconazole and its analogs. *Clin. Cancer Res. Off. J. Am. Assoc. Cancer Res.* 13, 2488–2495. <https://doi.org/10.1158/1078-0432.CCR-06-1592>
- Wang, H., Li, H., Moore, L.B., et al., 2008. The Phytoestrogen Coumestrol Is a Naturally Occurring Antagonist of the Human Pregnane X Receptor. *Mol. Endocrinol.* 22, 838–857. <https://doi.org/10.1210/me.2007-0218>
- Wang, H., Venkatesh, M., Li, H., et al., 2011. Pregnane X receptor activation induces FGF19-dependent tumor aggressiveness in humans and mice. *J. Clin. Invest.* 121, 3220–3232. <https://doi.org/10.1172/JCI41514>
- Wang, W., Zhan, M., Li, Q., et al., 2016. FXR agonists enhance the sensitivity of biliary tract cancer cells to cisplatin via SHP dependent inhibition of Bcl-xL expression. *Oncotarget* 7, 34617–34629. <https://doi.org/10.18632/oncotarget.8964>
- Ward, R.A., Fawell, S., Floc'h, N., Flemington, V., McKerrecher, D., Smith, P.D., 2020. Challenges and opportunities in cancer drug resistance. *Chem. Rev. acs.chemrev.0c00383*. <https://doi.org/10.1021/acs.chemrev.0c00383>

- Watkins, R.E., Maglich, J.M., Moore, L.B., et al., 2003. 2.1 A crystal structure of human PXR in complex with the St. John's wort compound hyperforin. *Biochemistry* 42, 1430–1438. <https://doi.org/10.1021/bi0268753>
- Wistuba, W., Gnewuch, C., Liebisch, G., Schmitz, G., Langmann, T., 2007. Lithocholic acid induction of the FGF19 promoter in intestinal cells is mediated by PXR. *World J. Gastroenterol.* 13, 4230–4235. <https://doi.org/10.3748/wjg.v13.i31.4230>
- Wu, Q., Wang, R., Yang, Q., et al., 2013a. Chemoresistance to gemcitabine in hepatoma cells induces epithelial-mesenchymal transition and involves activation of PDGF-D pathway. *Oncotarget* 4, 1999–2009. <https://doi.org/10.18632/oncotarget.1471>
- Wu, B., Li, S., Dong, D., 2013b. 3D structures and ligand specificities of nuclear xenobiotic receptors CAR, PXR and VDR. *Drug Discov. Today* 18, 574–581. <https://doi.org/10.1016/j.drudis.2013.01.001>
- Wu, M.H., Yan, B., Humerickhouse, R., Dolan, M.E., 2002. Irinotecan activation by human carboxylesterases in colorectal adenocarcinoma cells. *Clin. Cancer Res. Off. J. Am. Assoc. Cancer Res.* 8, 2696–2700.
- Xue, Y., Chao, E., Zuercher, W.J., Willson, T.M., Collins, J.L., Redinbo, M.R., 2007. Crystal structure of the PXR-T1317 complex provides a scaffold to examine the potential for receptor antagonism. *Bioorg. Med. Chem.* 15, 2156–2166. <https://doi.org/10.1016/j.bmc.2006.12.026>
- Yang, G., Xu, S., Peng, L., Li, H., Zhao, Y., Hu, Y., 2016. The hypoxia-mimetic agent CoCl₂ induces chemotherapy resistance in LOVO colorectal cancer cells. *Mol. Med. Rep.* 13, 2583–2589. <https://doi.org/10.3892/mmr.2016.4836>
- Yasuda, M., Kishimoto, S., Amano, M., Fukushima, S., 2019. The involvement of pregnane X receptor-regulated pathways in the antitumor activity of cisplatin. *Anticancer Res.* 39, 3601–3608. <https://doi.org/10.21873/anticancer.13507>
- Yoshida, H., Teramae, M., Yamauchi, M., et al., 2013. Association of copper transporter expression with platinum resistance in epithelial ovarian cancer. *Anticancer Res.* 33, 1409–1414.
- Zhang, W., Feng, M., Zheng, G., et al., 2012. Chemoresistance to 5-fluorouracil induces epithelial-mesenchymal transition via up-regulation of Snail in MCF7 human breast cancer cells. *Biochem. Biophys. Res. Commun.* 417, 679–685. <https://doi.org/10.1016/j.bbrc.2011.11.142>
- Zhang, Y.-K., Zhang, G.-N., Wang, Y.-J., et al., 2016. Bafetinib (INNO-406) reverses multidrug resistance by inhibiting the efflux function of ABCB1 and ABCG2 transporters. *Sci. Rep.* 6, 25694. <https://doi.org/10.1038/srep25694>
- Zhao, H., Guo, L., Zhao, H., Zhao, J., Weng, H., Zhao, B., 2015. CXCR4 over-expression and survival in cancer: a system review and meta-analysis. *Oncotarget* 6, 5022–5040. <https://doi.org/10.18632/oncotarget.3217>
- Zhou, J., Zhai, Y., Mu, Y., et al., 2006a. A novel pregnane X receptor-mediated and sterol regulatory element-binding protein-independent lipogenic pathway. *J. Biol. Chem.* 281, 15013–15020. <https://doi.org/10.1074/jbc.M511116200>
- Zhou, C., Tabb, M.M., Nelson, E.L., et al., 2006b. Mutual repression between steroid and xenobiotic receptor and NF-kappaB signaling pathways links xenobiotic metabolism and inflammation. *J. Clin. Invest.* 116, 2280–2289. <https://doi.org/10.1172/JCI26283>
- Zhou, C., Poulton, E.-J., Grün, F., et al., 2007. The dietary isothiocyanate sulforaphane is an antagonist of the human steroid and xenobiotic nuclear receptor. *Mol. Pharmacol.* 71, 220–229. <https://doi.org/10.1124/mol.106.029264>
- Zhou, J., Liu, M., Zhai, Y., Xie, W., 2008. The antiapoptotic role of pregnane X receptor in human colon cancer cells. *Mol. Endocrinol. Baltim. Md* 22, 868–880. <https://doi.org/10.1210/me.2007-0197>
- Zhu, H., Chen, Z., Ma, Z., et al., 2017a. Tanshinone IIA Protects Endothelial Cells from H₂O₂-Induced Injuries via PXR Activation. *Biomol. Ther.* 25, 599–608. <https://doi.org/10.4062/biomolther.2016.179>
- Zhu, S., Shanbhag, V., Wang, Y., Lee, J., Petris, M., 2017b. A Role for The ATP7A Copper Transporter in Tumorigenesis and Cisplatin Resistance. *J. Cancer* 8, 1952–1958. <https://doi.org/10.7150/jca.19029>
- Zhu, W., Song, L., Zhang, H., Matoney, L., LeCluyse, E., Yan, B., 2000. Dexamethasone differentially regulates expression of carboxylesterase genes in humans and rats. *Drug Metab. Dispos. Biol. Fate Chem.* 28, 186–191.
- Zhu, Z., Kim, S., Chen, T. et al., 2004. Correlation of high-throughput pregnane X receptor (PXR) transactivation and binding assays. *J. Biomol. Screen.* 9, 533–540. <https://doi.org/10.1177/1087057104264902>
- Zisowsky, J., Koegel, S., Leyers, S., et al., 2007. Relevance of drug uptake and efflux for cisplatin sensitivity of tumor cells. *Biochem. Pharmacol.* 73, 298–307. <https://doi.org/10.1016/j.bcp.2006.10.003>
- Zou, M., Hu, X., Xu, B., et al., 2019. Glutathione S-transferase isozyme alpha 1 is predominantly involved in the cisplatin resistance of common types of solid cancer. *Oncol. Rep.* 41, 989–998. <https://doi.org/10.3892/or.2018.6861>

Zucchini, N., de Sousa, G., Bailly-Maitre, B. et al., 2005. Regulation of Bcl-2 and Bcl-xL anti-apoptotic protein expression by nuclear receptor PXR in primary cultures of human and rat hepatocytes. *Biochim. Biophys. Acta* 1745, 48–58. <https://doi.org/10.1016/j.bbamcr.2005.02.005>

9. Appendices

Appendix table 1. Genes, that were determined from the Ls-R-C or Ls-R-I cells.

Gene	MOC-class	Relevance to cisplatin or irinotecan resistance	Effect by PXR activation
ABCA2	Ib	Cis treatment ↑ expression (Herraez et al., 2012) ↓ in cis-R (Herraez et al., 2012)	↑(Benson et al., 2016)
ABCB1	Ib	Iri substrate(Iyer et al., 2002; Luo et al., 2002) ↑ in iri-R (Choi et al., 2015) ↓ in cis-R (Li et al., 2016; Takara et al., 2006) ≈ in cis-R (Wakamatsu et al., 2007)	↑(Martin et al., 2008; Moscovitz et al., 2018; Olinga et al., 2008)
ABCB11		Cis and iri substrates (Pan et al., 2016) Cis treatment ↑ expression (Herraez et al., 2012; Vaquero et al., 2013) ↓ in cis-R (Herraez et al., 2012)	↑/↓(Moscovitz et al., 2018; Olinga et al., 2008)
ABCC1	Ib	Cis treatment ↑ expression (Herraez et al., 2012) ≈ in cis-R (Li et al., 2016; Wakamatsu et al., 2007) ↑ in cis-R (Herraez et al., 2012) ↑ in SN38-R (Takara et al., 2009)	↑(Martin et al., 2008)
ABCC2	Ib	Cis treatment ↑ expression (Herraez et al., 2012) Cis/iri substrates (Luo et al., 2002; Pan et al., 2016) ↑ in cis-R (Herraez et al., 2012; Liedert et al., 2003; Wakamatsu et al., 2007)	↑(Olinga et al., 2008)
ABCC3	Ib	Cis treatment ↑ expression (Herraez et al., 2012) Cis substrate (Benson et al., 2016) ↑ in SN38-R (Takara et al., 2009) ↑ in cis-R (Herraez et al., 2012; Wakamatsu et al., 2007)	
ABCC4	Ib	Cisplatin substrate (Benson et al., 2016) ↑ in cis-R (Herraez et al., 2012; Wakamatsu et al., 2007) Overexpression increases iri/SN38 resistance (Tian et al., 2005)	
ABCC5	Ib	↑ in SN38-R (Takara et al., 2009) ↑ in cis-R(Herraez et al., 2012; Wakamatsu et al., 2007)	↑(Moscovitz et al., 2018)
ABCG2	Ib	Iri/SN38 substrates (Nakatomi et al., 2001; Pan et al., 2016) Cis treatment ↑ expression (Herraez et al., 2012) ↑ in SN38-R (Candeil et al., 2004; Jandu et al., 2016; Takara et al., 2009) ↑ in iri-R (Choi et al., 2015)	↑(Moscovitz et al., 2018; Naspinski et al., 2008; Planque et al., 2016)
ALDH1A1		Colon cancer stem cell marker (Planque et al., 2016)	↑(Planque et al., 2016)
ATP7A	Ib	Cis treatment ↑ expression (Herraez et al., 2012) Cis substrate (Samimi et al., 2004b, 2004a) ≈ in cis-R (Song et al., 2004) ↑ in cis-R (Inoue et al., 2010; Li et al., 2016)	

		Deletion increases cis sensitivity (Zhu et al., 2017b)	
ATP7B	Ib	Cis substrate (Samimi et al., 2004a) Cis treatment ↑ expression (Herraez et al., 2012) ↑ in cis-R (Herraez et al., 2012; Li et al., 2016)	
BAG3		Antiapoptotic (Zhou et al., 2008; Zucchini et al., 2005)	↑(Zhou et al., 2008)
BAK1		Proapoptotic (Zhou et al., 2008)	↓(Zhou et al., 2008)
BAX	V	Proapoptotic (Verma et al., 2009)	↑(Verma et al., 2009)
BBC3		Proapoptotic (Verma et al., 2009)	↑(Verma et al., 2009)
BCL2	V	Antiapoptotic (Zucchini et al., 2005)	↑(Zucchini et al., 2005)
BCL2L1	V	Antiapoptotic (Zucchini et al., 2005)	↑(Zucchini et al., 2005)
BIRC2	V	Antiapoptotic (Zhou et al., 2008)	↑(Zhou et al., 2008)
CDKN1A	V	Negative regulator of cell cycle, suppressor of apoptosis (Abbas and Dutta, 2009) ↑ in iri-R (Choi et al., 2015)	↑/↓(Robbins et al., 2016; Verma et al., 2009)
CES1	II	Iri activation to SN38 (Humerickhouse et al., 2000; Wu et al., 2002)	↑(Moscovitz et al., 2018)
CES2	II	Iri activation to SN38 (Humerickhouse et al., 2000; Wu et al., 2002)	↑(Zhu et al., 2000)
CYP1A1	II		↑(Naspinski et al., 2008)
CYP1A2	II		↑(Naspinski et al., 2008)
CYP3A4	II	Iri inactivation (Haaz et al., 1998; Santos et al., 2000)	↑(Moscovitz et al., 2018; Olinga et al., 2008)
CXCR4		Colon cancer stem cell marker (Planque et al., 2016)	↑(Planque et al., 2016)
EGFR	V	↑ in SN38-R cells (Petitprez and Larsen, 2013)	
ERCC1	IV	↑ by cis (Li et al., 1998) Inhibition increases cis cytotoxicity (Arora et al., 2010) Low expression associated with better response in cis-treated patients (Bai et al., 2012)	
FGF19		↑ cell growth, migration, invasion of cells (Wang et al., 2011)	↑(Wang et al., 2011)
GADD45A	IV	Cis treatment ↑ expression (Liu et al., 2018b) Suppression increases cis sensitivity (Liu et al., 2018b; Smith et al., 2000)	
GADD45B		↑ migration of cancer cells (Kodama and Negishi, 2011)	↑(Kodama and Negishi, 2011)
GSTA1	II	Low expression associated with better response to cis (Nishimura et al., 1996) ↑ in cis-R (Zou et al., 2019) ≈ in cis-R (Saburi et al., 1989) Knock down increased cis toxicity (Zou et al., 2019)	↑(Moscovitz et al., 2018; Naspinski et al., 2008)
GSTP1	II	↑ in cis-R (Saburi et al., 1989; Zou et al., 2019) ≈ in cis-R (Li et al., 2016; Wakamatsu et al., 2007) Knock down increases cis toxicity (Zou et al., 2019) Overexpression decreased cis toxicity (De Luca et al., 2019)	↑(Moscovitz et al., 2018)
MCL1		Antiapoptotic (Zhou et al., 2008)	↑(Zhou et al., 2008)

MSH2	IV	Knock down increases cis resistance (Kothandapani et al., 2013) ↓ in cis-R (Lage et al., 1999)	
NFκB	V		
NR0B2		Cis-treatment ↑ expression (Vaquero et al., 2013) Cis-treatment ↓ expression (Wang et al., 2016)	
NR1H4		Farnesoid X receptor	
NR1I2		Pregnane X receptor	
OLMF4		Colon cancer stem cell marker (Planque et al., 2016)	↑(Planque et al., 2016)
PRAMEF10		Negative regulator of apoptosis, positive regulator of proliferation (Uniprot, 2020a)	↑(Kandel et al., 2016)
PRAMEF17		Negative regulator of apoptosis, positive regulator of proliferation (Uniprot, 2020b)	↑(Kandel et al., 2016)
SLC10A1	Ia		↑(Moscovitz et al., 2018)
SLC10A2	Ia		
SLC22A1	Ia		↑(Moscovitz et al., 2018)
SLC31A1	Ia	Uptake of cisplatin (Ishida et al., 2002; Song et al., 2004) Higher expression in cis-sensitive patients (Ishida et al., 2010; Lee et al., 2011) Cis treatment ↓ expression (Holzer and Howell, 2006) ↓ in cis-R (Song et al., 2004; Zisowsky et al., 2007)	
SLC31A2		Induction of cleavage of SLC31A1 (Öhrvik et al., 2016) Suppression of SLC31A2 increases cis sensitivity (Yoshida et al., 2013) Higher expression associated with cis resistance (Lee et al., 2011)	
SLCO1B1	Ia	Uptake of SN38 (Iusuf et al., 2014) ≈ in SN38-R (Takara et al., 2009)	
SLCO2B1	Ia	Uptake of SN38 (Fujita et al., 2016)	↑(Benson et al., 2016; Moscovitz et al., 2018)
TOP1	III	Molecular target of iri/SN38 (Kawato et al., 1991)	
TP53	V		↑/↓(Verma et al., 2009; Zhou et al., 2008)
UGT1A1	II	SN38 inactivation (Gagné et al., 2002; Iyer et al., 1998)	↑(Olinga et al., 2008)
UGT1A9	II	SN38 inactivation (Gagné et al., 2002; Iyer et al., 1998)	

Cis, cisplatin; iri, irinotecan; cis-R, cisplatin resistance; iri-R, irinotecan resistance; ↑, induction, ↓, suppression; MOC-class, mechanism of chemoresistance-classes according to Marin et al. 2010.

Appendix table 2. Relative expression of genes in Ls-R-C cells compared to Ls-P cells.

Gene	Relative expression (+/-SD)	Gene	Relative expression (+/-SD)
ABCA2	0.74* (0.1)	CYP1A2	0.54* (0.4)
ABCB1	0.0074**** (0.003)	ERCC1	1.6** (0.3)
ABCB11	12.5** (6.5)	GADD45A	4.4**** (1.0)
ABCC1	2.1**** (0.3)	GSTP1	0.61** (0.1)
ABCC2	2.6*** (0.9)	NR0B2	2.2** (0.6)
ABCC3	2.8** (0.9)	NR1I2	0.42* (0.1)
ABCG2	32.8* (29.6)	OLFM4	0.017**** (0.008)
ATP7A	1.8**** (0.3)	SLC10A2	0.070** (0.005)
BBC3	2.9** (0.8)	SLC31A1	0.50**** (0.1)
BCL2	0.54** (0.1)	SLC31A2	1.5** (0.3)
BCL2L1	4.0*** (1.4)	SLCO2B1	0.37** (0.1)
CDKN1A	5.1** (2.4)		

Only significant relative expression changes >1.5 or <0.75 to Ls-P cells were included. Data is shown as mean relative expression compared to the normalized mean expression of Ls-P. Statistically significant differences are illustrated with asterisks. * p <0.05, ** p <0.01, *** p <0.001, **** p <0.0001 compared to Ls-P cells analyzed by unpaired t-test.

Appendix table 3. Relative expression of genes in Ls-R-I cells compared to Ls-P cells.

Gene	Relative expression (+/-SD)	Gene	Relative expression (+/-SD)
ABCB1	1.8** (0.4)	GADD45A	2.1*** (0.3)
ALDH1A1	0.089**** (0.01)	NR0B2	4.3**** (1.1)
BCL2L1	2.3**** (0.3)	OLFM4	0.13*** (0.04)
CDKN1A	3.3**** (0.5)	SLC10A2	0.086**** (0.02)
CES2	1.6**** (0.1)	SLCO2B1	2.5**** (0.4)
CYP3A4	4.6** (2.1)	TOP1	0.58*** (0.05)
CXCR4	16.3* (9.0)	UGT1A1	0.58** (0.08)
FGF19	3.3** (1.0)	UGT1A9	0.28*** (0.2)
EGFR	1.6** (0.3)		

Only significant relative expression changes >1.5 or <0.75 to Ls-P cells were included. Data is shown as mean relative expression compared to the normalized mean expression of Ls-P. Statistically significant differences are illustrated with asterisks. * p <0.05, ** p <0.01, *** p <0.001, **** p <0.0001 compared to Ls-P cells analyzed by unpaired t-test.

10. Acknowledgements

First, I want to express my gratitude to Dr. Oliver Burk for the excellent supervision, the patience to answer my almost endless questions and for the scientific discussions we had. I also want to thank Prof. Matthias Schwab for the opportunity to do my doctoral studies in the Dr. Margarete-Fischer-Bosch-Institute for Clinical Pharmacology and for the supervision and reviewing my doctoral thesis. I am also thankful for Prof. Peter Ruth for the supervision and reviewing of my doctoral thesis on the part of the University of Tübingen. Next, I want to thank the collaborators in Tübingen for their contributions to this work: Prof. Stefan Laufer, Dr. Tatu Pantsar and Azam Rashidian. I am also very thankful for Karina Abuazi Rincones for her great technical assistance and all the help she has provided in the laboratory. I also want to thank Katja Löffler for her help. I am also grateful for the Interfaculty Centre for Pharmacogenomics and Pharma Research (ICEPHA) for funding this work.

Special thanks go to my parents for their support. I am also very thankful for my friends in Finland for all the moments we have shared during these years either in Finland or in Germany. Finally, I want to express my deepest gratitude to my husband Tatu for all the support and love you have provided.